THESIS

MODELING SNOW-FREE CONCRETE SURFACES USING HYDRONIC RADIANT HEAT

Submitted by

Trai Ngoc Nguyen

Department of Civil and Environmental Engineering

In partial fulfillment of the requirements

For the Degree of Master of Science

Colorado State University

Fort Collins, Colorado

Spring 2018

Master's Committee:

Advisor: Paul R.Heyliger

Rebecca Atadero
Scott A. Glick

ABSTRACT

MODELING SNOW-FREE CONCRETE SURFACES USING HYDRONIC RADIANT HEAT

U.S roads and bridges were graded as D and C+, respectively by the American Society of Civil Engineers (ASCE) in 2013. Snow accumulation during the winter results in many issues affecting national strategic goals. More specifically, it hinders the overall transportation system which significantly affects economic competitiveness. Moreover, it causes many traffic accidents in the winter affecting people's lives and assets. Traditional methods for snow accumulation are the use of deicing agents such as salt-based chemical (NaCl, $MgCl_2$) and sand. However, the application of these chemicals leads to the adverse effects on environment, drainage system and especially infrastructure (corrosion, premature failure). This remarkably raises the maintenance costs on structures. Therefore, it is necessary to conduct an alternative technology for snow removal which is environmentally safe and highly effective to avoid the negative effects of those deicing agents. Heated snow melting systems are potential solutions to prevent snow accumulation that has increasingly drawn attention during the last few decades in many countries.

This research presents the method of snow melting with hydronic radiant heat to avoid the negative effects of traditional agents on environment as well as infrastructure systems. Two-dimensional (2D) and three-dimensional (3D) finite element models are developed to investigate the influence of input parameters on the performance of snow melting in various environmental conditions. Intensive parametric studies are conducted to analyze and determine the key factors in the snow melting process. Consequently, appropriate values of those parameters are proposed for future experiments, design and construction in the U.S.

ACKNOWLEDGEMENTS

I would like to thank Dr. Paul Heyliger who provided guidance and support as the advisor for my thesis work. Under the guidance of Dr. Paul Heyliger, I have learned tremendous amount of knowledge in both engineering theories and practical research at Colorado State University - Fort Collins. I am so grateful to have such a great opportunity to study and to work under his supervision. Also, I would like to thank my committee members Dr. Rebecca Atadero and Dr. Scott Glick for their time and helpful direction. The funding for this research was provided by grant from Mountain Plains Consortium (MPC).

TABLE OF CONTENTS

CHAPTER 1 - OVERVIEW OF STUDY

1.1 INTRODUCTION

Snow accumulation during winter has many negative impacts on people's lives. More specifically, it causes many traffic accidents during winter (Figure 1.1). Snow accumulation also hinders the overall transportation systems as the vehicle mobility is reduced. According to official statistics, there are more than 1.5 million accidents due to bad weather conditions, resulting in about 7,000 fatalities as well as 800,000 injuries annually [1]. Furthermore, this issue could lead to tremendous economic losses, directly affecting the national economic competitiveness. For instance, crashes due adverse weather conditions cause $42 billion of economic cost annually [2]. The impacts of adverse weather conditions on the highway system are significant. It was reported that $2.3 billion were spent annually by the U.S for the snow removal on infrastructures including roadways and bridges [3].

Figure 1.1 Car accident during snow storm [14]

The use of deicing agents including salt-based chemicals (NaCl, $CaCl_2$ and $MgCl_2$) (Figure 1.3 and Figure 1.4) or snow plowing (Figure 1.2) is the most traditional technology to prevent snow accumulation during the winter. It is estimated that the use of salt can reduce the traffic accidents by 85% during the winter. According to some statistics, 15 million tons of salts (NaCl) are used by the U.S government annually for deicing snow [4]. It is estimated that salts (NaCl) and sand represented for about 93% of the total deicing agents applied to the roadways and bridges annually. Overall, 55% of salt (NaCl) and 38% of sand are used for snow removal by the US government [5].

There are several negative issues associated with the use of these salt-based deicing chemicals. The use of these deicers can lead to potentially harmful effects on the environment and corrosion of drainage systems. They can potentially increase the level of poisonous substances in water. Infrastructure including reinforced concrete structures or steel bridges can also be exposed to corrosion or premature failure. The maintenance costs for these structural systems are remarkably high. According to statistics, the cost of about $250 million - $650 million has been used for repairing old bridges annually [6]. For these reasons, the need for an alternative environmentally safe and low cost deicing technology is necessary.

Figure 1.2 Snow plowing [15]

Figure 1.3 Salt for snow melting [12]

Figure 1.4 Sand for snow melting [13]

The application of heating systems offers a potential solution for snow removal which has been used widely in many countries in the last few decades. The advantages of this system are not only to remove ice from the pavements, roadways or bridges but also to provide an intelligent system control strategies (snow detection control or idling control). At this point, this system is commonly used for small residential areas. More research should be conducted in order to further study the applications of this system to other critical trouble spots including airports and parking spaces. This would contribute significantly to the overall transportation system of the U.S.

1.2 LITEREATURE REVIEW

There are mainly two types of heating system: electric system (Figure 1.5 and 1.6) and hydronic system (or heat pipe) (Figure 1.7). Both are briefly reviewed below.

In electric systems, heating cables are embedded in the concrete. When the system is powered, the heating cables are warmed due to the electric current and the thermal energy (heat) will be transferred from the cables to the concrete that increases the concrete temperature. The applications of electric system include airports and pavements. There are some issues in using the electric system such as steel cable corrosion and the high resistivity of cable, resulting in the significant increase of operating costs and maintenance costs. Hou and coworkers suggested a new method for electric system using carbon fiber instead of traditional steel cables. This method has improved the electric system significantly [6]. However, this material is expensive to use in practice.

Snow accumulation can also be prevented by the use of hydronic system or heated pipe. Instead of using heating cables, pipes are embedded within the concrete slab. When the system is powered, fluids heated by boiler systems will elevate the temperature of the pipes, resulting in the increase in concrete temperature. When the surface temperature is hot enough, the snow is melted.

One advantage of using hydronic system is that many heat sources can be used such as natural gas boilers, fuel oil boilers and electric heaters. The first steady-state model of hydronic system considering heat losses was developed by Chapman [8]. A numerical model of hydronic system has been described by Liu and coworkers [7].

In terms of installation costs, the hydronic system is higher than the electric system as the boiler systems, piping systems, or circulating fluid must be obtained. However, in the case of the

operating costs, the hydronic system is lower than electric system. Fluid holds heat very well and pipes can carry thermal energy even when its temperature is low, resulting in a short operating time. On the other hand, there can be a very long operating time, leading to the increase in the cost for electricity usage. Therefore, hydronic systems have a long-term benefit in comparison to the electric systems regarding the costs.

The level of heat transfer in conduction is determined by thermal conductivity k. According to Japanese Concrete Institute (JCI), typical values of thermal conductivity of concrete are in the range 2.15-2.51 kcal/m.h.^{o}C [10]. However, typical values of k are about 1.7-2.53 kcal/ m.h.^{o}C according to American Concrete Institute (ACI) [9]. The value of thermal conductivity of concrete used in this research is 2.42 W/m.h.^{o}C or 0.062 W/in.h.^{o}C.

Similarly, the level of heat transfer in convection is determined by convection coefficient β. This heat transfer coefficient ranges 12-13 kcal/m^2.h.^{o}C according to the JCI [10] and 8-11 kcal/m^2.h.^{o}C [11]. Furthermore, convection coefficient is dependent upon wind speed as proposed by Ohzawa [19]. The value of convection coefficient of concrete used in this research is 0.009 W/in^2.h.^{0}C if the wind velocity of 2 m/s is assumed.

Specific heat is also an important factor in the transient analysis of hydronic systems. This is the key representation of heat capacity and depends on the physical properties of concrete including porosity and cement type. JCI proposed the value of specific heat in the range of 0.27-0.31 kcal/kg.^{o}C [10]. Also, the value of specific heat is in the range 0.22-0.24 kcal/kg.^{o}C according to ACI [9]. In this research, the value of specific heat is 0.3Wh/kg. ^{o}C as normal weight concrete is considered

Figure 1.5 Electric heating installation [16]

Figure 1.6 Snow sensor installation in electric system [17]

Figure 1.7 Hydronic snow melting system [18]

1.3 ORGANIZATION OF THE THESIS

This thesis is categorized into five chapters. Chapter 1 includes the introduction about some issues in using traditional deicing methods such as salt and sand. This chapter also introduces new methods of using heating snow melting systems including electric heating and hydronic heating. Chapter 2 covers detailing information about the hydronic snow melting system such as piping system, installation techniques and fluid specification. Chapter 3 provides a general background on finite element methods and heat transfer theory for steady-state and transient conditions. Both two-dimensional and three-dimensional models of hydronic snow melting system are developed to provide the preliminary results of the hydronic system. Chapter 4 performs intensive parametric studies to analyze the sensitivity as well as influence of key parameters on the hydronic system. As a consequence, the optimal value for each parameter is proposed for the future design, construction and experiment. Chapter 5 summaries the previous 4 chapters and provides some recommendations for future research.

CHAPTER 2 - HYDRONIC SNOW MELTING SYSTEM

2.1 OVERVIEW OF HYDRONIC SYSTEM

As opposed to electric systems, hydronic pipes (or heated pipes) are used in hydronic systems (Figure 2.1). Hydronic pipes are embedded in a concrete slab so that warm fluid will flow in these pipes and generate thermal energy (heat). Heat will be transferred from warm fluid to the pipes and then from heated pipes to the concrete. Consequently, the temperature of concrete increases, resulting in a warmer surface in which the snow will melt.

Closed-loop hydronic systems are typically used in many areas including residential areas or light commercial areas. One special characteristic of hydronic systems is that the life expectancy of the pipes is about 100 years and the same fluid can circulate in the piping systems for a very long time. Therefore, hydronic systems offer long-term benefits in comparison to electric systems.

Figure 2.1 Hydronic snow melting system [18]

Typically, there are four basic components of hydronic system: heat source, circulator, fluid and piping system (Figure 2.2). The most important component is the piping system.

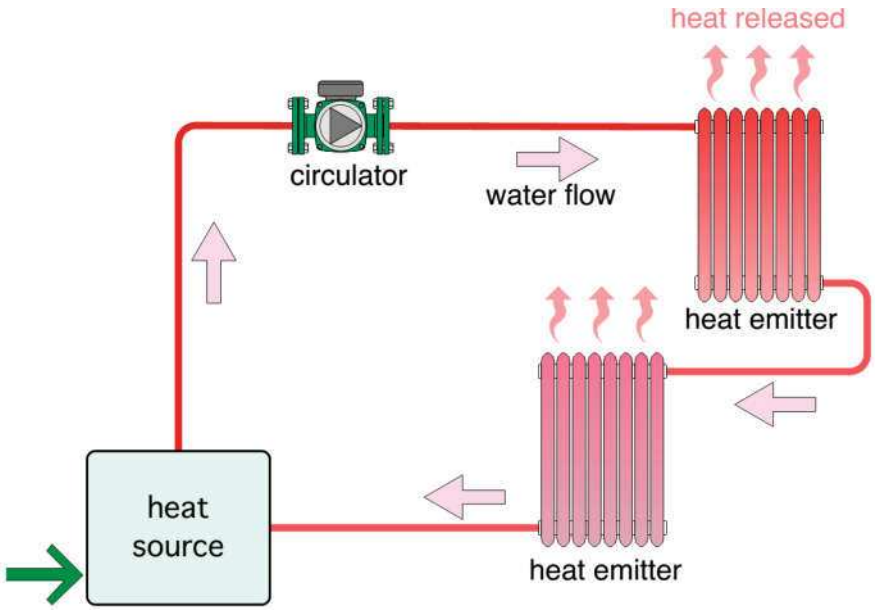

Figure 2.2 Basic components in hydronic system [23]

2.1.1 HEAT SOURCE

A potential heat source can be any device that can introduce heat in the system. Typically, there are two fundamental types of heat source. Traditional heat sources are natural gas boilers or fuel oil boilers. These heat sources are traditionally used in smaller areas such as residential areas or light commercial areas. Modern heat sources are boilers supplied with solar collector arrays, geothermal water-to-water heat pumps and biomass-fuel boilers. For some complicated systems, multiple boilers and heat pumps are used to provide enough heat for large areas in severe weather conditions. Each of these heat sources has strengths and weaknesses. Many factors including cost and fuel availability can have big impact on the selection of heat source. Typical boiler systems are shown in Figure 2.3 and Figure 2.4.

Figure 2.3 Typical snowmelt boiler systems [24]

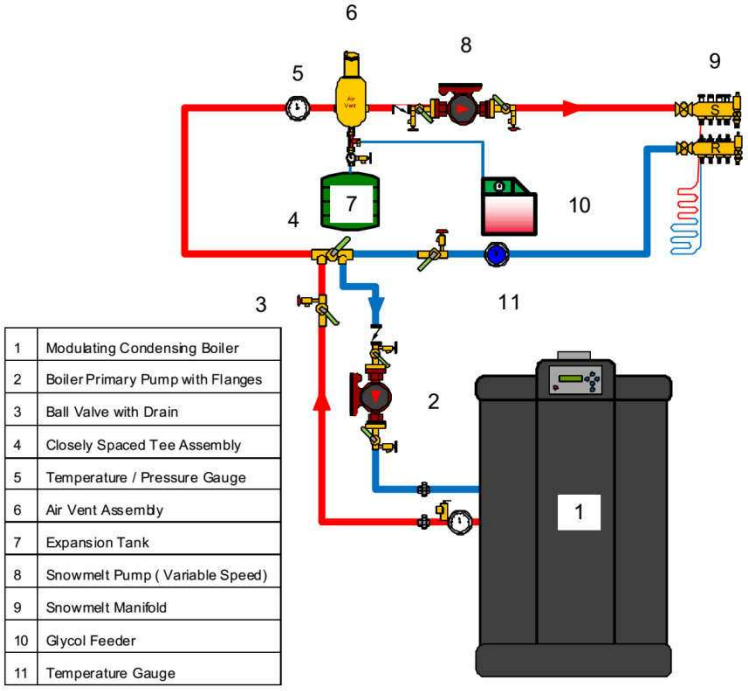

1	Modulating Condensing Boiler
2	Boiler Primary Pump with Flanges
3	Ball Valve with Drain
4	Closely Spaced Tee Assembly
5	Temperature / Pressure Gauge
6	Air Vent Assembly
7	Expansion Tank
8	Snowmelt Pump (Variable Speed)
9	Snowmelt Manifold
10	Glycol Feeder
11	Temperature Gauge

Figure 2.4 Dedicated snowmelt boiler system [24]

2.1.2 CIRCULATOR

The basic idea to design hydronic snow melting system is to design a closed-loop piping pathways so that fluid flows from the circulator's outlet to its inlet. This would allow the fluid circulate in the pipe and transfer heat throughout the entire system equally without creating any "strips" on the surface with low temperatures.

The purpose of a circulator (or pump) is to motivate fluid to flow in the pipes in an appropriate rate and direction. More specifically, the fluid leaves the circulator's inlet with higher pressure and then circulates in a designed piping pathways and finally gets back to the circulator's inlet with lower pressure. Figure 2.5 shows a typical modern 3-speed wet-rotor circulator commonly used in hydronic systems.

Figure 2.5 A modern 3-speed wet-rotor circulator [23]

2.1.3 FLUID SPECIFICATION

The working fluid (or circulating fluid) in hydronic snow melting system is a mixture of water and glycol. The purpose of using glycol is to lower the freezing temperature of the circulating fluid/solution. If the circulating fluid is just water alone, the fluid freeze when the ambient temperature decreases leading to the damage of the hydronic piping system. The use of additional glycol is to avoid system damage due to freezing.

Typically, there are two types of glycol: propylene glycol and ethylene glycol (Figure 2.6). Propylene glycol is recommended by many manufacturers as it is environmentally friendly while ethylene glycol is considered poison or toxic. However, neither of these choices has negative effects on the pipes. The level of glycol in solution is dependent upon many factors including weather conditions. However, 40% of glycol combined with 60% of water by volume is commonly used in hydronic systems.

There are two things to notice about the circulating fluid of hydronic systems. First, the fluid temperature must be increased slowly. Second, the temperature difference between the supply temperature and return temperature should be less than 25^{o}F. The reason is to avoid any thermal shock to the concrete.

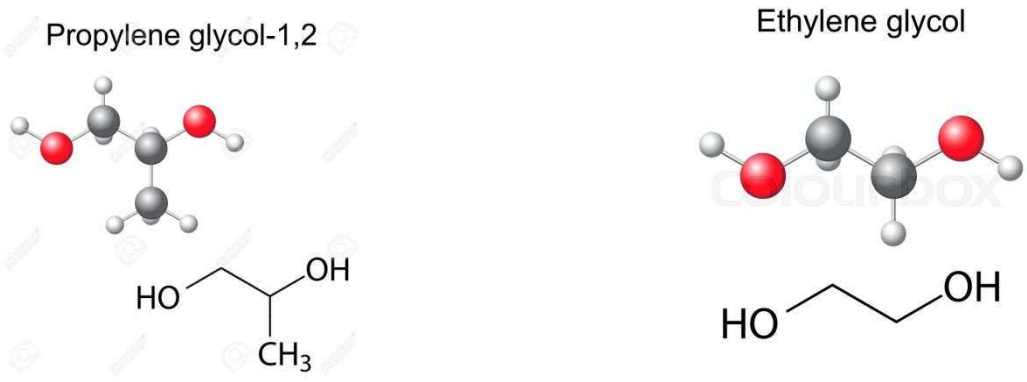

Figure 2.6 Glycol structures [25]

2.1.4 HYDORNIC PIPING SYSTEM

2.1.4.1 PIPE SPECIFICATION

A relatively new pipe called cross-linked polyethylene (a.k.a. PEX) was developed in Europe and has been popular in the American market since 1980s. This molecular structure shown in Figure 2.7 has proven to be very stable and durable which is extremely important for hydronic systems. The unique structure helps the pipes avoid the adverse effects of chemicals/solution circulating in the pipes. This type of piping can withstand a maximum temperature of 200^0F and a maximum pressure of $80psi$ [18]. Furthermore, its life expectancy is possibly over 100 years. These are very important properties in hydronic system. Typical dimensions of this pipe are shown in Table 2.1.

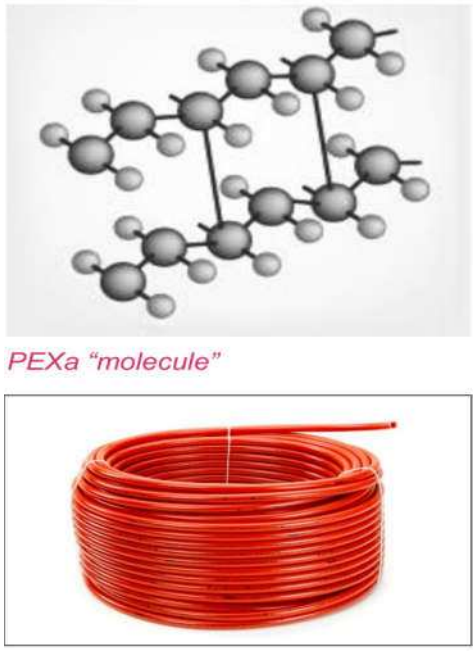

Figure 2.7 PEX [18]

Table 2.1 PEX table data [26]

Nominal Size	Outside Diameter (in)	Inside Diameter (in)	Max. Coil Length (in)	Water Content (gal/ft)
1/2 "	0.625	0.475	150	0.009
5/8 "	0.75	0.574	250	0.014
3/4 "	0.875	0.671	400	0.018
1 "	1.125	0.862	500	0.03

2.1.4.2 INSULATION

An insulated layer (i.e polystyrene insulation) is very important in any hydronic snow melting system as it keeps thermal energy (heat) generated from the heating source in the system during the snow melting process. In other words, it prevents wasted thermal energy (heat) from flowing out of the system. Insulated layers can be installed horizontally or vertically (either at the bottom surface or edges of the system).

2.1.4.3 PIPING LAYOUT PATTERNS

Making a decision on which piping pattern to use in a hydronic system is extremely important. Hydronic pipes should be installed so that the thermal energy (heat) is distributed equally on the surface to melt the snow without creating any "strips". Typically, there are two basic types of pattern: reverse-return pattern and serpentine pattern. Regarding the reverse-return pattern, the supply and return portion run parallel to each other. This provides an even heat to the entire surface. Figure 2.8 shows the reverse-return pattern used in hydronic system. In the case of serpentine pattern, this pattern is not as effective as the previous pattern since it does not provide heat equally to the entire surfaces. It can melt some areas very well however, ice/snow formation will still occur at some locations. However, this can be used in some special area such as stairs. Figure 2.9 shows the serpentine pattern used in hydronic system.

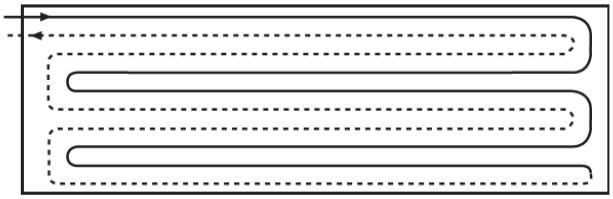

Figure 2.8 Reverse-return pattern [23]

Figure 2.9 Serpentine pattern [23]

2.1.4.4 INSTALLATION TECHNIQUES

The first step in piping installation is to prepare the base material as the compacted grade. Then the insulated layers are placed over the compacted grade in order to prevent wasted heat from flowing out of the system. Wire mesh or rebar usually lays over these layers. The piping is secured to the wire mesh or rebar by using either wire ties, foam stables or plastic zip ties as shown in Figure 2.10 - Figure 2.14. This enables the pipes to be stable during the construction/pour.

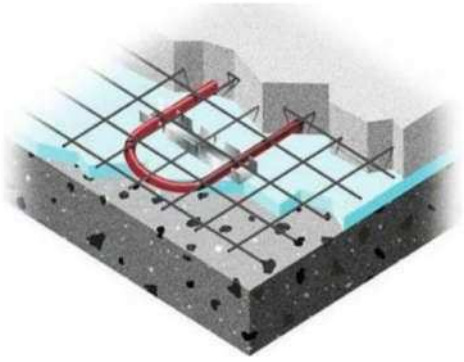

Figure 2.10 Tubing installed with wire ties [18]

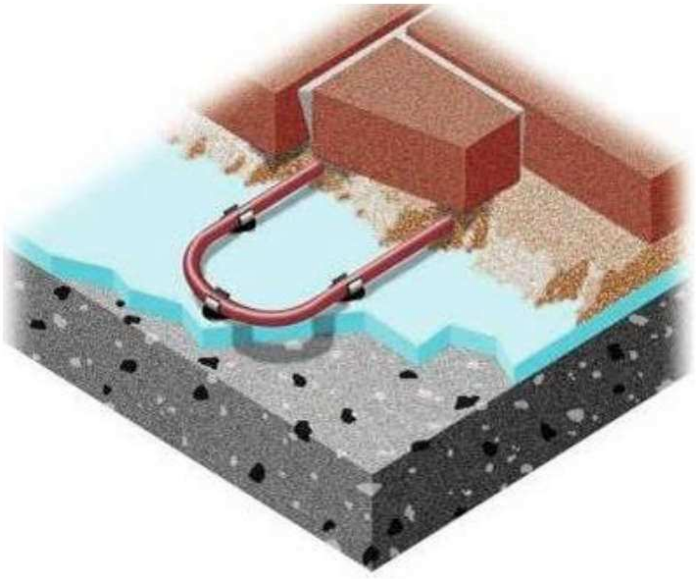

Figure 2.11 Tubing installed with foam stables [18]

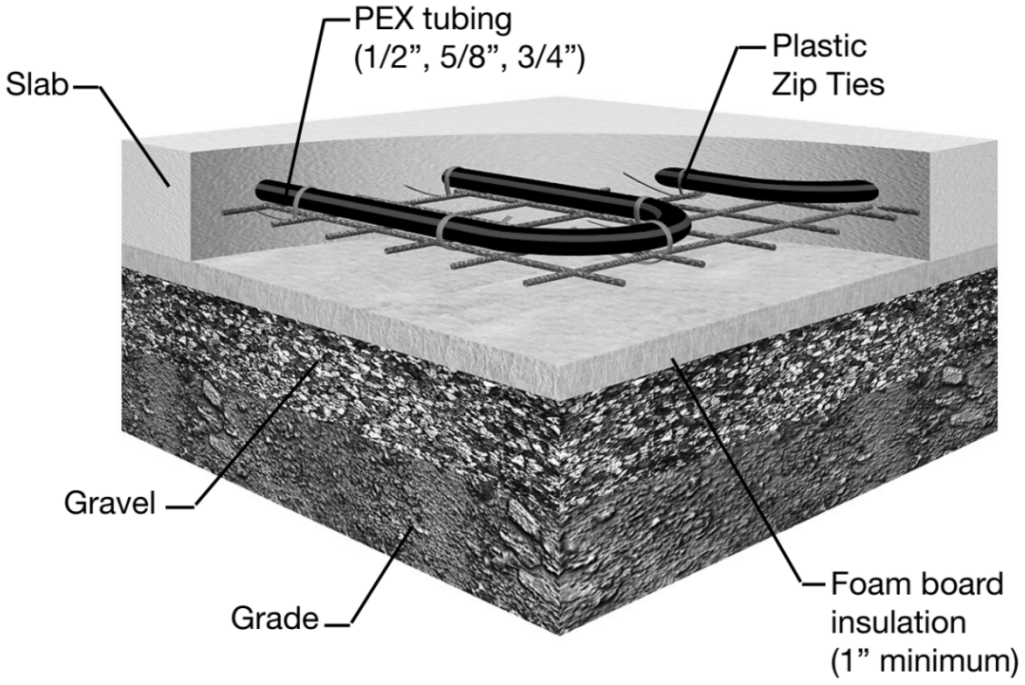

Figure 2.12 Tubing installed with plastic zip ties [26]

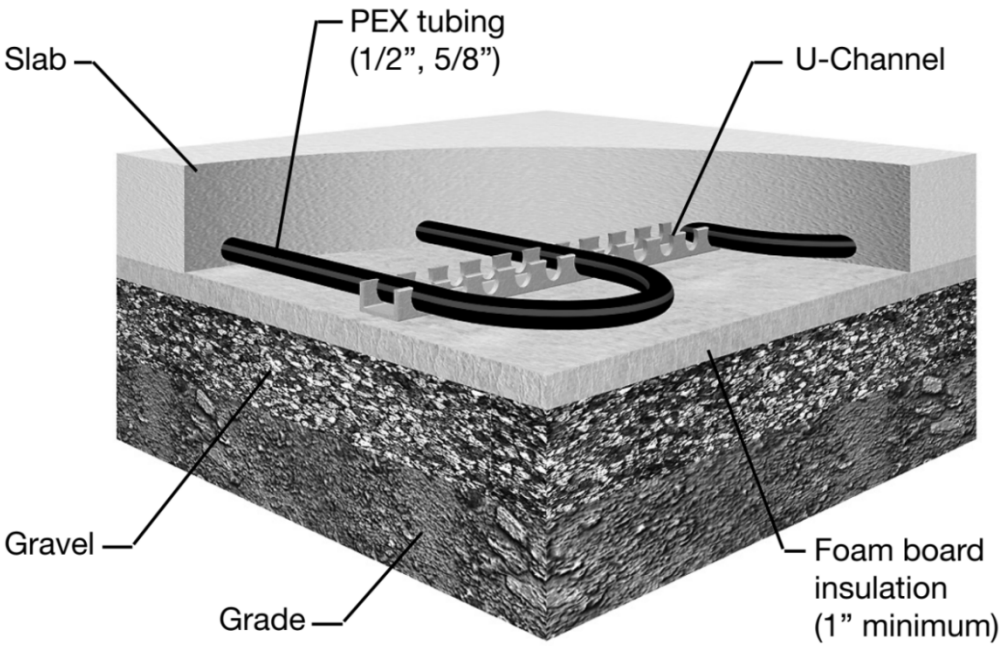

Figure 2.13 Tubing installed with U-Channel [26]

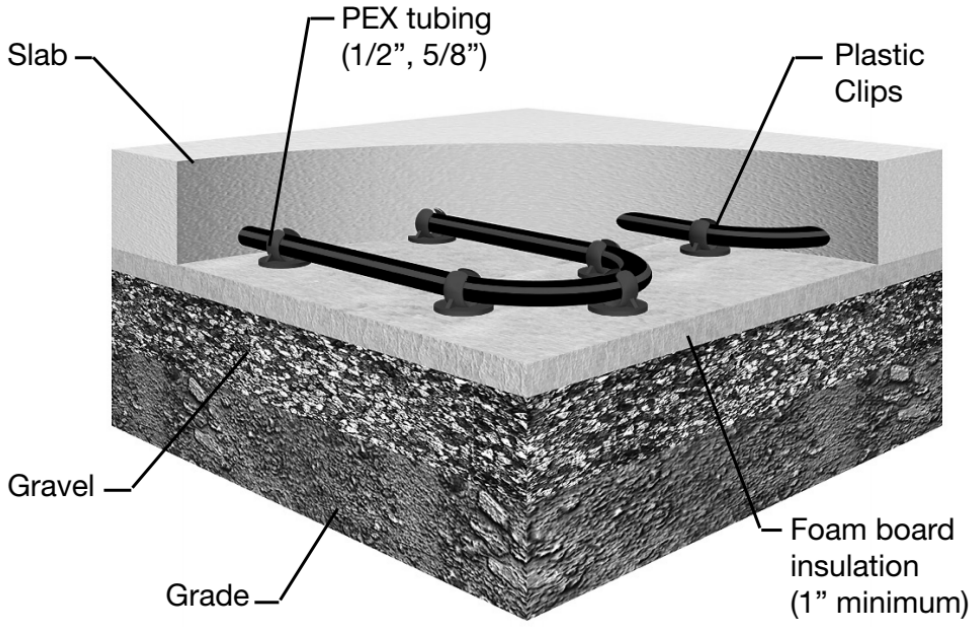

Figure 2.14 Tubing installed with plastic clips [26]

2.1.4.5 PRIMARY TYPES OF PIPING INSTALLATION

The pipe can be installed within the reinforce concrete. This procedure is commonly used for reinforced concrete structures including sidewalks or driveways. The first step is to prepare the base material to be a compacted grade before the piping installation. After that, under-slab insulation layers or edge insulation layers are installed to prevent heat from flowing out of the system. The heated pipe is then secured to the wire mesh or rebar using either wire ties or foam stables. Alternative methods can be used for securing the tubing to the insulation layers including plastic clips or U-channel. Figure 2.15 shows pipes installed within a reinforced concrete slab.

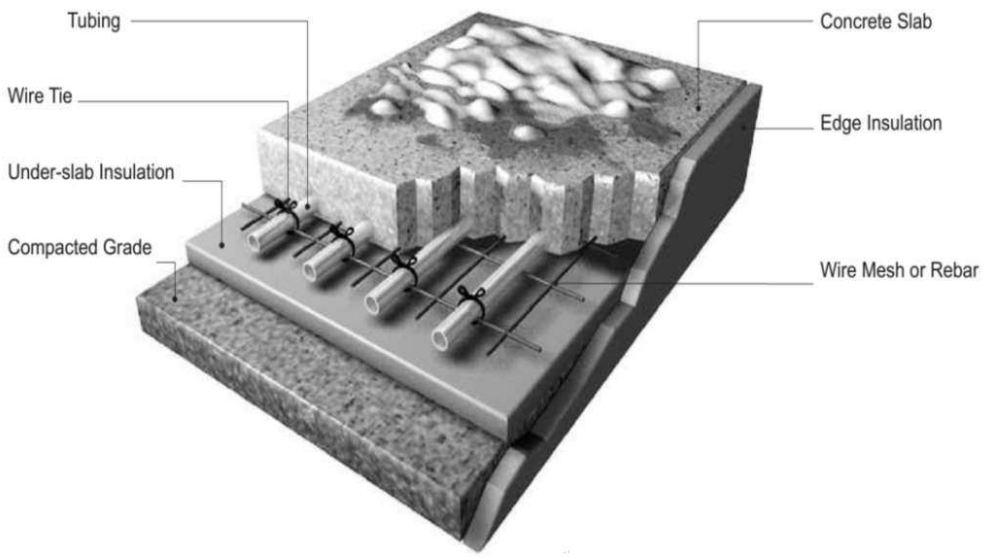

Figure 2.15 Pipes installed within reinforced concrete slab [22]

The pipe can also be installed within pre-stressed concrete slabs as shown in Figure 2.16. This type of installation is applicable for some pre-stressed concrete structures such as parking rams or suspended ramps. The base material must be compacted grade prior to any installations. A thermal break is then maintained between the hydronic system and normal slab by installing under-slab insulation and edge insulation. This is a critical step in the hydronic system since it

prevents the heat loss. There are also several methods to secure the tubing to the insulation by using wire ties, foam stables, plastic clips, U-channels.

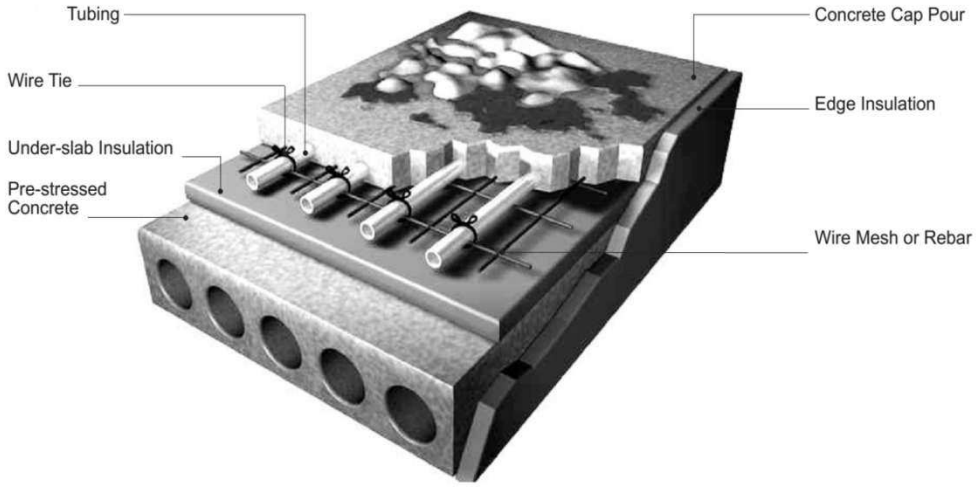

Figure 2.16 Pipes installed within pre-stressed concrete [22]

Pipe can be installed within concrete slab over insulated steel decking as shown in Figure 2.17. This installation is widely used in steel bridges or suspended ramps. The PEX tubing is fastened to the wire mesh or rebar using wire ties. The tubes are placed about 3"-4" from the top of the reinforced concrete slab. Horizontal insulated layers and vertical insulated layers are installed to prevent the heat loss and keep enough heat to melt the snow.

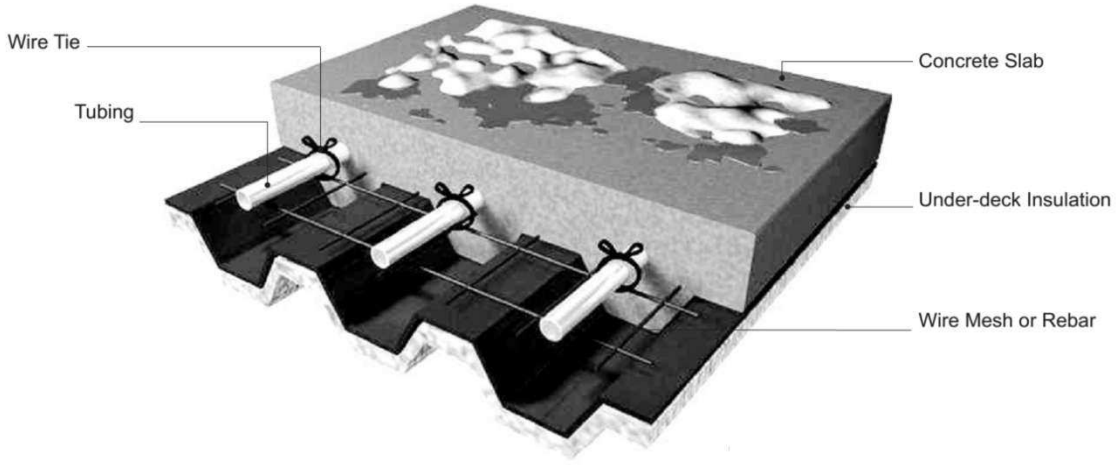

Figure 2.17 Slab over insulated steel decking [22]

Stair installation is a very special structure. A serpentine pattern is usually used as shown in Figure 2.18. Heat loss is minimized by installing the vertical insulation and horizontal insulation. Some other types of installation such asphalt pour installation and paver installation are shown in Figure 2.19 and Figure 2.20.

Figure 2.18 Stair installation [18]

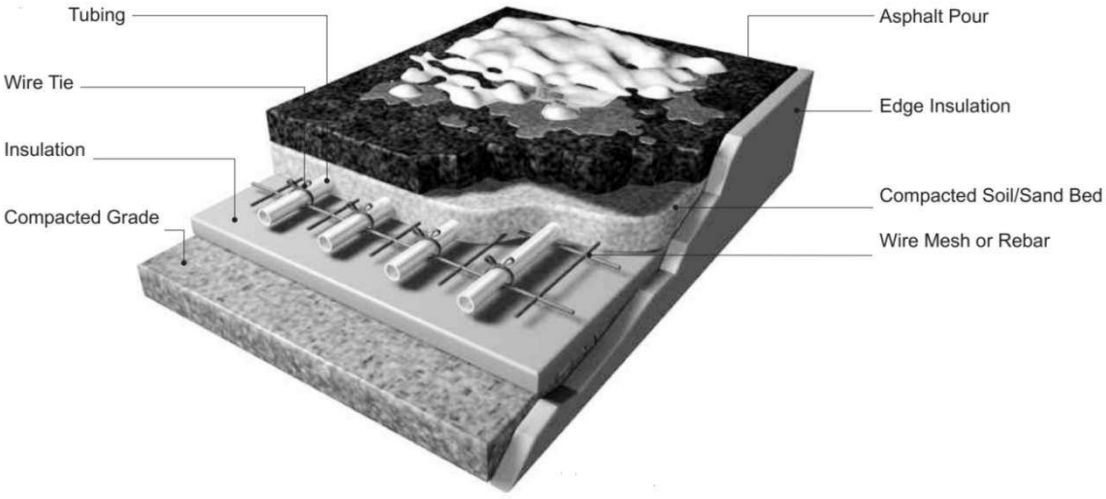

Figure 2.19 Asphalt pour installation [22]

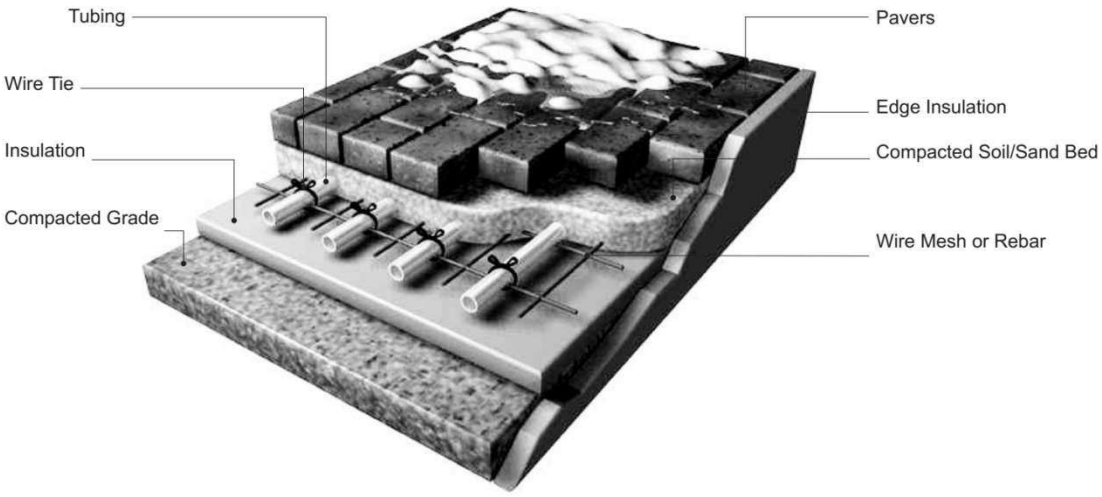

Figure 2.20 Paver installation [22]

2.2 TYPES OF APPLICATION

2.2.1 TYPE A - LEVEL I (RESIDENTIAL SYSTEMS)

This is applicable for some residential areas such as walkways (Figure 2.21), driveways with slight snow accumulation. The snow-free ratio (Ar) ranges from 0 (surface is covered with snow during snow storm or 0% snow-free) to 0.5 (some accumulation during snow storm or 50% snow-free).

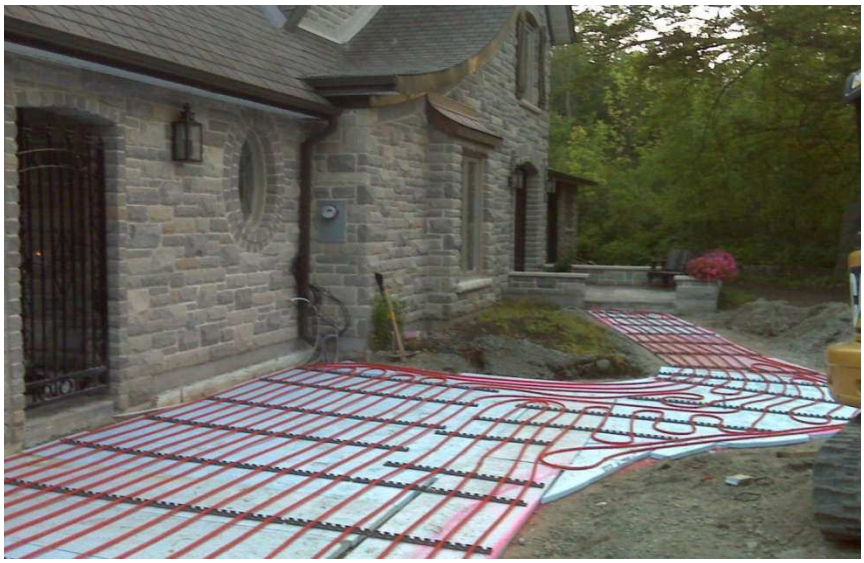

Figure 2.21 Residential sidewalk [18]

2.2.2 TYPE B - LEVEL II (COMMERICAL SYSTEMS)

This is applicable for some residential areas such as walkways and driveways with slight snow accumulation. The snow-free ratio (Ar) ranges from 0.5 (50% snow-free) to 1 (no accumulation during snow storm or 100% snow-free).

2.2.3 TYPE C - LEVEL III (INDUSTRIAL SYSTEMS)

This is commonly used in some critical areas such as hospital emergency entrances, parking ramp inclines and airports. Hence, it is required that the snow-free ratio is 100% at all times (there is no accumulation during snowfall in these areas).

2.3 SYSTEM CONTROL STRATEGY

Typically, there are two types of system control: manual and automatic control. Manual control is governed by any on/off switch to activate or turn off the system. This is the least expensive method to control the system. Therefore, it is commonly used in some small residential areas.

Automatic control includes two types: snow detection control and idling control. Regarding the snow detection control, some sensors are placed in the system to detect the environmental conditions such as ambient temperature, precipitation and moisture level as shown in Figure 2.22. If the ambient temperature is low enough and sensors detect precipitation on the surfaces then the system will be automatically activated to melt the snow. Similarly, if nothing is detected by sensors, the system will turn off automatically after a specific heating time. It is very important to choose the location to place the sensors so that the system can turn on and off properly during the snowfall. Otherwise, a huge amount of energy can be wasted.

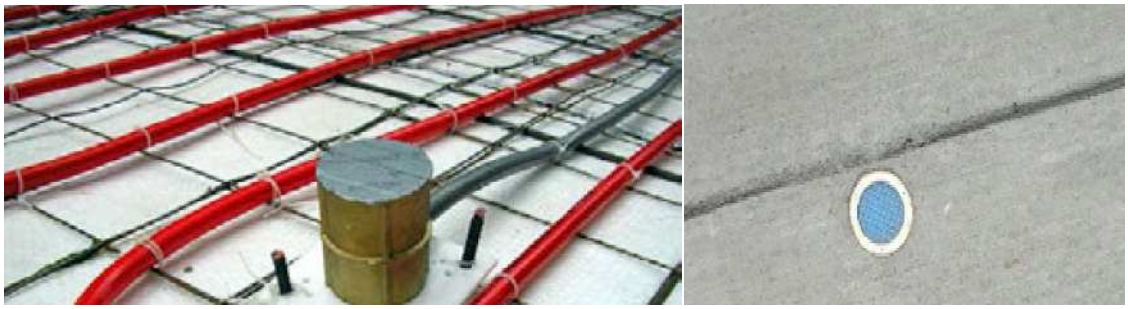

Figure 2.22 Snow detection sensor [24]

Idling control allows the slab to be maintained at a pre-determined temperature to prevent the system from being damaged during the winter. The pre-selected temperature is usually above 0^{o}C. The snow detector will increase the slab temperature to melt the snow if precipitation is detected by smart sensors.

CHAPTER 3 - NUMERICAL MODELING

3.1 OVERVIEW OF HEAT TRANSFER

3.1.1 GOVERNING EQUATIONS

In this section, the governing equations for one-dimensional (1D), two-dimensional (2D) and three-dimensional (3D) heat conduction are derived.

Heat (or thermal energy) and temperature $T(x)$ are two fundamental quantities in heat transfer. The heat flux $q_x(x)$ represents how much thermal energy is transferred through a specific cross-section of the system per unit sectional area and per unit time (in steady-state, time is not considered). When the heat flux $q_x(x)$ is added to the system, it is considered as positive quantity. When heat flux is flowing out of the system, it is considered as negative quantity. Another important quantity regarding the heat is the internal heat source Q (heat generated per unit time, unit volume).

A physical insight of heat conduction can be understood from the derivation in this section. Volume for one-dimensional (1D) and two-dimensional (2D) heat conduction are shown in Figure 3.1 and Figure 3.2

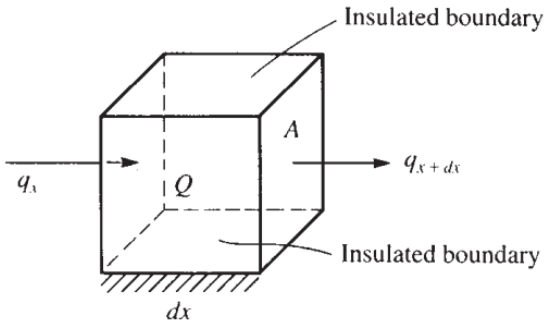

Figure 3.1 Volume for one-dimensional (1D) heat conduction [19]

Based on the conservation of energy principle:

$$E_{in} + E_{generated} = \Delta U + E_{out}$$

$$q_x A dt + Q A dx dt = \Delta U + q_{x+dx} A dt$$

E_{in} is the energy added to the volume (in J or kWh) and ΔU is the change in stored energy (in kWh). While q_x is the heat flux flowing into the domain at surface edge x (in $\frac{kW}{m^2}$), q_{x+dx} is the heat flux flowing out of the domain at surface edge $x + dx$ (in $\frac{kW}{m^2}$). Also, Q is the internal heat source (in $\frac{kg}{m^3}$) and A is the cross-sectional area perpendicular to heat flux q (in m^2).

By Fourier's law of heat conduction, heat flux can be expressed as $q_x = -k_x \frac{dT}{dx}$ where k_x is the thermal conductivity on the x direction (in $\frac{kW}{m.C}$) and T is the temperature (in C or F). The change in stored energy is of the form $\Delta U = c \times (\rho A dx) \times dT$ where c is the specific heat (or heat capacity) (in $\frac{kWh}{kg.C}$) and ρ is the mass density (in $\frac{kg}{m^3}$).

Dividing the equation $q_x A dt + Q A dx dt = c(\rho A dx) dT + q_{x+dx} A dt$ by $dV dt = A dx dt$. The following equations are obtained.

$$\frac{q_x}{dx} + Q = \rho c \frac{dT}{dt} + \frac{q_{x+dx}}{dx}$$

$$\frac{q_x - q_{x+dx}}{dx} + Q = \rho c \frac{dT}{dt}$$

Substituting $q_x = -k_x \frac{dT}{dx}$ to above equations, one-dimensional heat conduction equation can be obtained $\frac{d}{dx}\left(k_x \frac{dT}{dx}\right) + Q = \rho c \frac{dT}{dt}$. For steady-state conditions $\frac{dT}{dt} = 0$, the above equation becomes $\frac{d}{dx}\left(k_x \frac{dT}{dx}\right) + Q = 0$

Similarly, consider the two-dimensional (2D) steady-state heat conduction problem in Figure 3.2, governing differential equation can be obtained $\frac{d}{dx}\left(k_x\frac{\partial T}{\partial x}\right)+\frac{d}{dy}\left(k_y\frac{\partial T}{\partial y}\right)+Q=0$

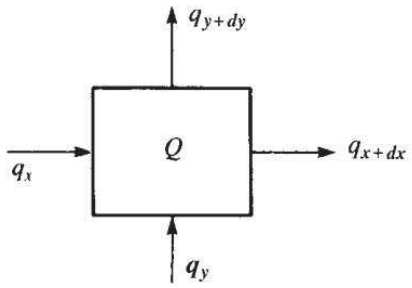

Figure 3.2 Volume for two-dimensional (2D) heat conduction [19]

Three-dimensional (3D) steady-state heat conduction governing differential equation can also be obtained. In summary, the equations for one-dimensional, two-dimensional and three-dimensional steady-state heat conduction are given as:

One-dimensional (1D): $\frac{d}{dx}\left(k_x\frac{dT}{dx}\right)+Q=0$

Two-dimensional (2D): $\frac{d}{dx}\left(k_x\frac{\partial T}{\partial x}\right)+\frac{d}{dy}\left(k_y\frac{\partial T}{\partial y}\right)+Q=0$

Three-dimensional (3D): $\frac{d}{dx}\left(k_x\frac{\partial T}{\partial x}\right)+\frac{d}{dy}\left(k_y\frac{\partial T}{\partial y}\right)+\frac{d}{dz}\left(k_z\frac{\partial T}{\partial z}\right)+Q=0$

3.1.2 BOUNDARY CONDITIONS

As can be seen from Figure 3.3, the boundary conditions take the form $T=T_B$ where T_B is known temperature at boundary S_1. These are considered as essential boundary conditions (EBC). From Figure 3.3, the boundary conditions can also take the form $q_n^*=\hat{q}$ where $\hat{q}$ is specified heat flux on S_2. Specifically, on an insulated boundary, there is no heat flux or $q_n^*=\hat{q}=0$. q_n^* is positive when the heat is added into the body while q_n^* is negative when thermal energy flows out of the analysis domain. These are natural boundary conditions (NBC) of the problem.

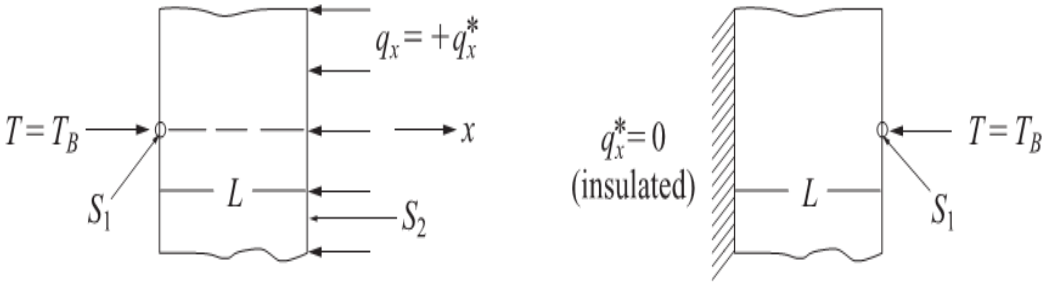

Figure 3.3 Examples of typical EBCs and NBCs [19]

At convection surface as shown in Figure 3.4, there will be heat transfer from solid to air or fluid due to the temperature difference between surface and air/fluid. One of the reasons for convection is the movement of air/fluid. Therefore, there are typically two types of convection including natural convection (or free convection) and forced convection. If the heated solid is exposed to the ambient temperature and there is no external source of motion. This is considered natural convection (or free convection). However, if there is a source of external motion such as a fan blowing air then forced convection occurs.

By Newton's law of cooling, heat flow by convection, or $q_h = \beta(T - T_\infty)$. For a convective boundary condition, the natural boundary condition (NBC) is the balance of thermal energy transfer across the boundary/surface due to convection and/or conduction. Equating $q_n^* = q_h$, the above equation has the form:

$$-k_x \frac{\partial T}{\partial x} n_x - k_y \frac{\partial T}{\partial y} n_y - k_z \frac{\partial T}{\partial z} n_z = \beta(T - T_\infty)$$

The first term accounts for thermal energy (heat flux) by conduction and the second is heat transfer by convection. Specified heat flux is not considered in this case. q_h is heat flow (heat flux) by convective heat transfer, β is the convection or film coefficient (in $\frac{kW}{m.C}$) while T_∞

is the ambient temperature of surrounding fluid medium and n_x, n_y, n_z are the direction cosines of the unit vector $\hat{n}$, normal to the surface as shown in Figure 3.5.

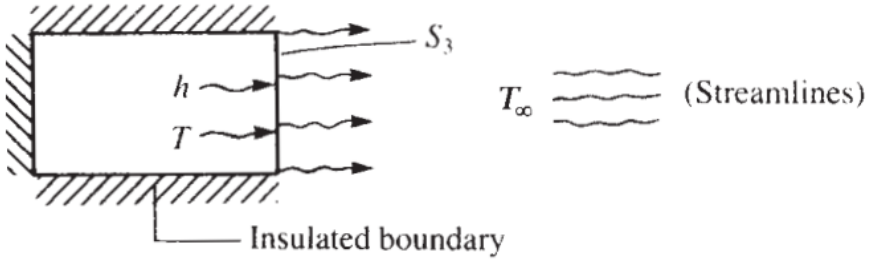

Figure 3.4 Convective boundary condition (arrows indicate heat transfer by convection) [19]

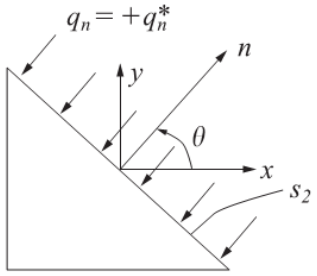

Figure 3.5 Unit vector normal to the surface (2D) [19]

3.1.3 INITIAL CONDITION

In transient analysis, the initial conditions applied to the calculation can be just as significant as the boundary conditions. The slab temperatures have to be initialized according to the weather conditions. For the hydronic snow melting system, the bottom layer is insulated and therefore the only initial condition is the temperature of concrete at $t = 0$. For this research, the temperatures are equal to the ambient temperature at $t = 0$: $T_0(x, y, z) = T_\infty$.

3.1.4 FLOWCHART OF HEAT TRANSFER PROGRAM

Flowchart of finite element process for two-dimensional and three-dimensional heat-transfer problems is shown in the Figure 3.6.

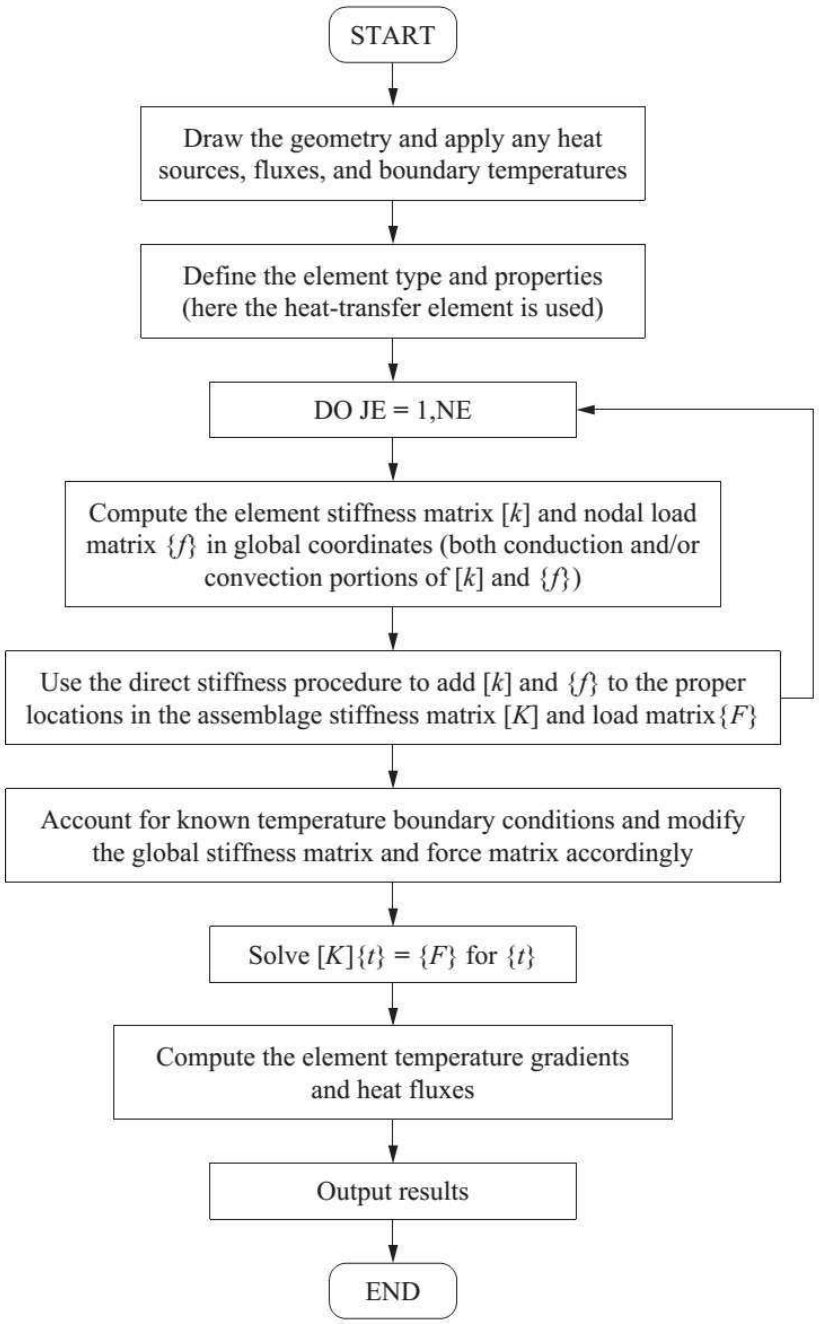

Figure 3.6 Flowchart of two-dimensional and three-dimensional heat-transfer process [19]

3.2 FINITE ELEMENT ANALYSIS OF HYDRONIC SNOW MELTING SYSTEM

Figure 3.7 - Figure 3.10 show a typical hydronic snow melting system. This system includes a concrete slab/pavement and hydronic pipes (for simplicity, there is no need to model insulation as the slab is on the ground). The embedded heated pipes in the concrete slab are U-tube structures.

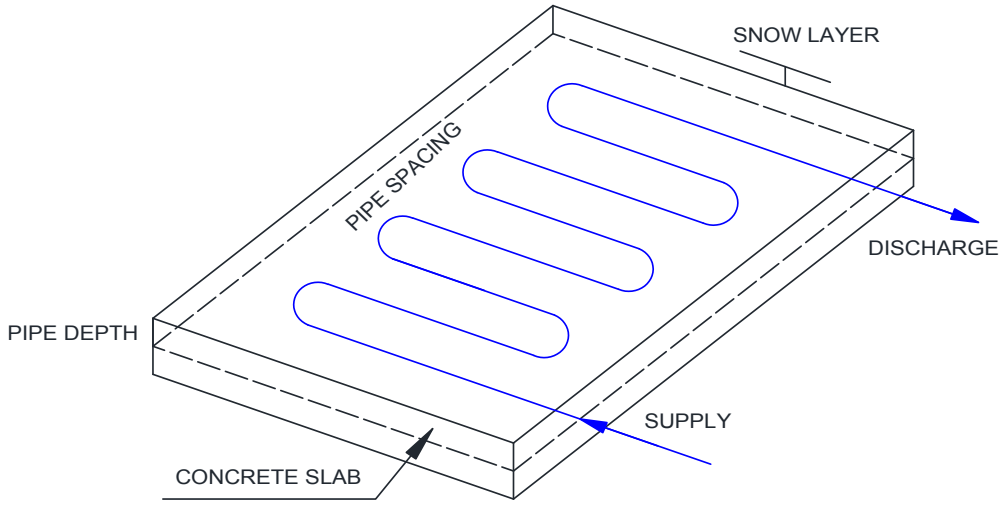

Figure 3.7 Simple hydronic snow melting system

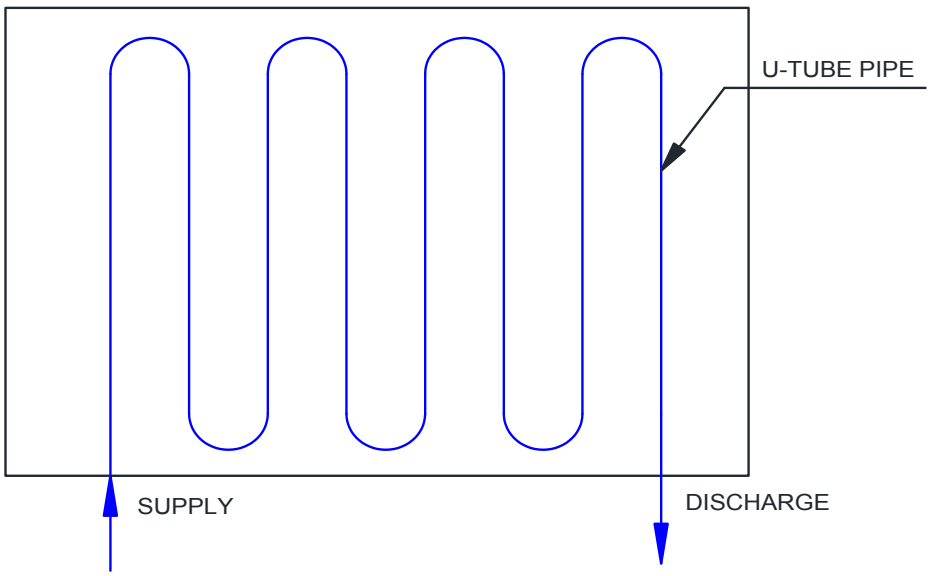

Figure 3.8 Plan view

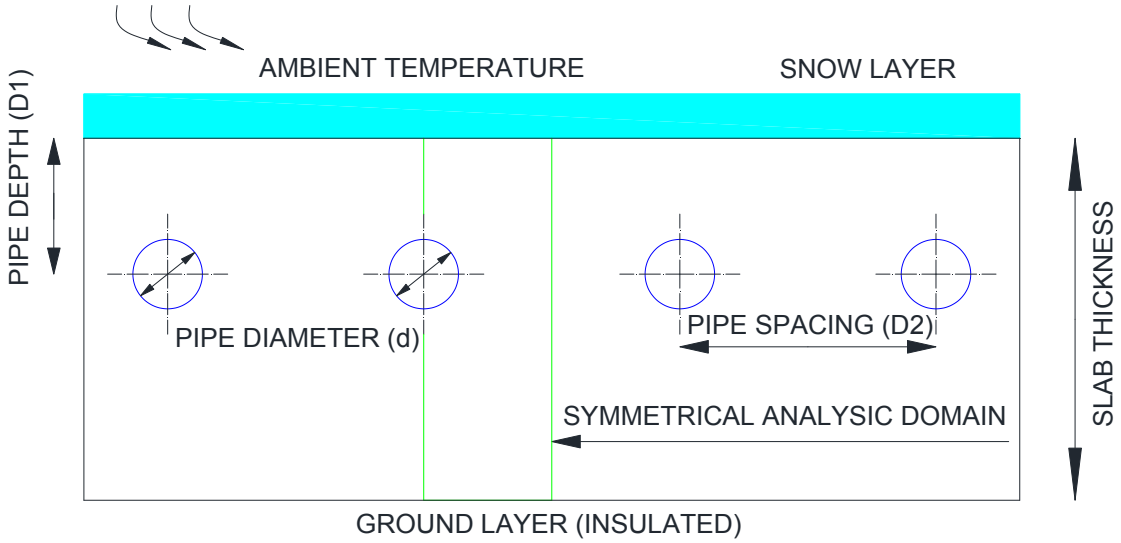

Figure 3.9 Cross section

Due to the symmetry, symmetrical domain as shown in Figure 3.9 is considered for the analysis.

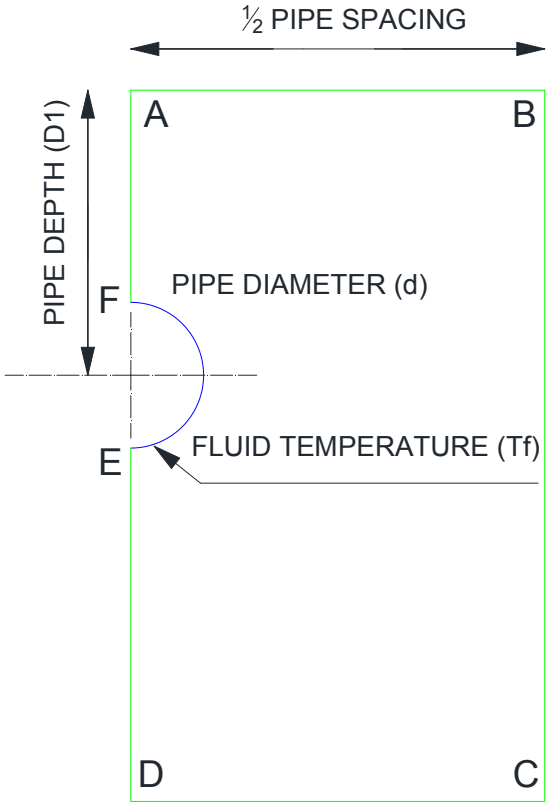

Figure 3.10 Analysis domain

All the above figures show a simple diagram of the concrete slab/pavement with heat pipes. Some assumptions are stated for simplicity and convenience:

- The concrete pavement is homogeneous and isotropic.
- The effect of thermal deformation is not considered.
- The pipe thickness is negligible (just consider nominal diameter for calculation).
- Convection between pipe and fluid is not considered.
- Neglect the evaporation of ice and snow melting and radiation effect.
- Flow rate of fluid is not taken into consideration.
- Heat losses within the pipe are not considered during the analysis.

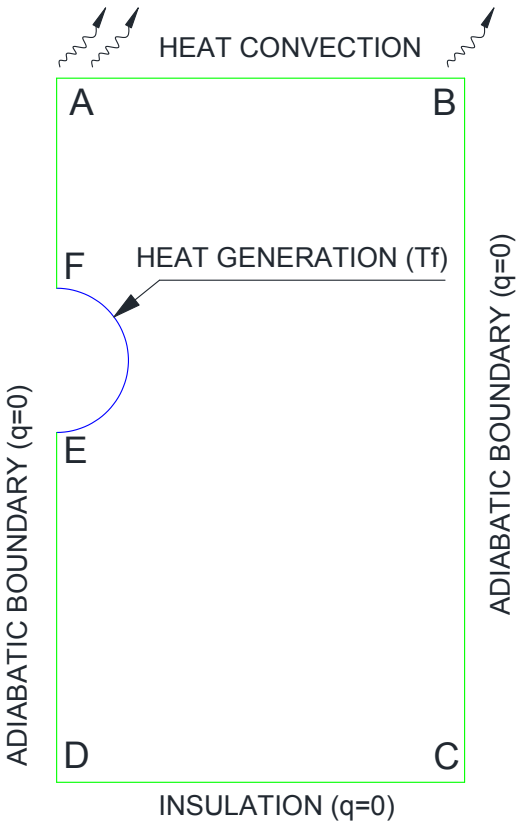

Figure 3.11 Boundary conditions

The top surface of the concrete slab is exposed to the fluid and ambient temperature which means that there will be the transfer of heat from one place to another by the movement of fluid. In other words, the thermal energy will be transferred from the surface to the environment. Therefore, convection occurs between concrete surface and fluid/air. The level of heat transfer by air convection is determined by convection coefficient of film coefficient β and the convection coefficient depends on the wind speed v. Ohzawa [19] proposed the convection coefficient β as a function of wind velocity as: $\beta = 9.6 + 1.12v$, in $(\frac{kcal}{m^2.h.C})$ where v is the wind velocity (m/s). At $v = 2m/s$, $\beta = 11.84\frac{kcal}{m^2.h.C} = 13.8\frac{W}{m^2.h.C} = 0.009\frac{W}{in^2.h.C}$. This value will be assumed in this chapter to get the preliminary results.

Along the curved EF, the essential boundary condition is imposed $T = T_f$ (fluid temperature). Along BC, AF, DE, natural boundary conditions are imposed. Due to symmetry, these lines (or surfaces in 3D) are set to adiabatic boundary conditions. In other words, there will be no heat flux or $q = 0$ on these surfaces/curves. Furthermore, there is an insulated layer under the bottom surface of the concrete slab (along CD), hence there is no heat flux or $q = 0$.

3.2.1 TWO-DIMEMSIONAL MODEL

The governing differential equation for steady-state heat transfer in plane system is given by:

$$-\frac{\partial}{\partial x}\left(k_x\frac{\partial T}{\partial x}\right) - \frac{\partial}{\partial y}\left(k_y\frac{\partial T}{\partial y}\right) = f(x,y) \quad in \quad \Omega.$$

For a convective boundary, the natural boundary condition is a balance of energy transfer across the boundary due to conduction and/or convection as discussed above:

$$k_x\frac{\partial T}{\partial x}n_x + k_y\frac{\partial T}{\partial y}n_y + \beta(T - T_\infty) = \hat{q}_n.$$

The first term is thermal energy transfer by conduction, the second term is heat transfer by convection and the third accounts for specified heat flux (if any). Ω is the two-dimensional domain and T is temperature within the concrete slab/pavement (in C or K). Also, k_x, k_y are thermal conductivities of the concrete along the x and y directions (in $\frac{W}{m.K}$) and $f(x,y)$ is internal heat generation per unit volume (in $\frac{W}{m^3}$). $\hat{q}_n$ is specified heat flux (in this case there is no internal heat or $\hat{q}_n = 0$) and β is convection or film coefficient on the top (in $\frac{W}{m^2.K}$) and T_∞ is the ambient temperature on the top of the slab (in C or K)

The weak form over an element Ω_e is given by:

$$0 = \int_{\Omega^e}(k_x \frac{\partial w}{\partial x}\frac{\partial T}{\partial x} + k_y \frac{\partial w}{\partial y}\frac{\partial T}{\partial y} - wf)dxdy - \oint_{\Gamma^e} w\left(k_x \frac{\partial T}{\partial x}n_x + k_y \frac{\partial T}{\partial y}n_y\right)ds$$

$$= \int_{\Omega^e}(k_x \frac{\partial w}{\partial x}\frac{\partial T}{\partial x} + k_y \frac{\partial w}{\partial y}\frac{\partial T}{\partial y} - wf)dxdy - \oint_{\Gamma^e} w[q_n - \beta(T - T_\infty)]ds$$

where w is the arbitrary function commonly used on finite element analysis.

The finite element model is obtained by substituting the finite element approximation of the form $T = \sum_{j=1}^{n} T_j^e \psi_j^e(x,y)$ and $w = \psi_i^e(x,y)$ into the above weak form. This results in:

$$\sum_{j=1}^{n}(K_{ij}^e + H_{ij}^e)T_j^e = F_i^e + P_i^e$$

The above coefficients can be defined by:

$$K_{ij}^e = \int_{\Omega^e}(k_x \frac{\partial \psi_i}{\partial x}\frac{\partial \psi_j}{\partial x} + k_y \frac{\partial \psi_i}{\partial y}\frac{\partial \psi_j}{\partial y})dxdy$$

$$H_{ij}^e = \beta \oint_{\Gamma^e} \psi_i \psi_j ds$$

$$F_i^e = \int_{\Omega^e} f\psi_i \, dxdy + \oint_{\Gamma^e} q_n \psi_i ds$$

$$P_i^e = \beta \oint_{\Gamma^e} \psi_i T_\infty ds$$

There are two new terms (H_{ij}^e and P_i^e). These additional terms arise due to convection boundary condition and can be computed by calculating above integrals. These coefficients can only be computed for those elements and boundaries that are subjected to a convection boundary condition (by setting the heat transfer coefficient $\beta = 0$, the heat conduction model with no account taken of convection is obtained). [21]

The coefficients H_{ij}^e and P_i^e for a linear triangular element are defined by:

$$H_{ij}^e = \beta_{12}\int_0^{h_{12}} \psi_i\psi_j ds + \beta_{23}\int_0^{h_{23}} \psi_i\psi_j ds + \beta_{34}\int_0^{h_{34}} \psi_i\psi_j ds + \beta_{41}\int_0^{h_{41}} \psi_i\psi_j ds$$

$$P_i^e = \beta_{12}T_\infty^{12}\int_0^{h_{12}} \psi_i ds + \beta_{23}T_\infty^{23}\int_0^{h_{23}} \psi_i ds + \beta_{34}T_\infty^{34}\int_0^{h_{34}} \psi_i ds + \beta_{41}T_\infty^{41}\int_0^{h_{41}} \psi_i ds$$

where β_{ij} is the convection coefficient (assumed to be constant) for the side connecting nodes i and j of the element Ω^e, T_∞^{ij} is the ambient temperature on the side and h_{ij} is the length of the side. For linear rectangular elements, the matrices have the form:

$$[H^e] = \frac{\beta_{12}h_{12}}{6}\begin{bmatrix}2&1&0&0\\1&2&0&0\\0&0&0&0\\0&0&0&0\end{bmatrix} + \frac{\beta_{23}h_{23}}{6}\begin{bmatrix}0&0&0&0\\0&2&1&0\\0&1&2&0\\0&0&0&0\end{bmatrix} + \frac{\beta_{34}h_{34}}{6}\begin{bmatrix}0&0&0&0\\0&0&0&0\\0&0&2&1\\0&0&1&2\end{bmatrix}$$
$$+ \frac{\beta_{41}h_{41}}{6}\begin{bmatrix}2&0&0&1\\0&0&0&0\\0&0&0&0\\1&0&0&2\end{bmatrix}$$

$$[P^e] = \frac{\beta_{12}T_\infty^{12}h_{12}}{2}\begin{Bmatrix}1\\1\\0\\0\end{Bmatrix} + \frac{\beta_{23}T_\infty^{23}h_{23}}{2}\begin{Bmatrix}0\\1\\1\\0\end{Bmatrix} + \frac{\beta_{34}T_\infty^{34}h_{34}}{2}\begin{Bmatrix}0\\0\\1\\1\end{Bmatrix} + \frac{\beta_{41}T_\infty^{41}h_{41}}{2}\begin{Bmatrix}1\\0\\0\\1\end{Bmatrix}$$

3.2.2 TWO DIMENSIONAL NUMERICAL RESULTS

A concrete slab is considered with thermal conductivity $k = 2.42\frac{W}{m.C} = 0.062\frac{W}{in.C}$ exposed to the ambient temperature $T_\infty = -10^0C = 14^0F$. It is also subjected to the convective boundary condition on the top surface, the convection or film coefficient $\beta = 0.009\frac{W}{in^2.C}$. There is no internal heat generation or $f(x) = 0$.

Additionally, in order to consider the transient heat transfer analysis, the specific heat or heat capacity of concrete of $c = 1090\frac{J}{kg.C} = 0.3\frac{Wh}{kg.C}$ is used, the mass density of concrete $\rho = 2400\frac{kg}{m^3} = 0.039\frac{kg}{in^3}$ and initial condition: $T_0(x, y, z) = T_\infty = -10^0C = 14^0F$. The input parameters are summarized in the Table 3.1

Table 3.1 Input parameters

Parameters	Values
Slab/pavement thickness	$H = 6"$
Thermal conductivity of concrete	$k_x = k_y = 0.062\frac{W}{in.C}$
Convective heat transfer coefficient	$\beta = 0.009\frac{W}{in^2.C}$
The specific heat or heat capacity of concrete	$c = 1090\frac{J}{kg.C} = 0.3\frac{Wh}{kg.C}$
The mass density of concrete	$\rho = 2400\frac{kg}{m^3} = 0.039\frac{kg}{in^3}$
Ambient temperature	$T_\infty = -10^0C = 14^0F$
Fluid temperature	$T_f = 30^0C = 86^0F$
Pipe depth	$D_1 = 4"$
Pipe spacing	$D_2 = 10"$
Pipe diameter	$d = 1"$

From the above derivations, temperature distribution (in degree Celsius) within the concrete slab can be obtained using MATLAB. However, the analyses will be performed in ABAQUS for convenience as two cases (steady-state and transient) are considered.

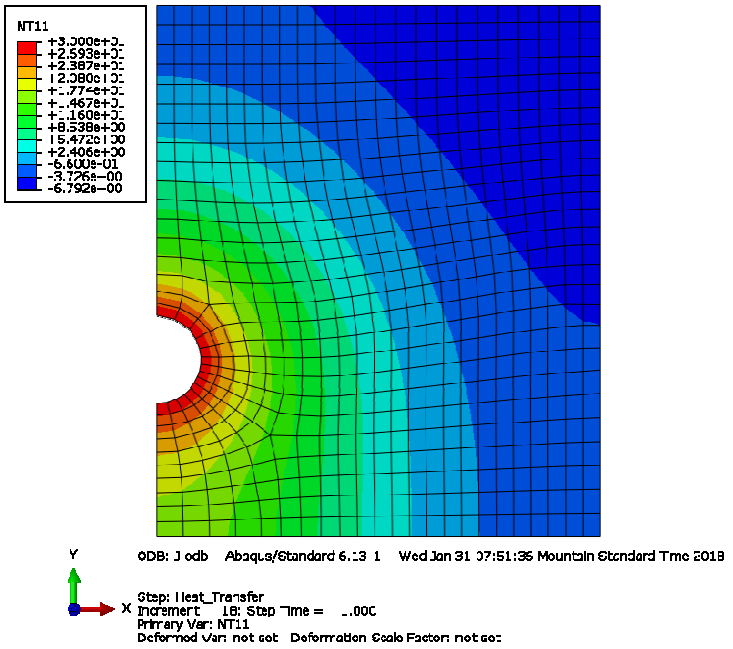

Figure 3.12 Temperature distribution in t=1h

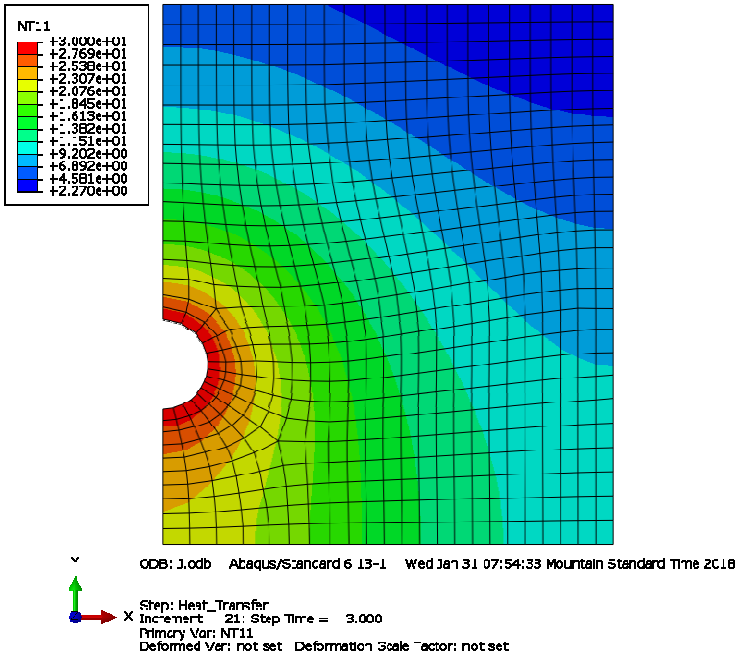

Figure 3.13 Temperature distribution in t=3h

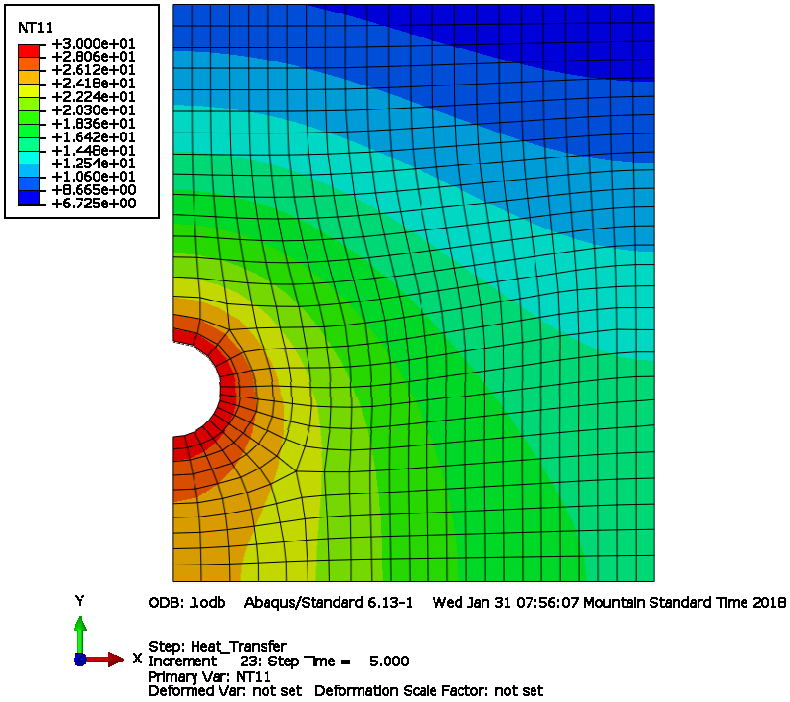

Figure 3.14 Temperature distribution in t=5h

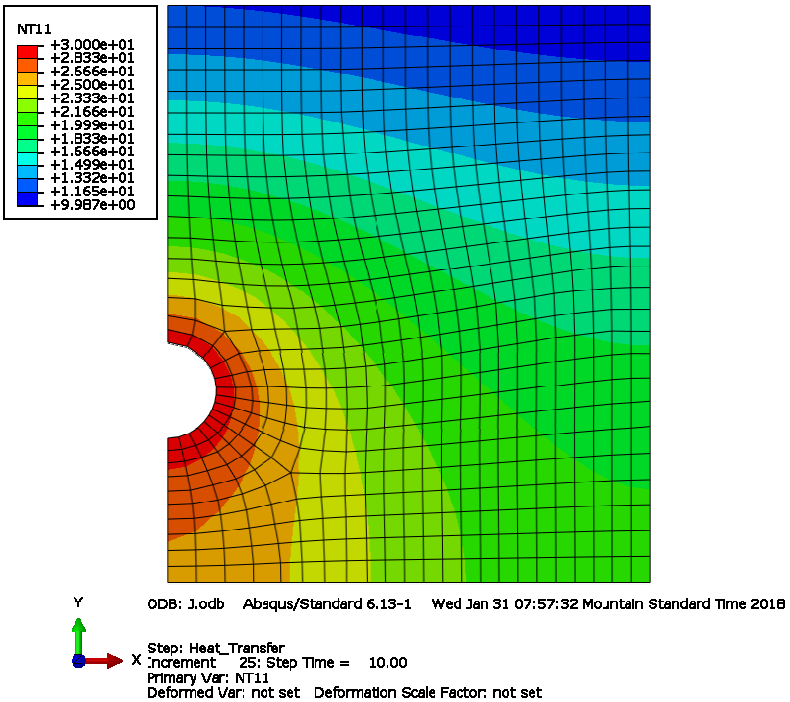

Figure 3.15 Temperature distribution in t=10h

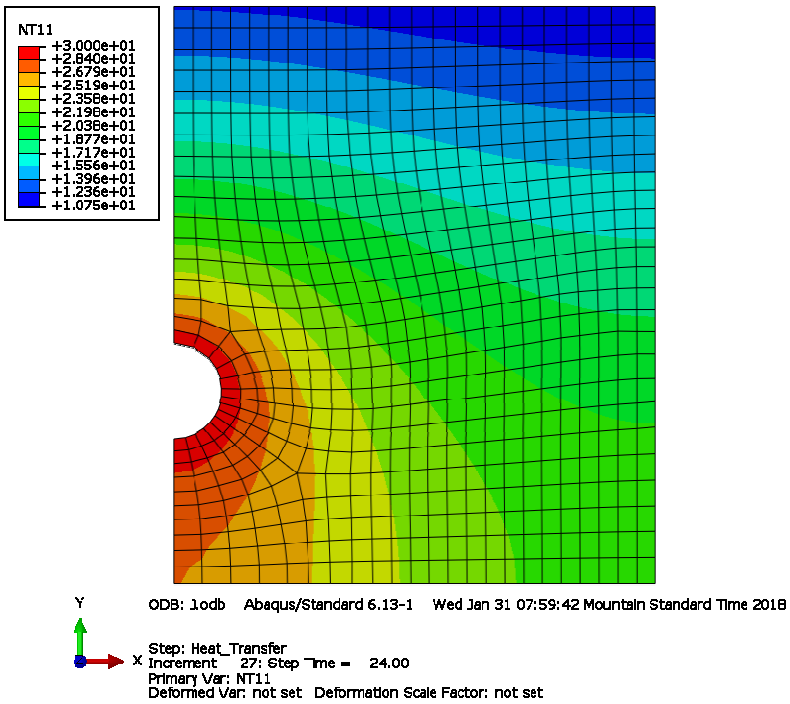

Figure 3.16 Temperature distribution in t=24h

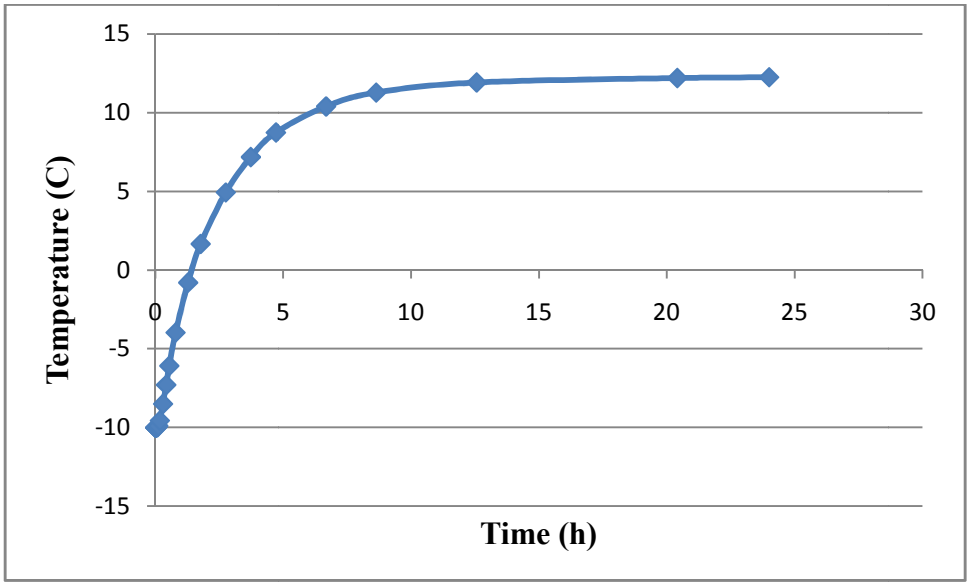

Figure 3.17 Temperature at point A in t=24h

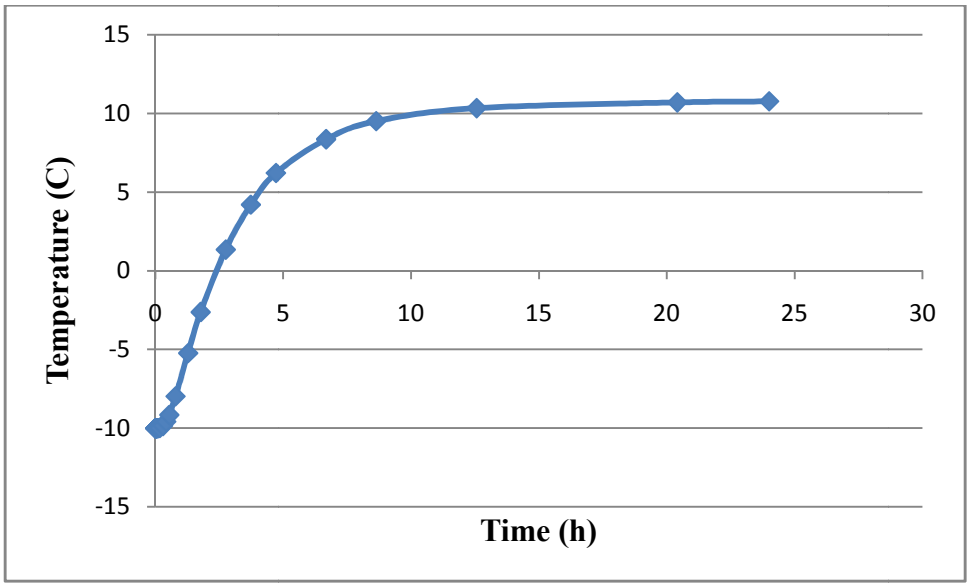

Figure 3.18 Temperature at point B in t=24h

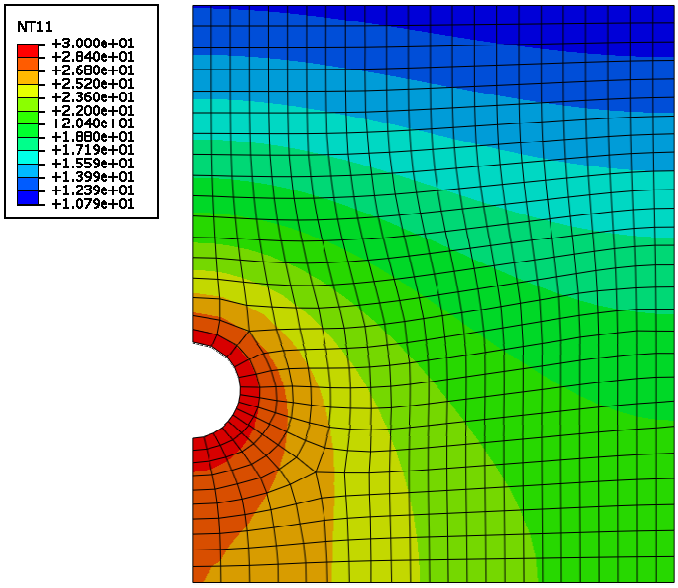

(a)

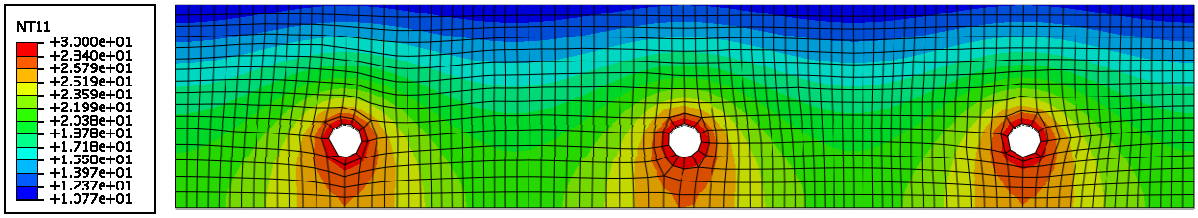

(b)

Figure 3.19 Temperature distribution in two cases: (a) analysis domain and (b) full domain

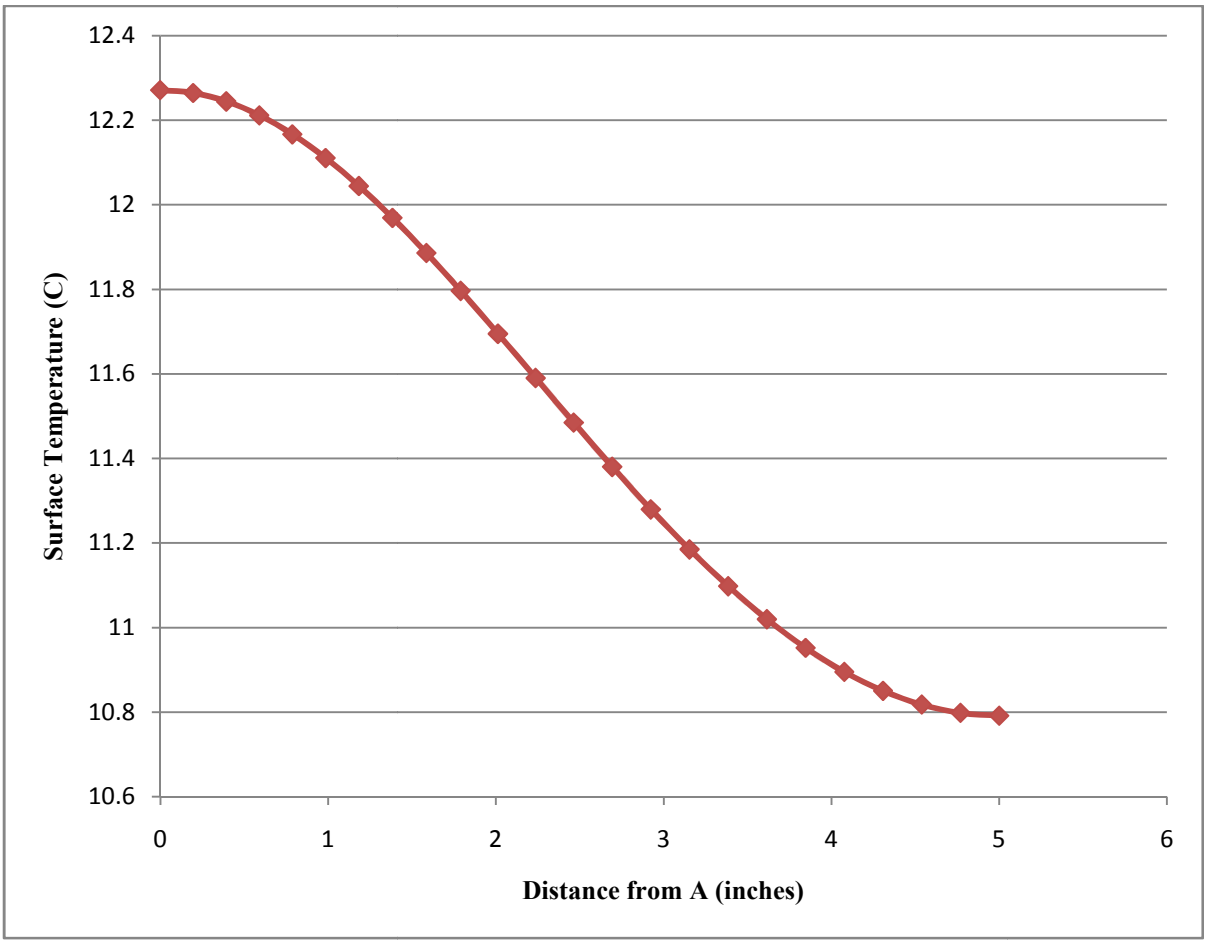

Figure 3.20 Surface temperature (steady-state)

3.2.3 THREE-DIMENSIONAL MODEL

Consider the Possion equation:

$$-\frac{\partial}{\partial x}\left(k_x\frac{\partial T}{\partial x}\right)-\frac{\partial}{\partial y}\left(k_y\frac{\partial T}{\partial y}\right)-\frac{\partial}{\partial z}\left(k_z\frac{\partial T}{\partial z}\right)=f(x,y,z)\quad in\quad \Omega$$

subjected to boundary conditions of the form

$$T=\hat{T}\ on\ \Gamma_1$$

$$k_x\frac{\partial T}{\partial x}n_x+k_y\frac{\partial T}{\partial y}n_z+k_z\frac{\partial T}{\partial z}n_x+\beta(T-T_\infty)=q_n\quad on\ \ \Gamma_2$$

$k_x, k_y\ and\ k_z$ are thermal conductivities of an isotropic solid. $f(x,y,z)$ is internal heat generation per unit volume in three-dimensional domain Ω as shown in Figure 3.21 (this is Q in the previous derivation) , $\hat{T}\ and\ q_n$ are specified functions of position on the portions $\Gamma_1\ and\ \Gamma_2$, respectively of the surface Γ of the domain while β is convection or film coefficient and T_∞ is ambient temperature. Figure 3.21 shows three-dimensional domain and typical finite element.

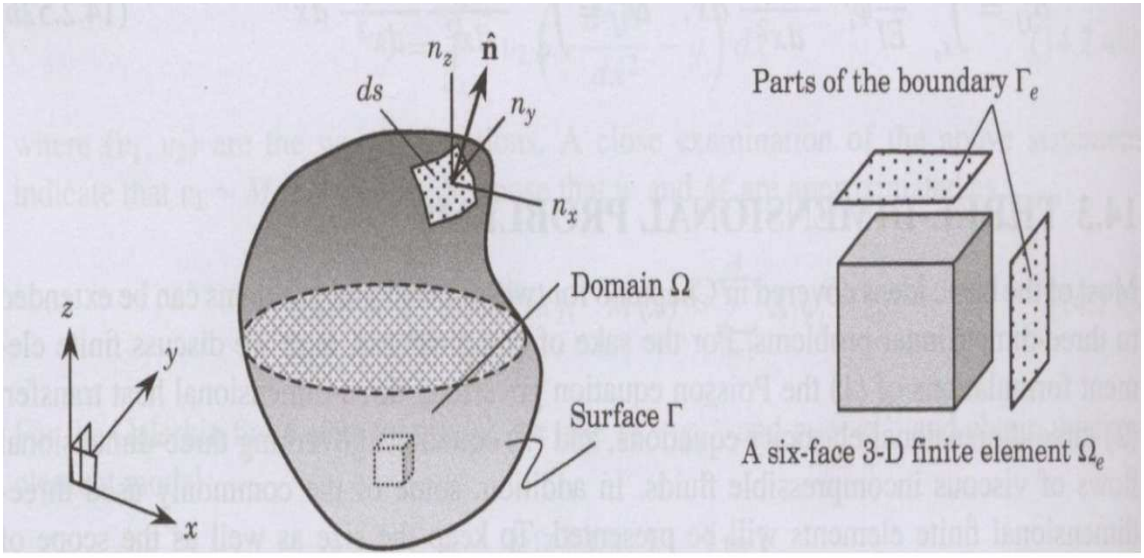

Figure 3.21 Three-dimensional (3D) domain and typical finite element [21]

The weak form over an element Ω_e is given by:

$$0 = \int_{\Omega^e}(k_x \frac{\partial w}{\partial x}\frac{\partial T}{\partial x} + k_y \frac{\partial w}{\partial y}\frac{\partial T}{\partial y} + k_z \frac{\partial w}{\partial z}\frac{\partial T}{\partial z} - wf)dxdydz$$

$$= \oint_{\Gamma^e} \beta wTds - \oint_{\Gamma^e} w[q_n + \beta T_\infty]ds$$

Assuming the finite element interpolation of a form:

$T = \sum_{j=1}^{n} T_j^e \psi_j^e(x, y, z)$ and $w = \psi_i^e(x, y, z)$ over an element Ω_e

The finite element model can be obtained:

$$(K_{ij}^e + H_{ij}^e)T_j^e = f_i^e + P_i^e + Q_i^e$$

where:

$$K_{ij}^e = \int_{\Omega^e}(k_x \frac{\partial \psi_i}{\partial x}\frac{\partial \psi_j}{\partial x} + k_y \frac{\partial \psi_i}{\partial y}\frac{\partial \psi_j}{\partial y} + k_z \frac{\partial \psi_i}{\partial z}\frac{\partial \psi_j}{\partial z})dxdydz$$

$$H_{ij}^e = \beta \oint_{\Gamma^e} \psi_i \psi_j ds$$

$$f_i^e = \int_{\Omega^e} f\psi_i \, dxdy$$

$$P_i^e = \oint_{\Gamma^e} \psi_i q_n \, ds$$

$$Q_i^e = \oint_{\Gamma^e} \psi_i \beta T_\infty ds$$

There are two new terms H_{ij}^e and Q_i^e. These coefficients can only be computed for elements and boundaries subjected to convection boundary condition. The numerical integration of volume and surface integrals is carried out in the same way as the above two-dimensional finite element model.

3.2.4 THREE-DIMENSIONAL NUMERICAL RESULTS

Consider the same concrete slab exposed to same weather condition. The results can be obtained from ABAQUS simulation.

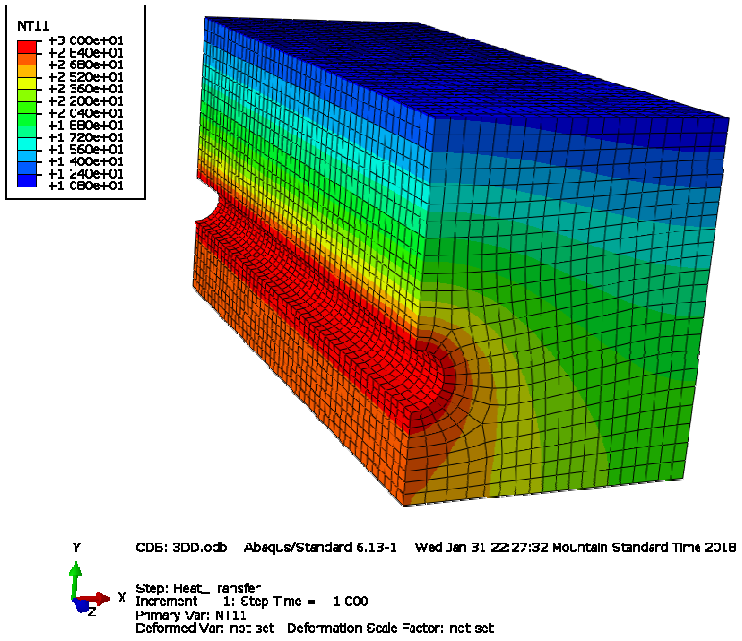

Figure 3.22 Three-dimensional temperature distribution (steady-state)

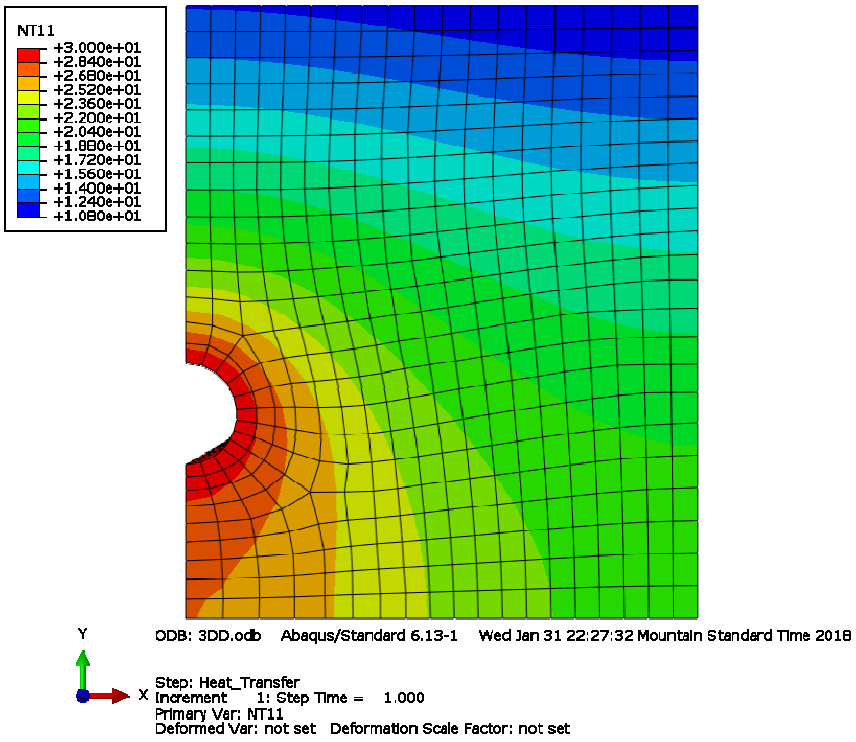

Figure 3.23 Temperature distribution in XY plane

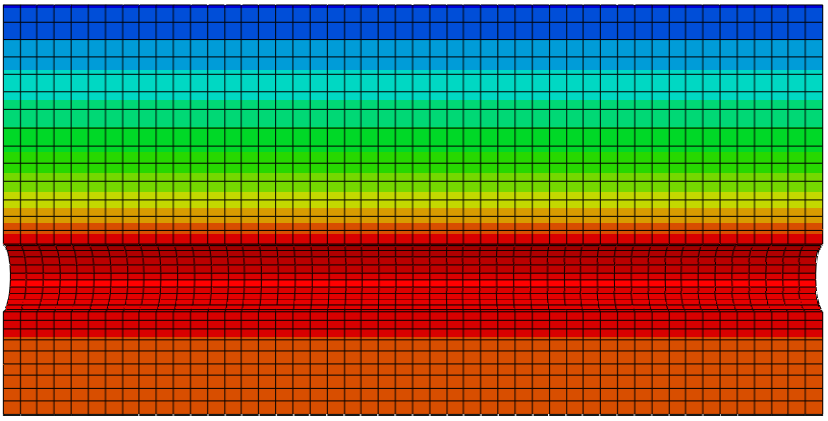

Figure 3.24 Temperature distribution in YZ plane

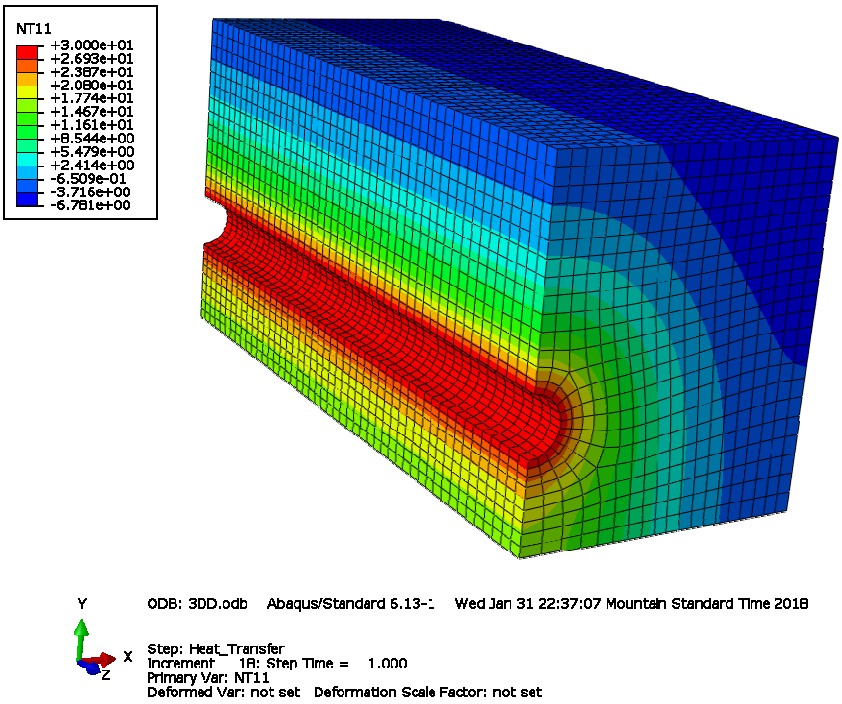

Figure 3.25 Temperature distribution in t=1h

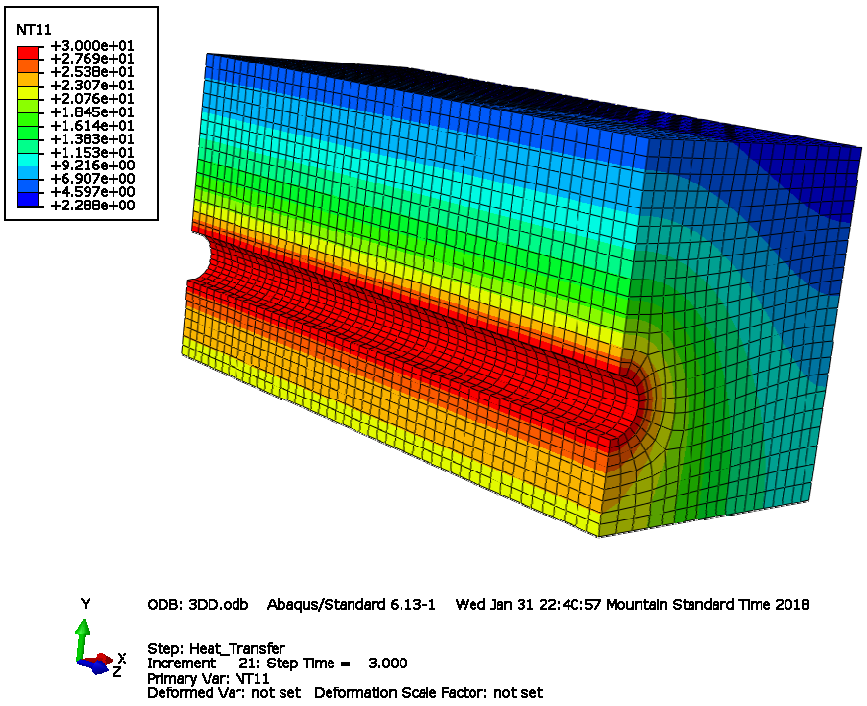

Figure 3.26 Temperature distribution in t=3h

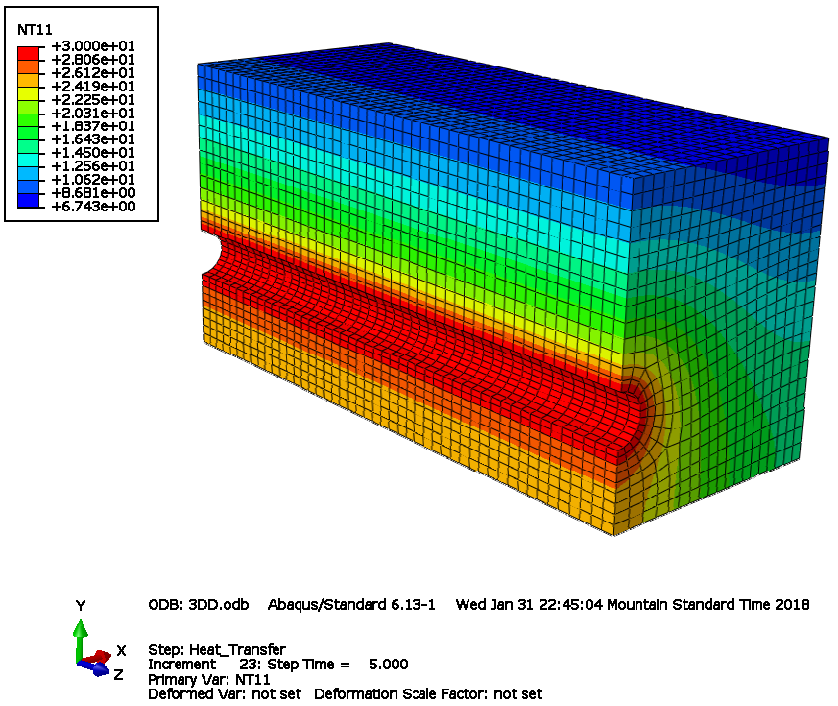

Figure ***3.27*** Temperature distribution in t=5h

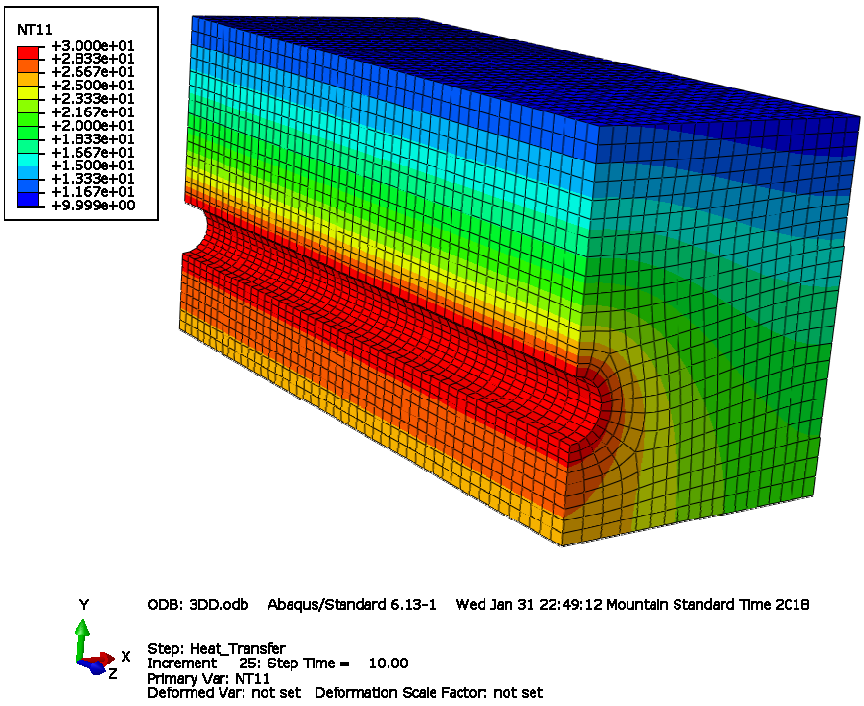

Figure 3.28 Temperature distribution in t=10h

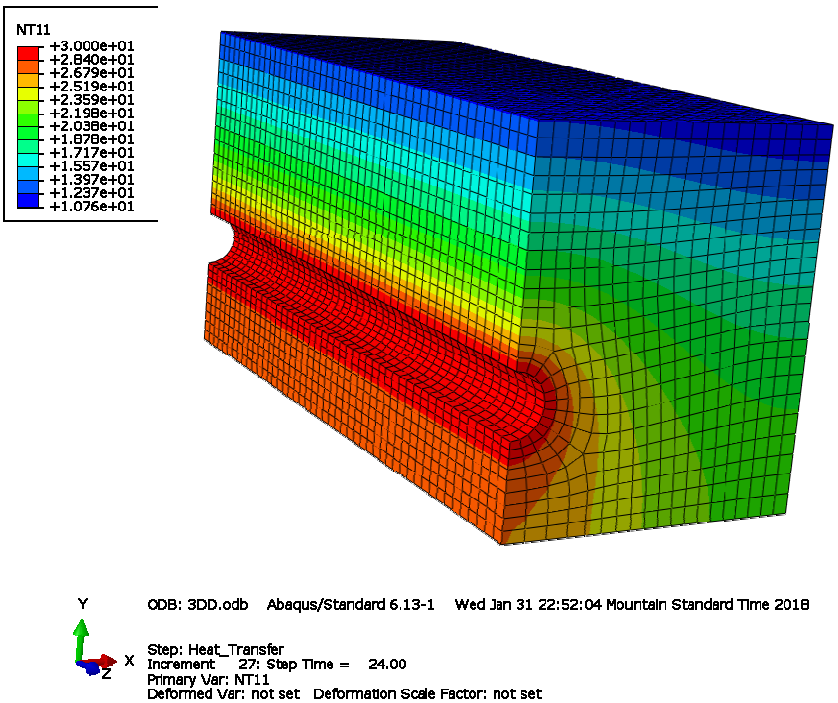

Figure 3.29 Temperature distribution in t=24h

3.3 CONLUSIONS

As expected, the surface temperature distribution is not uniform as it shows the sine/cosine form (Figure 3.19 and Figure 3.20). The maximum surface temperature is above the heated pipe (point A) whereas the minimum temperature is at the midway between the two adjacent pipes (point B). Pavement surface deicing was achieved when the lowest temperature was above 0^0C (or 33^0F - suggested by The American Society of Heating, Refrigerating and Air Conditioning Engineers or ASHARE). Hence, the main focus is the change in the lowest temperature of the concrete slab surface (at point B).

From the transient analyses (Figure 3.12 - Figure 3.18), the melting speed in the initial stages is remarkably fast and then becomes slow. This could be attributed to the fact that heat transfer gradually develops from the unsteady-state to a steady-state after a period of heating.

In general, the temperature variation of concrete surface can be categorized into four sub-stages: the starting stage, linear stage and accelerated stage and stable stage.

(i) During the starting period, the temperature increases very slowly due to the low ambient temperature at $t = 0$ ($T_0(x, y, z)$ is low). However, this stage occurs in short period of time.

(ii) The surface temperature then increases linearly with heating time as a result of the improvement in the heat transfer process (when surface temperatures become higher).

(iii) As the surface temperature reaches a relatively high temperature (over the melting point - 0^0C), the accelerated period begins and surface temperature rises exponentially. This can be attributed to the fact that the thermal energy generated by conduction is much higher than energy dissipated by convection. In other words, the absorbed thermal energy by conduction dominates the dissipated energy by convection.

(iv) The heat transfer process develops to the stable state (or steady state) when concrete surface absorbs most of the thermal energy transferred from heating source (fluid temperature).

The slope of temperature curve at point A is higher compared to point B, indicating that the temperature change at point A is faster than that of point B. Point A is closer to the heating source (heated pipe) then point B, resulting in the higher absorbed energy. Consequently, the surface areas near the pipe get melted first because of higher surface temperature. Then the surface temperatures at some locations far away from the pipe (i.e at point B) get higher after a period of time and hence the snow is fully melted.

From the three-dimensional analyses (Figure 3.22- Figure 3.29), it is apparent that three-dimensional results and two-dimensional results are similar for both cases: steady-state and transient. In other words, if three-dimensional domain is "sliced" in the z direction, the same results can be obtained for all slices. Therefore, two-dimensional model is good enough for future analysis throughout this research.

CHAPTER 4 - PARAMETRIC STUDY

From the derivation of differential equations in the previous chapter, it can be observed that thermal energy can be divided into two parts in the heat transfer process of the snow melting system:

(i) Part of the energy is absorbed by the concrete slab via conduction from the heating source (fluid temperature). In other words, thermal energy (heat) is transferred from the heating source to increase the temperature in the concrete slab by conduction.

(ii) The other energy portion is dissipated from the concrete slab to the ambient environment by convection due to the air movement near the concrete surface.

It is reasonable to categorize system parameters into two types: internal working conditions and external working conditions. The temperature within concrete slab depends upon several variables: internal working conditions including pipe depth D_1, pipe spacing D_2, fluid temperature T_f, pipe diameter d and external working conditions (or weather conditions) include ambient temperature T_∞ and wind velocity (v).

The objective of the parametric study undertaken in this research is to investigate the effects of these parameters. The parametric study allows us to systematically determine the key parameters for the performance of hydronic sytem. The approach for parametric study is to vary one parameter while holding other parameters constant to investigate the sensitivity of that parameter and to assess the impact that changing that parameter can have on the snow melting performance (i.e surface temperature, idling time).

The finite element method background from the previous chapter allows us perform the analysis in both cases: steady-state and transient. Consequently, typical values for these parameters will be proposed to optimize future construction, design and field experiments.

4.1 INTERNAL WORKING CONDITIONS

Consider the same concrete slab exposed to ambient temperature as the previous chapter. The system parameters for internal working conditions include pipe depth, pipe spacing, fluid temperature and pipe diameter. The table below shows inputs and ranges for the analysis.

Table 4.1 System parameters for internal working conditions

Parameters	Values
Fluid temperature $(T_f - C/F)$	$25^0C/77^0F$, $35^0C/95^0F$, $45^0C/113^0F$,$55^0C/131^0F$
Pipe diameter $(d - in)$	$0.5 - 0.625 - 0.75 - 1$
Pipe depth $(D_1 - in)$	$2 - 3 - 4 - 5$
Pipe spacing $(D_2 - in)$	$6 - 9 - 12 - 15$

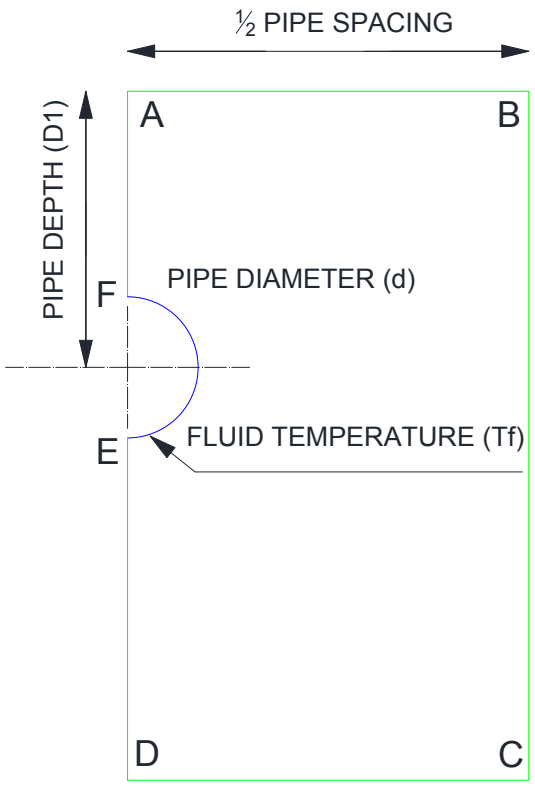

Figure 4.1 Two-dimensional (2D) analysis domain

4.1.1 PIPE DEPTH

Four depths are selected for this study ($D_1 = 2", 3", 4", 5"$). The depths are measured from the center of pipes to the concrete surface. All ABAQUS simulation inputs and ranges are summarized in the table below.

Table 4.2 System parameters for pipe depth analysis

Parameters	Values
Slab thickness (in)	6
Thermal conductivity $(k - \frac{W}{in.C})$	0.062
Specific heat $(c - \frac{Wh}{kg.C})$	0.3
Mass density $(\rho - \frac{kg}{in^3})$	0.039
Fluid temperature $(T_f - C\ or\ F)$	$30^0C/86^0F$
Ambient temperature $(T_\infty - C\ or\ F)$	$-10^0C/14^0F$
Convection coefficient$(\beta - \frac{W}{in^2.h.C})$	0.009
Initial condition $T(x, y, z, t = 0)$	$-10^0C/14^0F$
Pipe diameter $(d - in)$	0.75
Pipe spacing $(D_2 - in)$	10
Pipe depth $(D_1 - in)$	$2 - 3 - 4 - 5$

Table 4.3 Surface temperature distribution (in degree Celsius) with different depths

Distance (inches)	T (D1=2")	T (D1=3")	T (D1=4")	T (D1=5")
0	17.7358	14.0342	11.4639	9.22846
0.5	17.4414	13.9411	11.4229	9.20684
1	16.7481	13.6824	11.3075	9.14552
1.5	15.8563	13.3081	11.1344	9.0518
2	14.9273	12.879	10.9261	8.93634
2.5	14.0882	12.4514	10.7067	8.81149
3	13.3893	12.0652	10.4981	8.68971
3.5	12.8473	11.746	10.3187	8.5823
4	12.4637	11.5091	10.1813	8.49855
4.5	12.2356	11.3632	10.0953	8.44532
5	12.1599	11.3126	10.0659	8.4268

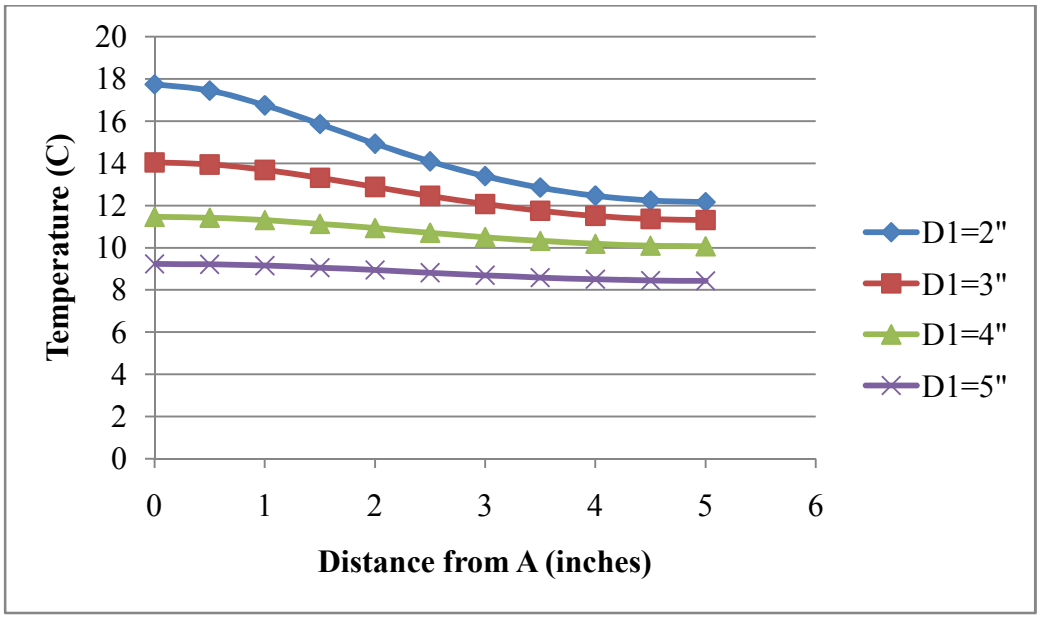

Figure 4.2 Surface temperature distribution with different depths

Table 4.4 Temperature difference with different depths

D1 (inches)	$\Delta T(C)$
2	5.5759
3	2.7216
4	1.398
5	0.80166

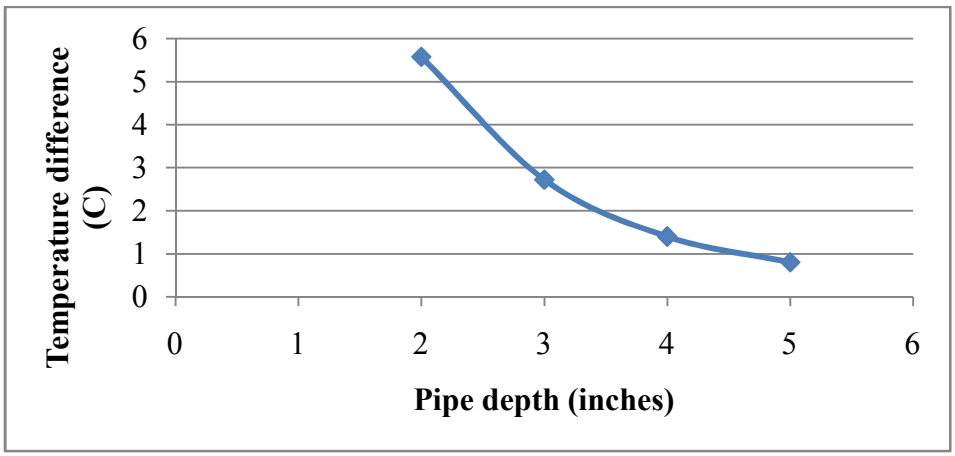

Figure 4.3 Temperature difference with different depths

Table 4.5 Temperature at B (t=10h) with different depths

D1=2"		D1=3"		D1=4"		D1=5"	
t (h)	**T (C)**	**t (h)**	**T (C)**	**t (h)**	**T (C)**	**t (h)**	**T (C)**
0	-10	0	-10	0	-10	0	-10
1.00E-03	-10	1.00E-03	-10	1.00E-03	-10	1.00E-03	-10
2.00E-03	-10	2.00E-03	-10	2.00E-03	-10	2.00E-03	-10
3.00E-03	-10	3.00E-03	-10	3.00E-03	-10	3.00E-03	-10
5.00E-03	-10	5.00E-03	-10	5.00E-03	-10	5.00E-03	-10
7.00E-03	-10	7.00E-03	-10	7.00E-03	-10	7.00E-03	-10
1.10E-02	-10	1.10E-02	-10	1.10E-02	-10	1.10E-02	-10
1.90E-02	-10	1.50E-02	-10	1.50E-02	-10	1.50E-02	-10
2.70E-02	-10	2.30E-02	-10	2.30E-02	-10	2.30E-02	-10
4.30E-02	-9.99998	3.90E-02	-10	3.90E-02	-10	3.89E-02	-10
7.50E-02	-9.99866	5.50E-02	-9.99998	5.50E-02	-10	5.48E-02	-10
1.07E-01	-9.99357	8.70E-02	-9.99923	8.70E-02	-9.9998	7.07E-02	-10
1.71E-01	-9.9417	1.51E-01	-9.98129	1.51E-01	-9.99292	1.03E-01	-9.9999
2.99E-01	-9.58852	2.15E-01	-9.9313	2.15E-01	-9.97099	1.34E-01	-9.9996
4.27E-01	-9.01357	3.43E-01	-9.64835	3.43E-01	-9.81515	1.98E-01	-9.9945
6.83E-01	-7.46684	5.99E-01	-8.53656	4.71E-01	-9.52982	2.62E-01	-9.9799
9.39E-01	-5.84413	8.55E-01	-7.1496	7.27E-01	-8.56362	3.89E-01	-9.8767
1.451	-2.99951	1.367	-4.31627	9.83E-01	-7.36767	6.44E-01	-9.327
2.475	1.05449	1.879	-1.77405	1.495	-4.82598	8.98E-01	-8.511
3.499	3.96368	2.903	1.97314	2.48455	-7.82E-01	1.40745	-6.4912
4.523	6.08445	3.927	4.6637	3.4741	2.26016	2.4259	-2.8227
6.571	8.56696	5.96918	7.63657	4.46365	4.47692	3.44435	7.92E-02
8.619	10.0318	8.01136	9.28029	6.44274	6.96074	4.4628	2.27074
10	10.7059	10	10.1756	8.42184	8.34277	6.4997	4.84687
				10	9.01528	8.5366	6.34769
						10	7.05813

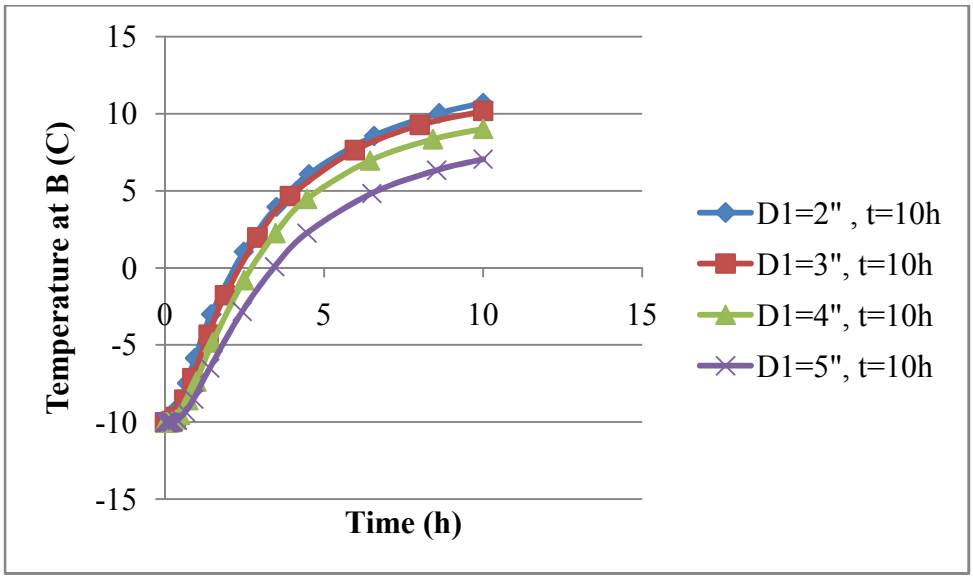

Figure 4.4 Temperature at B (t=10h) with different depths

Table 4.6 Heating rates at B with different depths

At point B	
D1 (inches)	**Heating rate (C/h)**
2	2.07059
3	2.01756
4	1.901528
5	1.705813

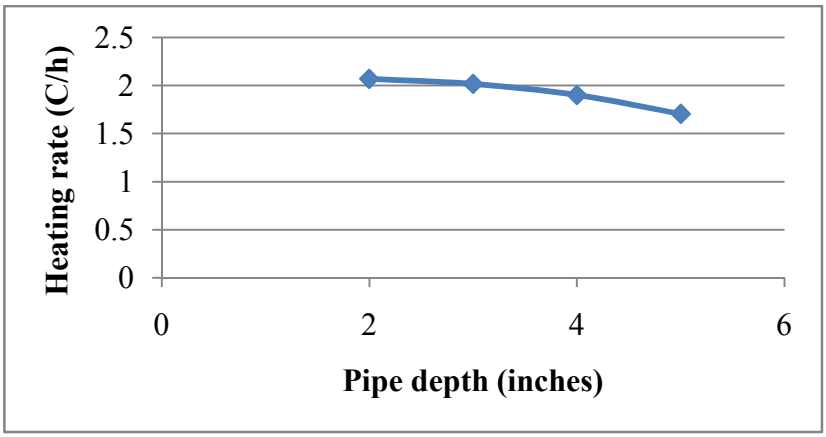

Figure 4.5 Heating rates at B with different depths

As the pipe depth increases, the surface temperature decreases and the temperature difference between point A and point B (ΔT) gets smaller (Figure 4.2 and Figure 4.3). Therefore, the temperature distribution curve is gradually flattening and becomes smoother and smoother. This can be explained by the fact that the shallower the pipe depth is, the more energy the concrete surface gets, regardless of the change in other variables.

Transient analyses were also performed to investigate the effects of pipe depth combined with heating time (t=10h) on surface temperature (at point B):

(i) As the pipe depth increases, it takes more time to transfer thermal energy from the heating pipes to the concrete surface. Figure 4.4 and Figure 4.5 show that the heating rate also gets smaller as the depth increases.

(ii) There are relatively no differences at the initial state of the snow melting process. This is attributed to the fact that when heating time is not long enough, the transferred energy is also small which does not have much effect on the surface temperature. The situation is changed when the heating time is long enough as the temperature at B increases significantly when the pipe depth gets smaller.

Increasing the pipe depths from 2" to 5" results in the decrease of temperature at B from 12.16^0C to 8.43^0C. In other words, increasing pipe depths by 1% results in the decrease of temperature (at B) by 0.204%. Also, by varying the pipe depths from 2" to 5", the heating rate decreases approximately 17.4%, from $2.07^0C/h$ to $1.71^0C/h$. Therefore, the heating rate will decrease approximately 0.116% when increasing the pipe depths by 1%. Notice that the relationship between surface temperature or heating rate at B and pipe depth varies linearly. Therefore, linear interpolations are performed to achieve above numerical evaluations.

From the above results and discussions, it is concluded that pipe depth is an important parameter. However, practically, shallow embedded pipes are exposed to more risk of damage including cracking under different loads. Additionally, the embedded pipes usually lay over the wire mesh or rebar which is about 2" from the bottom surface in practice. Hence, pipe depth can be considered as a fixed parameter for future design.

4.1.2 PIPE DIAMETER

This section presents the effects of pipe diameters on the snow melting performance. As mentioned previously, the pipe thickness is neglected for simplicity. Four diameters are selected for this study ($d = 0.5", 0.625", 0.75", 1"$). All fixed inputs are summarized in the table below.

Table 4.7 System parameters for pipe diameter analysis

Parameters	Values
Slab thickness (in)	6
Thermal conductivity $(k - \frac{W}{in.C})$	0.062
Specific heat$(c - \frac{Wh}{kg.C})$	0.3
Mass density $(\rho - \frac{kg}{in^3})$	0.039
Fluid temperature $(T - \ C \ or \ F)$	$30^0C/86^0F$
Ambient temperature $(T_\infty - \ C \ or \ F)$	$-10^0C/14^0F$
Convection coefficient $(\beta - \frac{W}{in^2.h.C})$	0.009
Initial condition $T(x, y, z, t = 0)$	$-10^0C/14^0F$
Pipe depth $(D_1 - in)$	4
Pipe spacing $(D_2 - in)$	10
Pipe diameter $(d - in)$	$0.5 - 0.625 - 0.75 - 1$

Table 4.8 Surface temperature distribution with different diameters

Distance (inches)	T (d=0.5")	T (d=0.625")	T (d=0.75")	T (d=1")
0	10.4816	10.9918	11.463	12.279
0.5	10.4431	10.952	11.4226	12.2358
1	10.335	10.8403	11.308	12.1135
1.5	10.1724	10.6725	11.1353	11.9296
2	9.97667	10.4706	10.9273	11.7086
2.5	9.77033	10.2579	10.708	11.4769
3	9.57392	10.0557	10.4995	11.2563
3.5	9.4048	9.8815	10.3199	11.0662
4	9.27531	9.74815	10.1828	10.9227
4.5	9.19422	9.66465	10.097	10.8319
5	9.16651	9.63612	10.0678	10.799

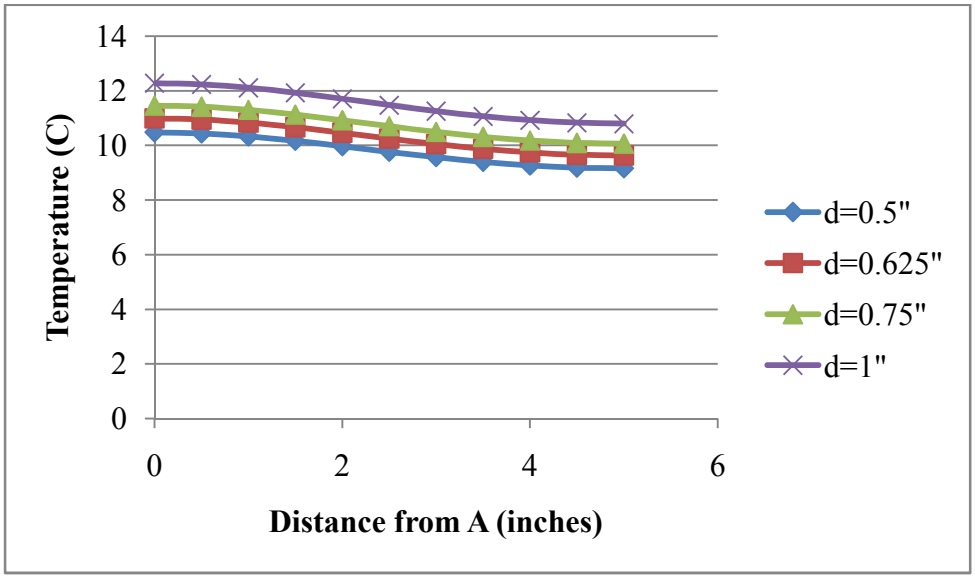

Figure 4.6 Surface temperature distribution with different diameters

Table 4.9 Temperature difference with different diameters

d (inches)	$\Delta T(C)$
0.5	1.31509
0.625	1.35568
0.75	1.3952
1	1.48

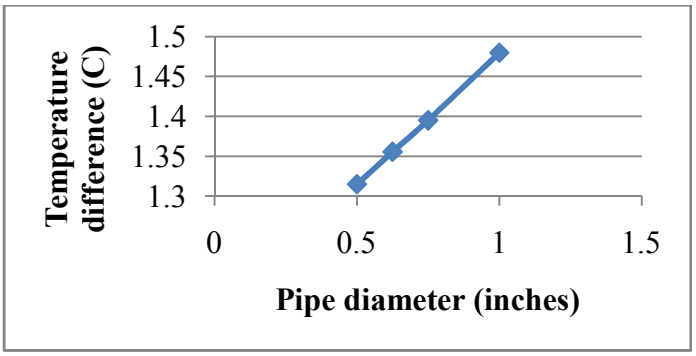

Figure 4.7 Temperature difference with different diameters

Table 4.10 Temperature at B (t=10h) with different diameters

d=0.5"		d=0.625"		d=0.75"		d=1"	
t (h)	T (C)	t (h)	T (C)	t (h)	T (C)	t (h)	T (C)
0	-10	0	-10	0	-10	0	-10
1.00E-03	-10	5.92E-04	-10	1.00E-03	-10	1.00E-03	-10
2.00E-03	-10	1.18E-03	-10	2.00E-03	-10	2.00E-03	-10
3.00E-03	-10	1.78E-03	-10	3.00E-03	-10	3.00E-03	-10
5.00E-03	-10	2.37E-03	-10	5.00E-03	-10	5.00E-03	-10
9.00E-03	-10	3.55E-03	-10	7.00E-03	-10	7.00E-03	-10
1.30E-02	-10	5.92E-03	-10	1.10E-02	-10	1.10E-02	-10
2.10E-02	-10	8.29E-03	-10	1.50E-02	-10	1.50E-02	-10
2.90E-02	-10	1.30E-02	-10	2.30E-02	-10	2.30E-02	-10
4.50E-02	-10	1.78E-02	-10	3.90E-02	-10	3.90E-02	-10
7.70E-02	-9.99992	2.73E-02	-10	5.50E-02	-10	5.50E-02	-10
1.09E-01	-9.9995	4.62E-02	-10	8.70E-02	-9.99979	8.70E-02	-9.9997
1.73E-01	-9.99214	6.52E-02	-10	1.51E-01	-9.99285	1.51E-01	-9.9902
3.01E-01	-9.90352	1.03E-01	-9.9995	2.15E-01	-9.97079	2.15E-01	-9.9608
4.29E-01	-9.71458	1.79E-01	-9.9866	3.43E-01	-9.81449	3.43E-01	-9.7623
6.85E-01	-8.9805	2.55E-01	-9.949	4.71E-01	-9.52863	4.71E-01	-9.4091
9.41E-01	-8.01186	4.06E-01	-9.7199	7.27E-01	-8.56154	7.27E-01	-8.2592
1.453	-5.8202	7.00E-01	-8.7786	9.83E-01	-7.36497	9.83E-01	-6.8718
1.965	-3.70709	9.94E-01	-7.5413	1.495	-4.82276	1.495	-4.0219
2.989	-3.50E-01	1.28837	-6.1774	2.48409	-7.80E-01	2.007	-1.4452
4.013	2.18178	1.87634	-3.5547	3.47317	2.2615	3.031	2.32387
6.061	5.13856	3.04926	4.08E-01	4.46226	4.47797	4.055	4.97058
8.109	6.84744	4.22218	3.23527	6.44043	6.96181	6.103	7.7587
10	7.7871	5.3951	5.21048	8.4186	8.34402	8.151	9.21542
		7.74094	7.3029	10	9.01772	10	9.93429
		10	8.38495				

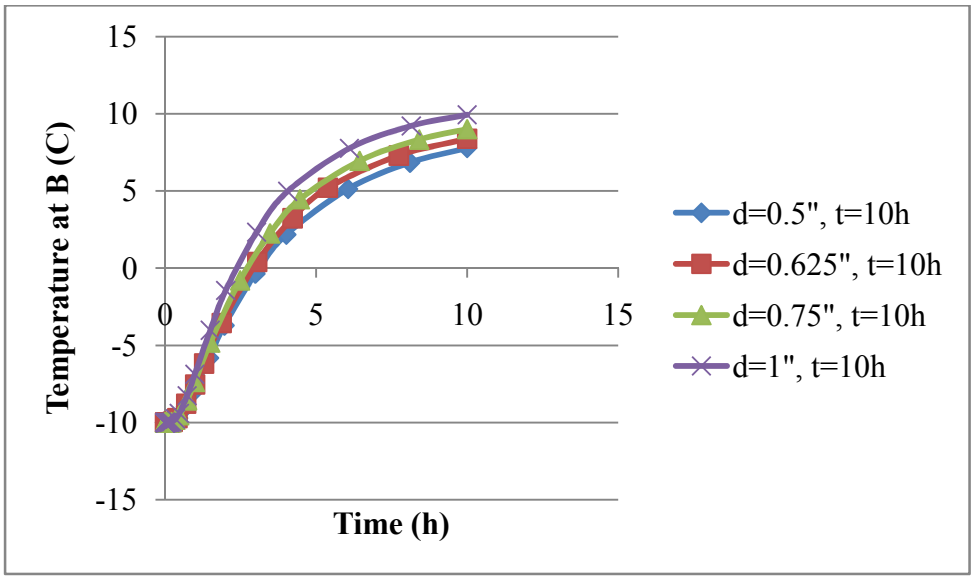

Figure 4.8 Temperature at B (t=10h) with different diameters

Table 4.11 Heating rates at B with different diameters

At point B	
d (inches)	**Heating rate (C/h)**
0.5	1.77871
0.625	1.838495
0.75	1.901772
1	1.993429

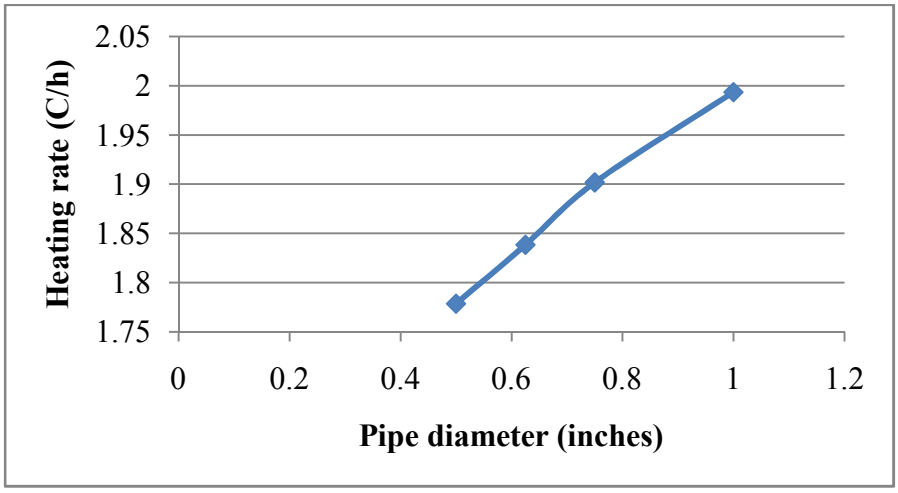

Figure 4.9 Heating rates at B with different pipe diameters

Figure 4.6 illustrates the relationship between surface temperature and pipe diameter, it can be observed that:

(i) Surface temperature increases as the pipe diameter increases.

(ii) The surface temperature distribution curves obtained at difference diameters are approximately parallel to one another as opposed to the pipe depth cases when the curves become smoother and smoother as the depth increases.

(iii) These curves are close one another. This can also be inferred from Figure 4.7 showing the relationship between temperature difference (point A and B) and pipe diameter. Increasing the diameter improves the temperature difference, however the rate of change is relatively slow.

More specifically, by increasing the diameters from 0.5" to 1", temperature at B increases from 9.17^0C to 10.8^0C and heating rate (at B) increases from $1.32^0C/h$ to $1.48^0C/h$. In other words, increasing the pipe diameters by 1% results in an increase of temperature (at B) by 0.177% and an increase of heating rate (at B) by 0.11%. These indicate that the surface temperature is not very sensitive to the pipe diameter, indicating slight effects of pipe diameter on the snow melting process.

Figure 4.8 shows the relationship between the lowest temperature on the surface (at point B) and time during the transient analysis.

(i) These curves virtually coincide, suggesting the slight sensitivity of pipe diameter to the surface temperature. The heating rate increases as the pipe diameter increases, however the rate changes very slowly as shown in Figure 4.9.

(ii) It is reasonable to conclude that pipe diameter is not an important parameter for the snow melting system.

Practically, when the pipe diameter is large, there will be negative effects on the structural behaviors of the overall system. Hence, it is suggested that the diameter is about 0.75" for typical snow melting system in the U.S.

4.1.3 PIPE SPACING

This section examines the effects of pipe spacing on snow melting process of hydronic snow melting system and analyzes the results to evaluate the importance and recommended values of pipe spacing for future design, construction and experiments. Four distances are taken into consideration for the study ($D_2 = 6", 9", 12", 15"$). All input values and ranges are summarized in Table 4.12.

Table 4.12 System parameters for pipe spacing analysis

Parameters	Values
Slab thickness (in)	6
Thermal conductivity $(k - \frac{W}{in.C})$	0.062
Specific heat$(c - \frac{Wh}{kg.C})$	0.3
Mass density $(\rho - \frac{kg}{in^3})$	0.039
Fluid temperature $(T_f - C\ or\ F)$	$30^0C/86^0F$
Ambient temperature $(T_\infty - C\ or\ F)$	$-10^0C/14^0F$
Convection coefficient $\beta - \frac{W}{in^2.h.C}$	0.009
Pipe depth $(D_1 - in)$	4
Pipe diameter $(d - in)$	0.75
Initial condition $T(x, y, z, t = 0)$	$-10^0C/14^0F$
Pipe spacing $(D_2 - in)$	$6", 9", 12", 15"$

Table 4.13 Surface temperature distribution (in C) with different pipe distances

D2=6"		D2=9"		D2=12"		D2=15"	
Distance (inches)	**T(C)**	**Distance (inches)**	**T(C)**	**Distance (inches)**	**T(C)**	**Distance (inches)**	**T(C)**
0	13.5303	0	11.9222	0	10.6068	0	9.66704
3.00E-01	13.5252	4.50E-01	11.8934	6.00E-01	10.5313	7.50E-01	9.51772
6.00E-01	13.5117	9.00E-01	11.8143	1.2	10.319	1.5	9.10859
9.00E-01	13.4907	1.35	11.6955	1.8	10.0064	2.25	8.52897
1.2	13.4643	1.8	11.5512	2.4	9.63993	3	7.87787
1.5	13.4354	2.25	11.3964	3	9.26507	3.75	7.23793
1.8	13.4069	2.7	11.2479	3.6	8.91847	4.5	6.66634
2.1	13.3812	3.15	11.1191	4.2	8.62661	5.25	6.1982
2.4	13.361	3.6	11.0199	4.8	8.40755	6	5.85357
2.7	13.3483	4.05	10.9569	5.4	8.27227	6.75	5.64322
3	13.3433	4.5	10.9346	6	8.22647	7.5	5.57245

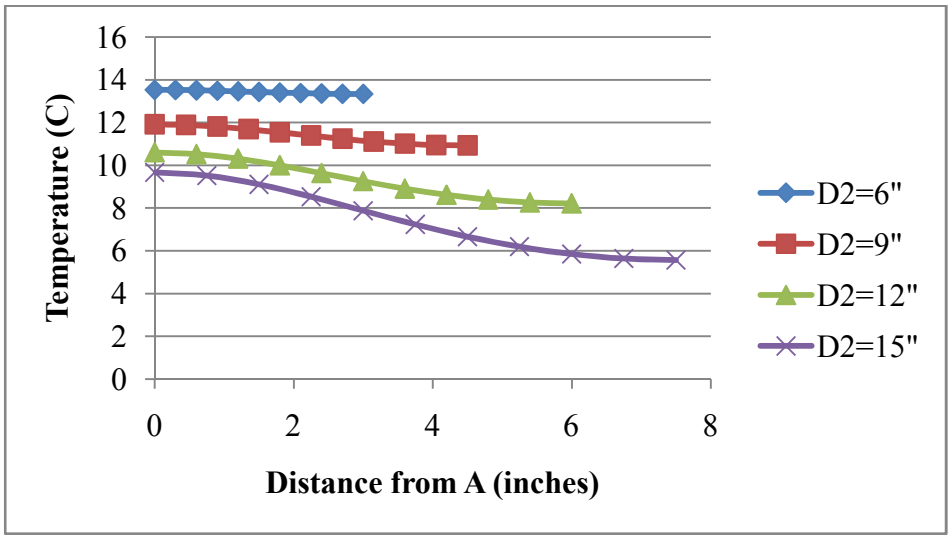

Figure 4.10 Surface temperature distribution with different pipe distances

Table 4.14 Temperature difference with different pipe distances

D2(inches)	ΔT(C)
6	0.187
9	0.9876
12	2.38033
15	4.09459

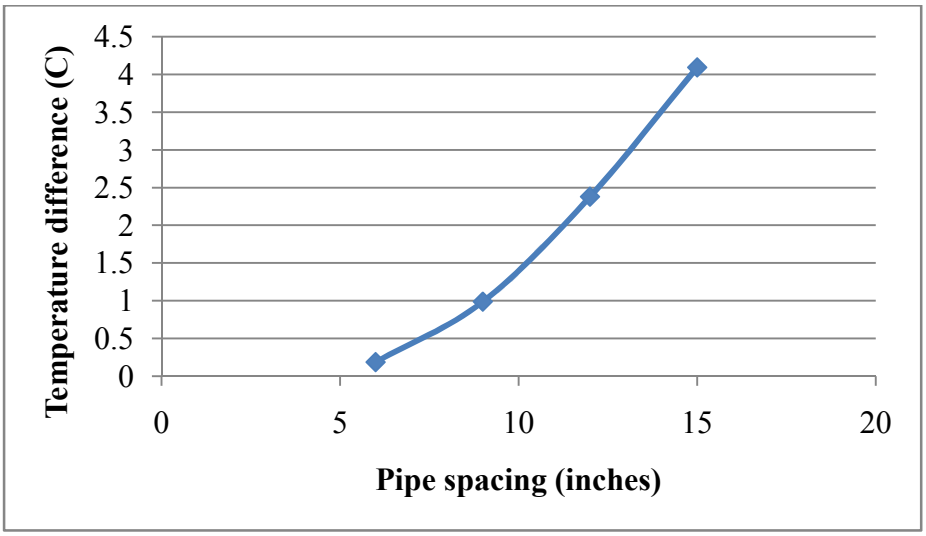

Figure 4.11 Temperature difference with different pipe distances

Table 4.15 Temperature at B (t=10h) with different pipe distances

D2=6"		D2=9"		D2=12"		D2=15"	
t (h)	T (C)	t (h)	T (C)	t (h)	T (C)	t (h)	T (C)
0	-10	0	-10	0	-10	0	-10
1.00E-03	-10	7.94E-04	-10	1.00E-03	-10	1.00E-03	-10
2.00E-03	-10	1.59E-03	-10	2.00E-03	-10	2.00E-03	-10
3.00E-03	-10	2.38E-03	-10	3.00E-03	-10	3.00E-03	-10
4.00E-03	-10	3.18E-03	-10	5.00E-03	-10	5.00E-03	-10
6.00E-03	-10	4.76E-03	-10	7.00E-03	-10	7.00E-03	-10
1.00E-02	-10	7.94E-03	-10	1.10E-02	-10	1.10E-02	-10
1.40E-02	-10	1.11E-02	-10	1.90E-02	-10	1.50E-02	-10
2.20E-02	-10	1.75E-02	-10	2.70E-02	-10	2.30E-02	-10
3.80E-02	-9.99996	3.02E-02	-10	4.30E-02	-10	3.90E-02	-10
5.40E-02	-9.99972	4.29E-02	-10	7.50E-02	-9.99999	5.50E-02	-10
8.60E-02	-9.99453	6.83E-02	-9.9999	1.07E-01	-9.9999	8.70E-02	-10
1.50E-01	-9.92001	1.19E-01	-9.99571	1.71E-01	-9.99751	1.51E-01	-9.99983
2.14E-01	-9.74982	1.70E-01	-9.98137	2.99E-01	-9.95518	2.15E-01	-9.99902
3.42E-01	-9.03096	2.72E-01	-9.86663	4.27E-01	-9.85062	3.43E-01	-9.98591
4.70E-01	-8.0399	4.66E-01	-9.27743	6.83E-01	-9.35764	4.71E-01	-9.95068
7.26E-01	-5.67258	6.61E-01	-8.4013	9.39E-01	-8.63613	7.27E-01	-9.74405
9.82E-01	-3.2939	8.55E-01	-7.34729	1.451	-6.81197	9.83E-01	-9.39629
1.238	-1.07078	1.24441	-5.07595	1.963	-4.93937	1.495	-8.33385
1.75	2.49979	2.02269	-1.16513	2.987	-1.78133	2.519	-5.91095
2.262	5.25936	2.80097	1.9077	4.011	6.92E-01	3.543	-3.69066

3.286	8.59456	3.57925	4.23915	6.059	3.71177	5.591	-5.49E-01
4.31	10.5708	5.13582	7.00871	8.107	5.5268	7.639	1.55882
6.358	12.2068	6.69238	8.63734	10	6.56242	9.687	2.94784
8.406	12.8786	9.80551	9.98576			10	3.14446
10	13.1249	10	10.0631				

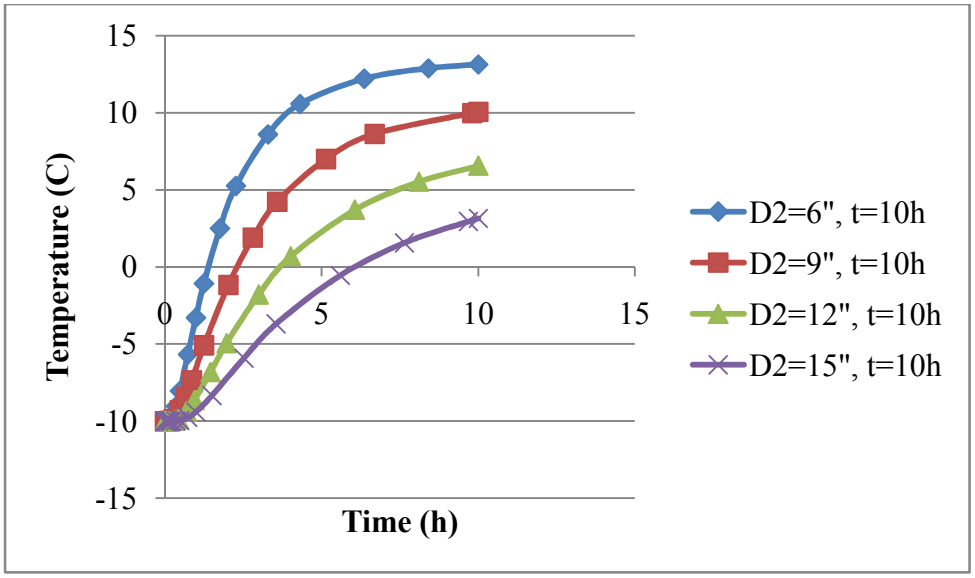

Figure 4.12 Temperature at B (t=10h) with different pipe distances

Table 4.16 Heating rate at B with different pipe distances

At point B	
D2 (inches)	**Heating rate (C/h)**
6	2.31249
9	2.00631
12	1.656242
15	1.314446

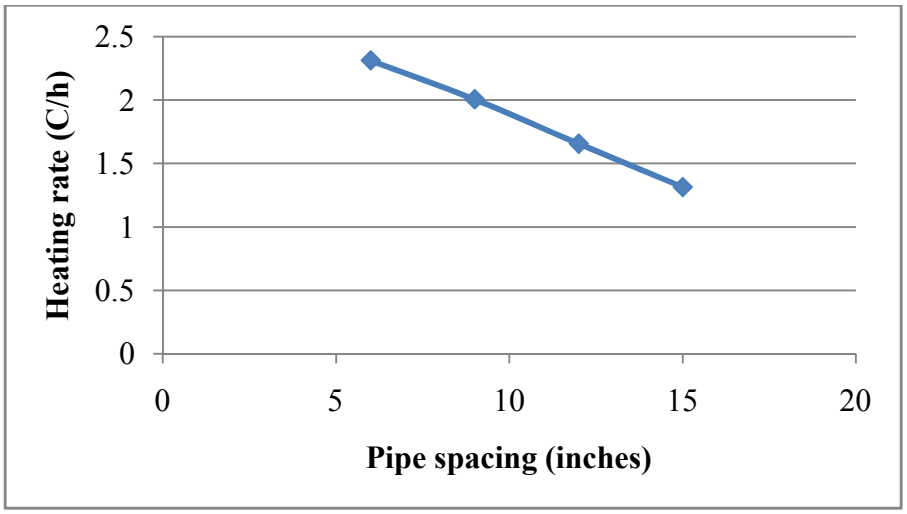

Figure 4.13 Heating rate at B with different pipe distances

As shown in Figure 4.10, by increasing the pipe spacing, the surface temperature decreases, resulting in the colder concrete surface. The effect of heating on surface temperature is smaller as the pipe location is far away from the thermal source (heating pipe).

It can also be seen from Figure 4.11 that the temperature difference between point A and B decreases when the spacing decreases. As a result, the heating curve becomes smoother and smoother as the pipe spacing decreases. The maximum temperature difference occurs when the pipe spacing reaches maximum value. However, when the distance is over 12", the temperature difference on the concrete surface is over 2^0C which does not meet the uniform temperature requirement for deicing and leads to "strips". Therefore, the recommended pipe spacing should be less than 12".

From the transient analysis, by increasing the distance, it takes longer to achieve a specific temperature, resulting in the large decrease of heating rate. This is illustrated by Figure 4.12 and Figure 4.13.

More specifically, by increasing the distances from 6" to 15", the temperature at B decreases by 58.3%, from 13.34^0C to 5.57^0C and heating rate (at B) decreases by 43.4%, from

$2.31^0C/h$ to $1.31^0C/h$. In other words, increasing the pipe diameters by 1% results in an increase of temperature and heating rate (at B) by 0.38% and 0.29%, respectively. These indicate that pipe spacing is an important parameter.

In practice, for a given configuration of a slab, the larger the distance is, the less number of pipes there are. However, closers pipes might result in segregation of aggregate of concrete during construction. Combining all the above analyses, pipe spacing should be around 6"-12".

4.1.4 FLUID TEMPERATURE

This section presents the effects of fluid temperature on the performance of snow melting process of the hydronically heated system. In this study, four fluid temperatures of $25^0C, 35^0C, 45^0C, 55^0C$ are taken into consideration. All fixed inputs are summarized in the Table 4.17.

Table 4.17 System parameters for fluid temperature analysis

Parameters	Values
Slab thickness (in)	6
Thermal conductivity $(k - \frac{W}{in.C})$	0.062
Specific heat$(c - \frac{Wh}{kg.C})$	0.3
Mass density $(\rho - \frac{kg}{in^3})$	0.039
Ambient temperature $(T_\infty - \ C \ or \ F)$	$-10^0C/14^0F$
Convection coefficient $(\beta - \frac{W}{in^2.h.C})$	0.009
Pipe depth $(D_1 - in)$	4
Pipe diameter $(d - in)$	0.75
Initial condition $T(x, y, z, t = 0)$	$-10^0C = 14^0F$
Pipe spacing $(D_2 - in)$	10"
Fluid temperature $(T_f - \ C \ or \ F)$	$25^0C, 35^0C, 45^0C, 55^0C$

Table 4.18 Surface temperature distribution (in C) with different T_f

Distance (inches)	$T_f = 25^0C$	$T_f = 35^0C$	$T_f = 45^0C$	$T_f = 55^0C$
0	8.77739	14.1424	19.5073	24.8723
0.5	8.73995	14.0942	19.4485	24.8028
1	8.63982	13.9655	19.2911	24.6168
1.5	8.48992	13.7728	19.0556	24.3384
2	8.30724	13.5379	18.7685	23.9992
2.5	8.11531	13.2911	18.4669	23.6427
3	7.93247	13.056	18.1796	23.3032
3.5	7.7746	12.8531	17.9315	23.01
4	7.65628	12.7009	17.7456	22.7902
4.5	7.58265	12.6063	17.6299	22.6535
5	7.55514	12.5709	17.5867	22.6024

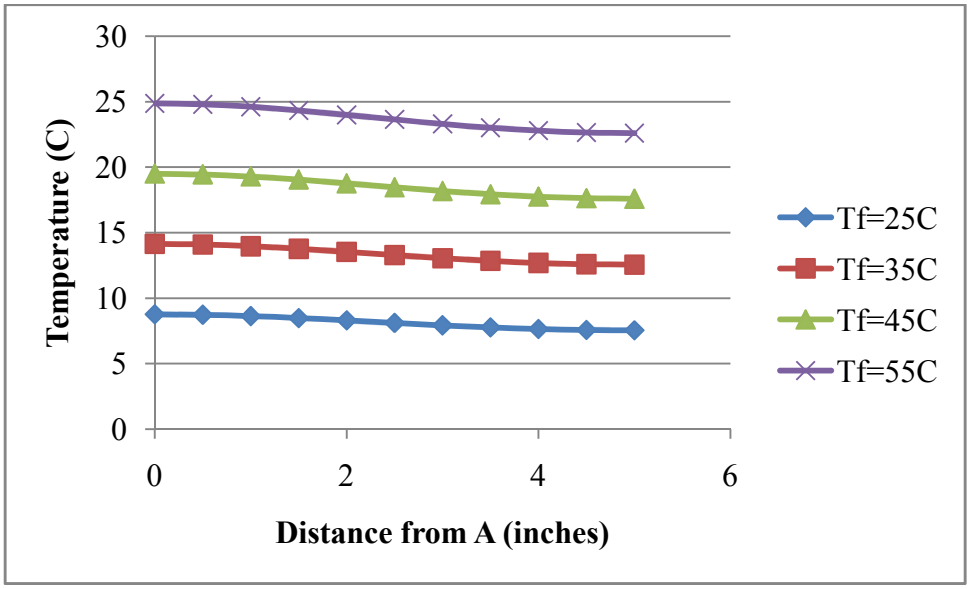

Figure 4.14 Surface temperature distribution with different T_f

Table 4.19 Temperature difference with different T_f

T_f	ΔT(C)
25	1.22225
35	1.5715
45	1.9206
55	2.2699

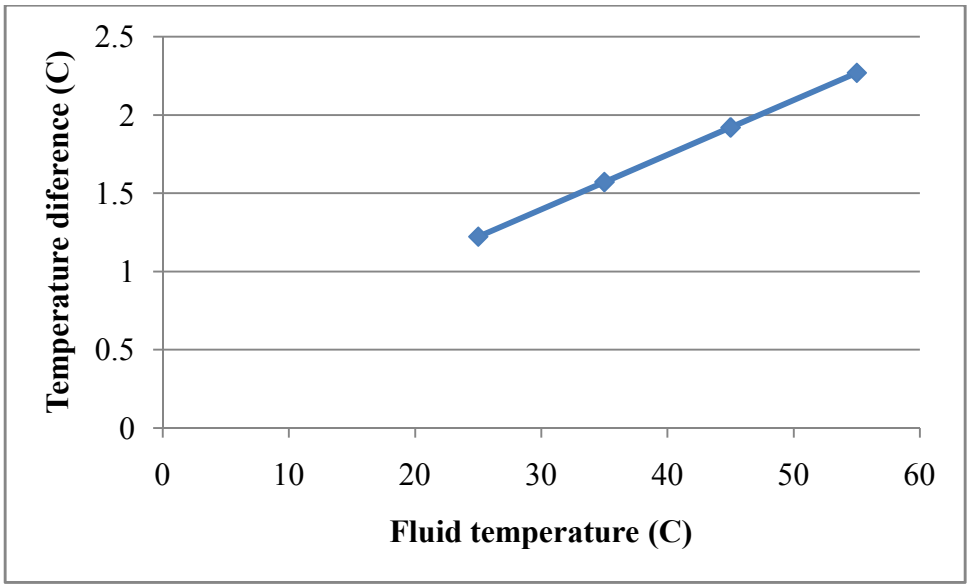

Figure 4.15 Temperature difference with different T_f

Table 4.20 Temperature at B in t=10h with different T_f

$T_f = 25^0C$		$T_f = 35^0C$		$T_f = 45^0C$		$T_f = 55^0C$	
t (h)	**T (C)**	**t (h)**	**T (C)**	**t (h)**	**T (C)**	**t (h)**	**T (C)**
0	-10	0	-10	0	-10	0	-10
1.00E-03	-10	1.00E-03	-10	8.05E-04	-10	6.81E-04	-10
2.00E-03	-10	2.00E-03	-10	1.61E-03	-10	1.36E-03	-10
3.00E-03	-10	3.00E-03	-10	2.42E-03	-10	2.04E-03	-10
5.00E-03	-10	4.00E-03	-10	3.22E-03	-10	2.73E-03	-10
7.00E-03	-10	6.00E-03	-10	4.83E-03	-10	4.09E-03	-10
1.10E-02	-10	8.00E-03	-10	6.44E-03	-10	5.45E-03	-10
1.90E-02	-10	1.20E-02	-10	9.66E-03	-10	6.81E-03	-10
2.70E-02	-10	2.00E-02	-10	1.29E-02	-10	9.54E-03	-10
4.30E-02	-10	2.80E-02	-10	1.93E-02	-10	1.50E-02	-10
7.50E-02	-9.9999	4.40E-02	-10	2.58E-02	-10	2.04E-02	-10
1.07E-01	-9.9994	6.00E-02	-9.99999	3.87E-02	-10	2.59E-02	-10
1.71E-01	-9.99068	9.20E-02	-9.99974	5.15E-02	-10	3.68E-02	-10
2.99E-01	-9.89007	1.56E-01	-9.99145	7.73E-02	-9.9999	4.77E-02	-10
4.27E-01	-9.68028	2.20E-01	-9.96557	1.03E-01	-9.9996	6.95E-02	-9.99997
6.83E-01	-8.89422	3.48E-01	-9.78588	1.55E-01	-9.9933	9.13E-02	-9.99982
9.39E-01	-7.8818	4.76E-01	-9.45997	2.55E-01	-9.9133	1.35E-01	-9.99659
1.45E+00	-5.6686	7.32E-01	-8.3659	3.56E-01	-9.7324	1.79E-01	-9.98629
2.475	-2.00328	9.88E-01	-7.01674	4.57E-01	-9.4376	2.66E-01	-9.8997
3.499	7.40E-01	1.5	-4.15721	6.58E-01	-8.4676	3.53E-01	-9.72047

5.547	3.81627	2.012	-1.50642	8.60E-01	-7.2403	4.40E-01	-9.43721
7.595	5.51006	3.036	2.51452	1.26302	-4.4558	6.15E-01	-8.50603
9.643	6.43759	4.06	5.43377	1.66609	-1.7132	7.89E-01	-7.30892
10	6.57888	5.084	7.51888	2.06915	8.20E-01	1.13785	-4.48388
		7.132	9.80881	2.87527	4.84627	1.48669	-1.60334
		9.18	11.0617	3.68139	7.94951	1.83554	1.14051
		10	11.4384	5.24134	11.672	2.51688	5.6194
				6.80129	13.9615	3.19821	9.23295
				8.36123	15.3658	3.87955	12.1033
				9.92118	16.2264	5.24221	15.831
				10	16.2685	6.60488	18.2391
						7.96755	19.7918
						9.33022	20.7922
						10	21.179

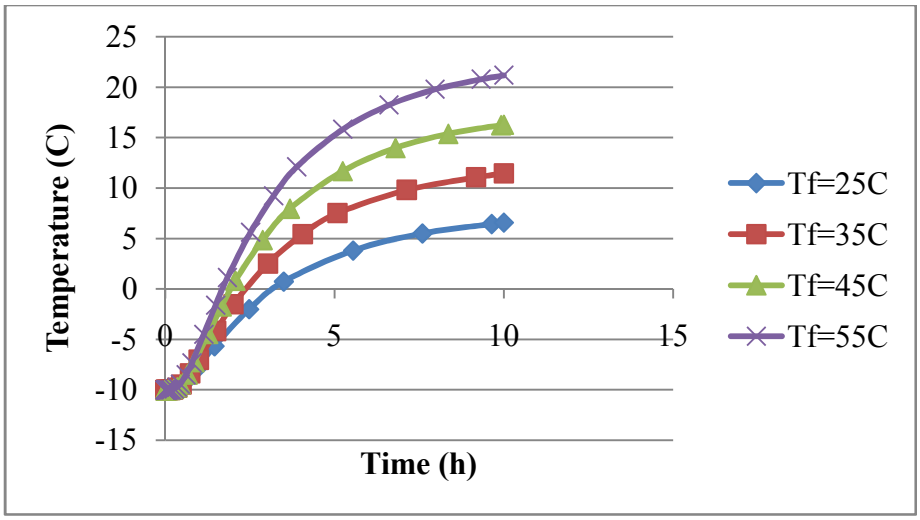

Figure 4.16 Temperature at B in t=10h with different T_f

Table 4.21 Heating rate at B with different T_f

At point B	
T	**Heating rate (C/h)**
25	1.657888
35	2.14384
45	2.62685
55	3.1179

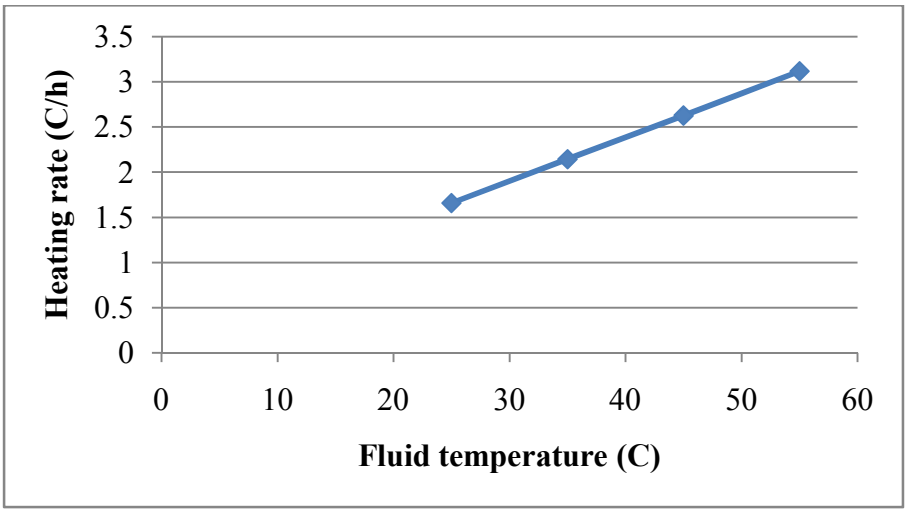

Figure 4.17 Heating rate at B with different T_f

In general, increasing the fluid temperature leads to an increase in thermal energy, resulting in the significant increase of surface temperature, as shown in Figure 4.14. In addition, it can be observed that the heating curves obtained at different temperatures are approximately parallel to one another. The distance between these curves are relatively large and as opposed to the pipe diameter and pipe spacing cases, the temperature difference rises linearly with the increase of fluid temperature.

Also, increasing the fluid temperature leads to the linear increase of heating rate. Specifically, the heating rate in this case is relatively larger than that of other cases. This is confirmed by Figure 4.17.

More specifically, by increasing the fluid temperatures from 25^0C to 55^0C, temperature (at B) increases by approximately 198%, from 7.56^0C to 22.6^0C and heating rate (at B) increases by 87.9%, from $1.66^0C/h$ to $3.12^0C/h$. In other words, increasing the fluid temperatures by 1% results in an increase of temperature and heating rate (at B) by 1.65% and 0.73%, respectively, indicating that the fluid temperature is a very important parameter.

Combining all above results, it is concluded that the surface temperature is very sensitive to the thermal energy (fluid temperature). In other words, fluid temperature plays an important role in the hydronic snow melting system. However, when the fluid temperature $T_f = 55^0C$, the temperature difference is over 2^0C, which does not meet the uniformity requirement for snow melting. Therefore, fluid temperature should be less than 55^0C. It is proposed that the fluid temperature should be around $25^0C - 50^0C$.

4.2 EXTERNAL WORKING CONDITIONS

In the previous section, the influences of internal working conditions such as fluid temperature, pipe spacing, pipe depth and pipe diameter on the snow melting performance were considered. Thermal energy represented by fluid temperature, is the most important factor in performance of hydronic snow melting system. However, examining those parameters is insufficient to fully assess the overall performance of the heat transfer process in the hydronic system. It is also necessary to investigate the importance of external working conditions including ambient temperature and wind velocity and how the internal working conditions combined with external conditions effect the snow melting performance. Specifically, the influences of fluid temperature (internal working condition) combined with ambient temperature as well as wind velocity (external working conditions) on idling time (transient analysis) and surface temperature (steady-state analysis) will be further investigated.

4.2.1 AMBIENT TEMPERATURE

The same concrete slab as used previously is exposed to the ambient temperature. Notice that the initial condition depends on the ambient temperature. All fixed inputs are summarized in Table 4.22.

Table 4.22 System parameters for temperature analysis

Parameters	Values
Slab thickness (in)	6
Thermal conductivity $(k - \frac{W}{in.C})$	0.062
Specific heat/ Heat capacity $(c - \frac{Wh}{kg.C})$	0.3
Mass density $(\rho - \frac{kg}{in^3})$	0.039
Convection coefficient $\beta - \frac{W}{in^2.h.C}$	0.009
Pipe depth $(D_1 - in)$	4
Pipe diameter $(d - in)$	0.75
Pipe spacing $(D_2 - in)$	10"
Fluid temperature $(T_f - \ C \ or \ F)$	$25^0C - \ 35^0C - \ 45^0C - \ 55^0C$
Ambient temperature $(T_\infty - \ C \ or \ F)$	$-1^0C, -3^0C, -5^0C, -7^0C$

4.2.1.1 EFFECTS ON IDLING TIME

Idling time is the waiting time for the concrete surface to reach the melting point of snow $(0^0C \ or \ 33^0F)$ from a fixed initial condition (ambient temperature). This section examines the influence of ambient temperature and fluid temperature on idling time. All results are shown in the tables and figures belows.

Table 4.23 Idling time

$v = 2m/s$	At point B				
$t(T_f, T_\infty)$	T_f/T_∞	-1	-3	-5	-7
	25	0.73653	1.3171	1.82328	2.38144
	35	0.63623	1.08824	1.46292	1.82306
	45	0.57752	0.95653	1.26072	1.54152
	55	0.55173	0.87205	1.12567	1.36354

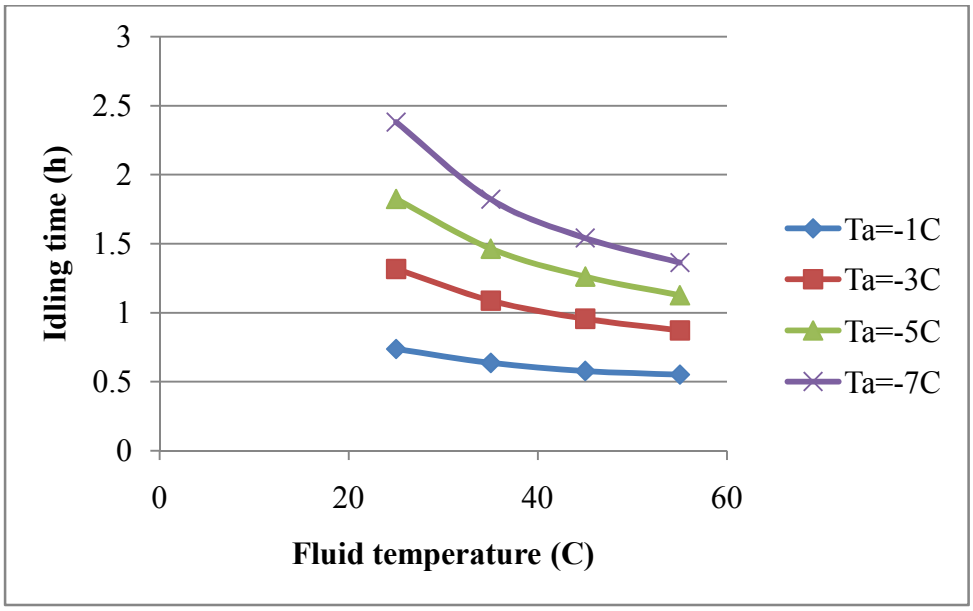

Figure 4.18 Idling time with different ambient temperatures

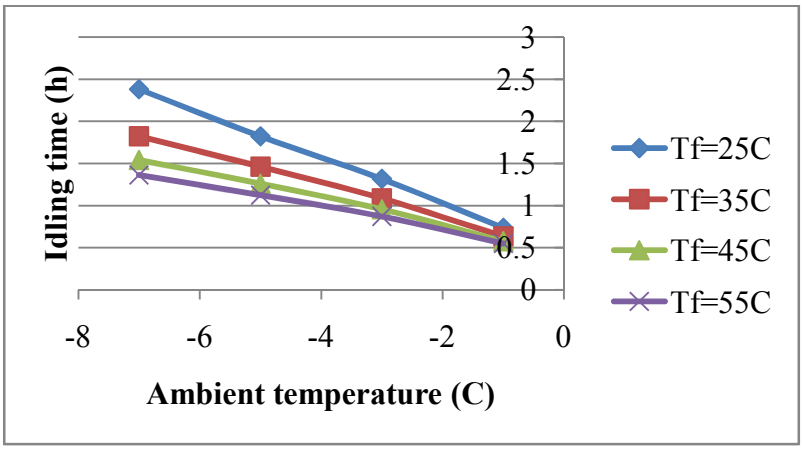

Figure 4.19 Idling time with different fluid temperatures

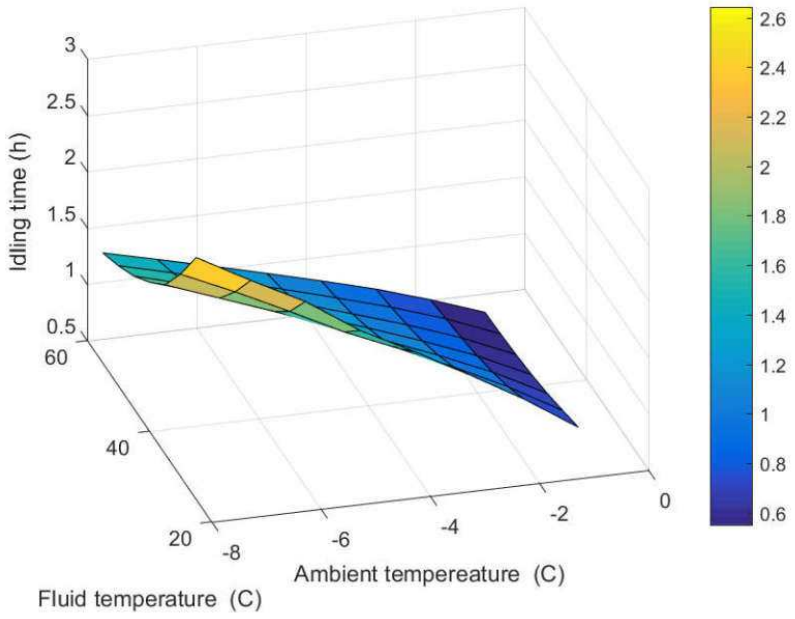

Figure 4.20 Idling time surface

From Figure 4.18 to Figure 4.20 , the effects of ambient temperature are depicted in two-dimensional and three-dimensional plots. At a fixed ambient temperature, the idling time decreases as thermal energy represented by fluid temperature rises. Intuitively, it is reasonable since the concrete slab absorbs more energy as the thermal energy increases and the idling time reduces exponentially.

Similarly, at a fixed fluid temperature, the idling time rises linearly as the air temperature reduces suggesting the negative effect of air temperature. This can be attributed to the fact that as the ambient temperature gets smaller, the energy dissipation increases. Therefore, the concrete surface needs more time to achieve the melting point.

It can also be seen from Figure 4.19, the idling time is more sensitive to the input thermal energy represented by fluid temperature as the surrounding temperature gets reduced. More specifically, when the ambient temperature is -1^0C, the idling times given at $T_f = 25^0C$ and $T_f = 35^0C$ are 0.74h and 0.64h, respectively. However, when ambient temperature is -7^0C, the

idling times given at $T_f = 25^0C$ and $T_f = 35^0C$ are 2.38h and 1.82h respectively. It can be observed that when the ambient temperature decreases from -1^0C to -7^0C, the idling time difference gets bigger (from 0.1h to 0.56h).

The longest idling time occurs when the ambient temperature and fluid temperature reach minimum values. This is attributed to the fact that the thermal energy transferred to the concrete surface is minimum (low fluid temperature) and thermal energy dissipation reaches maximum (low ambient temperature).

4.2.1.2 EFFECTS ON SURFACE TEMPERATURE

This section investigates the effects of ambient temperature (t=24h) on the surface temperature at fixed fluid temperature. Four ambient temperatures are selected to investigate the effect of surrounding temperature with a fixed working condition (fluid temperature). All results are shown in the tables and figures below.

Table 4.24 Surface temperature with different ambient temperatures (t=24h)

$T_f = 25^0C$							
$T_\infty = -1^0C$		$T_\infty = -3^0C$		$T_\infty = -5^0C$		$T_\infty = -7^0C$	
t (h)	**T (C)**	**t (h)**	**T (C)**	**t (h)**	**T (C)**	**t (h)**	**T (C)**
0	-1	0	-3	0	-5	0	-7
1.00E-03	-1	1.00E-03	-3	1.00E-03	-5	1.00E-03	-7
2.00E-03	-1	2.00E-03	-3	2.00E-03	-5	2.00E-03	-7
3.00E-03	-1	3.00E-03	-3	3.00E-03	-5	3.00E-03	-7
5.00E-03	-1	5.00E-03	-3	5.00E-03	-5	5.00E-03	-7
9.00E-03	-1	9.00E-03	-3	9.00E-03	-5	9.00E-03	-7
1.70E-02	-1	1.70E-02	-3	1.70E-02	-5	1.30E-02	-7
2.50E-02	-1	2.50E-02	-3	2.50E-02	-5	2.10E-02	-7
4.10E-02	-1.00E+00	4.10E-02	-3	4.10E-02	-5	3.70E-02	-7
7.30E-02	-1.00E+00	7.30E-02	-2.9999	7.30E-02	-4.9999	5.30E-02	-7
1.37E-01	-9.96E-01	1.37E-01	-2.9961	1.05E-01	-4.9995	8.50E-02	-6.9998
2.01E-01	-9.84E-01	2.01E-01	-2.983	1.69E-01	-4.9921	1.49E-01	-6.9944
3.29E-01	-8.91E-01	3.29E-01	-2.8824	2.97E-01	-4.9064	2.13E-01	-6.9772
5.85E-01	-4.08E-01	5.85E-01	-2.3629	5.53E-01	-4.3922	3.41E-01	-6.8538

8.41E-01	2.82E-01	8.41E-01	-1.6199	8.09E-01	-3.6243	5.97E-01	-6.243
1.353	1.89915	1.353	1.22E-01	1.321	-1.7724	8.53E-01	-5.3823
2.377	4.67293	2.377	3.10931	1.833	3.43E-02	1.365	-3.385
3.401	6.77382	3.401	5.37181	2.857	2.8582	1.877	-1.4654
5.449	9.14322	5.449	7.92347	4.905	6.08481	2.901	1.50933
7.497	10.4508	7.497	9.33164	6.953	7.8722	4.87499	4.8273
11.593	11.4378	11.593	10.3945	9.001	8.85339	6.84898	6.69417
19.785	11.8954	19.785	10.8874	13.097	9.59265	8.82298	7.73582
24	11.9824	24	10.9811	21.289	9.93528	12.771	8.53869
				24	9.98934	20.6669	8.92143
						24	8.9902

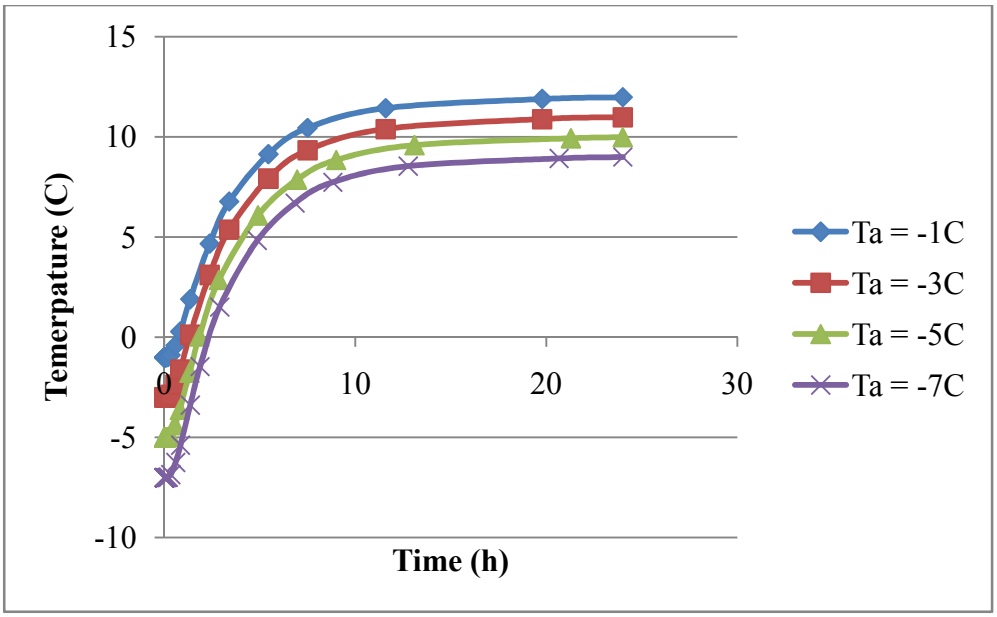

Figure 4.21 Surface temperature with different ambient temperatures (t=24h)

Figure 4.21 shows the relationship between surface temperature and heating time with different ambient temperatures as the fluid temperature is fixed at $T_f = 25^0C$. As the ambient temperature decreases, the surface temperature gets colder. This is reasonable as the energy dissipated (the thermal energy transferred to environment) by convection increases as the ambient temperature decreases. The heating curves obtained at different air temperatures are approximately parallel to one another and the distances of these curves are relatively even.

4.2.2 WIND VELOCITY

In the previous chapter, the degree of heat transferred from concrete to environment is determined by convection coefficient or film coefficient which is mainly dependent upon wind velocity. Ohzawa proposed the convection coefficient, β as a function of wind velocity v: $\beta = 9.6 + 1.12v$, in $(\frac{kcal}{m^2.h.C})$ where v is the wind velocity (m/s). This relationship is shown in Figure 4.22.

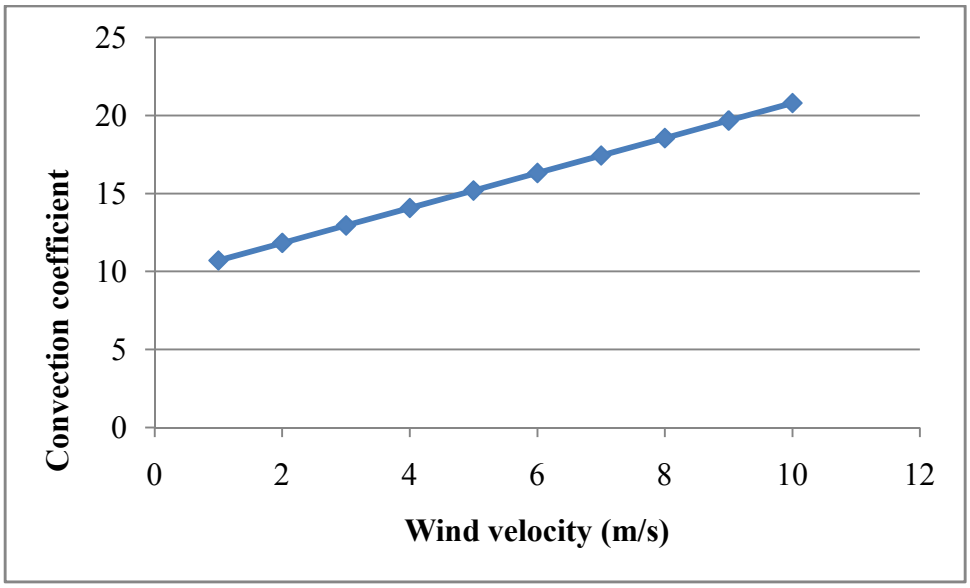

Figure 4.22 Convection coefficient (in $\frac{kcal}{m^2.h.C}$)

4.2.2.1 EFFECTS ON IDLING TIME:

This section will analyze the effect of wind velocity combined with fluid temperature at a fixed ambient temperature on idling time ($T_\infty = -5^0C$). Four wind velocities are taken into consideration. From these wind velocities, convection coefficients can be calculated for this study. All results are shown in the tables and figures below.

Table 4.25 Idling time

$T_\infty = -5^0C$	At point B				
$t(T_f, v)$	$T_f/v(\beta)$	1(0.008)	2(0.009)	3(0.00972)	4(0.01056)
	25	1.77861	1.82328	1.86255	1.912845
	35	1.43295	1.46292	1.48585	1.513113
	45	1.23849	1.26072	1.27698	1.296188
	55	1.10881	1.12567	1.13794	1.152713

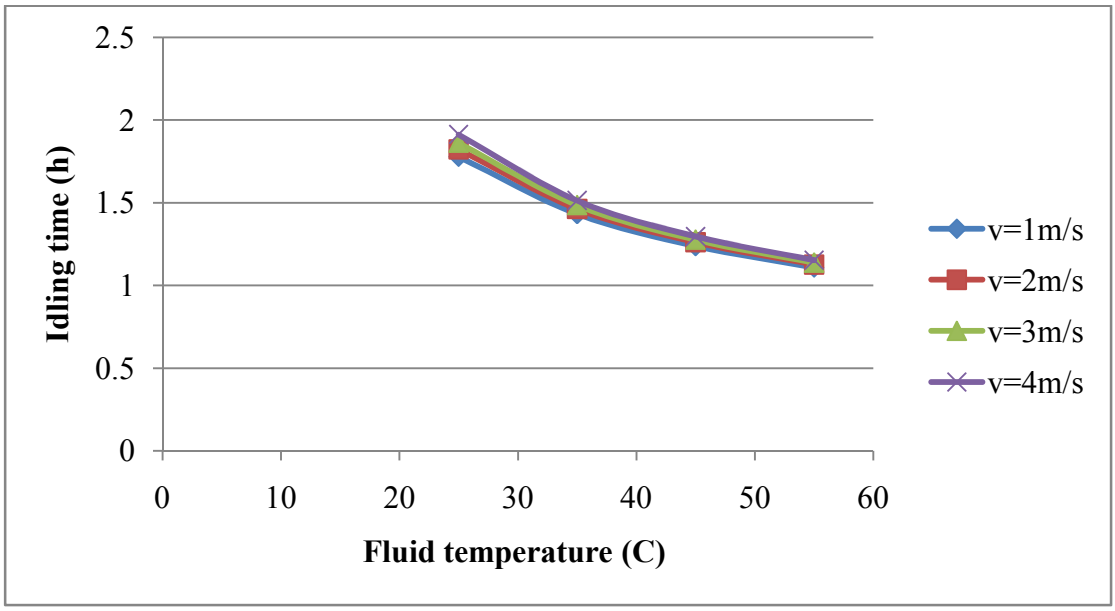

Figure 4.23 Idling time with various wind velocities

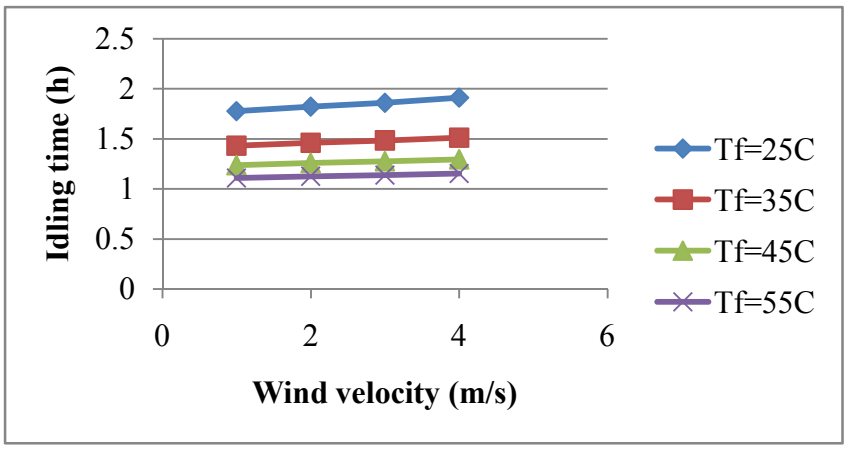

Figure 4.24 Idling time with various fluid temperatures

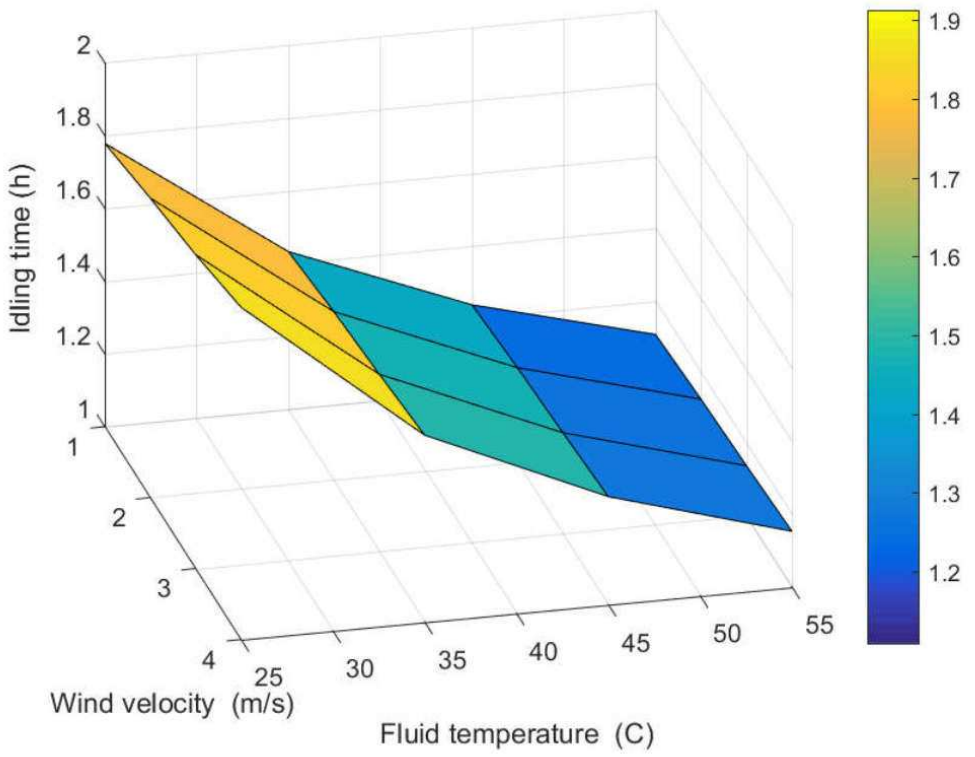

Figure 4.25 Idling time surface

From Figure 4.23 to Figure 4.25, the idling time curves obtained at different wind velocities are closed to one another as opposed to these curves obtained at different fluid temperatures. This indicates that idling time is not sensitive to wind velocity but thermal energy, represented by fluid temperature. Therefore, wind velocity is not an important parameter in investigating idling time.

4.2.2.2 EFFECTS ON SURFACE TEMPERATURE

The effects of wind velocity at a fixed ambient temperature ($T_\infty = -5^0C$) and fixed fluid temperature ($T_f = 25^0C$) on surface temperature are considered here. The relationship between surface temperature and heating time obtained at four wind velocities are shown in the Figure 4.26.

Table 4.26 Surface temperature at B in t=24h

v=1 m/s		v=2 m/s		v=3 m/s		v=4 m/s	
t (h)	**T (C)**	**t (h)**	**T (C)**	**t (h)**	**T (C)**	**t (h)**	**T (C)**
0	-5	0	-5	0	-5	0	-5
1.00E-03	-5	1.00E-03	-5	1.00E-03	-5	1.00E-03	-5
2.00E-03	-5	2.00E-03	-5	2.00E-03	-5	2.00E-03	-5
3.00E-03	-5	3.00E-03	-5	3.00E-03	-5	3.00E-03	-5
5.00E-03	-5	5.00E-03	-5	5.00E-03	-5	5.00E-03	-5
9.00E-03	-5	9.00E-03	-5	9.00E-03	-5	9.00E-03	-5
1.70E-02	-5	1.70E-02	-5	1.70E-02	-5	1.70E-02	-5
2.50E-02	-5	2.50E-02	-5	2.50E-02	-5	2.50E-02	-5
4.10E-02	-5	4.10E-02	-5	4.10E-02	-5	4.10E-02	-5
7.30E-02	-4.9999	7.30E-02	-4.9999	7.30E-02	-4.99991	7.30E-02	-4.99991
1.05E-01	-4.9995	1.05E-01	-4.9995	1.05E-01	-4.99949	1.05E-01	-4.99949
1.69E-01	-4.992	1.69E-01	-4.9921	1.69E-01	-4.99214	1.69E-01	-4.99222
2.97E-01	-4.9049	2.97E-01	-4.9064	2.97E-01	-4.90747	2.97E-01	-4.90866
5.53E-01	-4.3794	5.53E-01	-4.3922	5.53E-01	-4.40116	5.53E-01	-4.41129
8.09E-01	-3.5914	8.09E-01	-3.6243	8.09E-01	-3.64714	8.09E-01	-3.67287
1.321	-1.6782	1.321	-1.7724	1.321	-1.83723	1.321	-1.90989
1.833	1.99E-01	1.833	3.43E-02	1.833	-7.88E-02	1.833	-2.05E-01
2.857	3.16274	2.857	2.8582	2.857	2.65164	2.857	2.42303
4.904	6.59613	4.905	6.08481	4.905	5.74139	4.905	5.36505
6.951	8.52517	6.953	7.8722	6.953	7.43684	6.953	6.9626
8.998	9.59915	9.001	8.85339	9.001	8.35884	9.001	7.82236
13.092	10.4242	13.097	9.59265	13.097	9.0446	13.097	8.45279
21.28	10.8158	21.289	9.93528	21.289	9.35743	21.289	8.73542
24	10.8788	24	9.98934	24	9.40626	24	8.77901

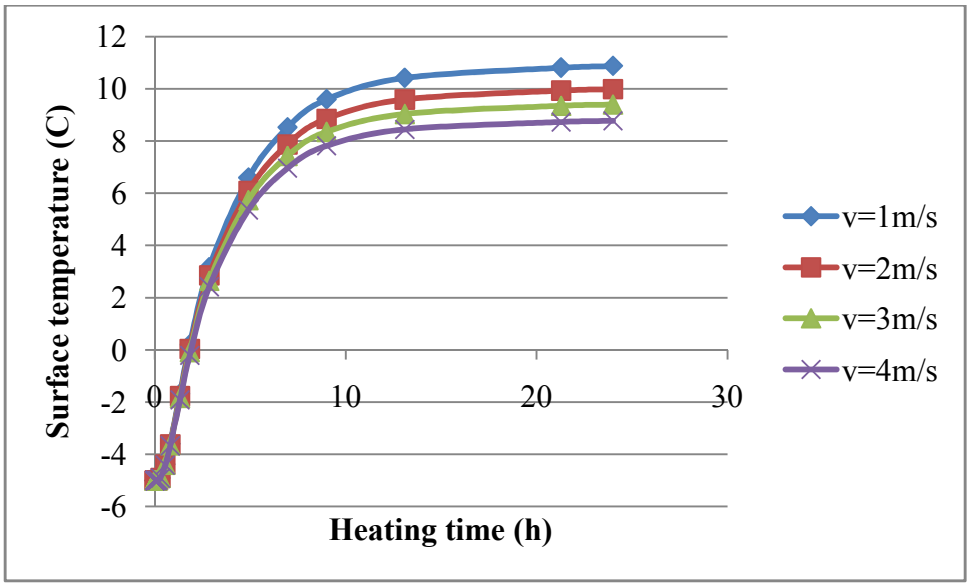

Figure 4.26 Surface temperature at B in t=24h

The table and figures above show the relationship between surface temperature and heating time at various wind velocity. At the initial stage and linear stage, these curves are very close to one another. This again confirms the minimal sensitivity of wind velocity in the snow melting performance.

4.2.3 AMBIENT TEMPERATURE AND WIND VELOCITY

In the previous sections, the influences of ambient temperature and wind velocity have been examined individually. This section will investigate the effect external working conditions represented by ambient temperature combined with wind velocity at a fixed working condition ($T_f = 30^0C$) on the performance of snow melting process (i.e idling time). This will provide a better comparison of ambient temperature with wind velocity. Four wind velocities and four ambient temperatures are selected for this study. Results are shown in the table and figures below.

Table 4.27 Idling time

At $T_f = 30^0C$		At point B			
$t(T_\infty, v)$	$T_\infty/v(\beta)$	1/0.008	2/0.009	3/0.00972	4/0.01056
	-1	0.6781	0.68446	0.68909	0.69455
	-3	1.16355	1.18403	1.19896	1.21656
	-5	1.57384	1.60865	1.63751	1.67585
	-7	2.01504	2.07953	2.12711	2.18377

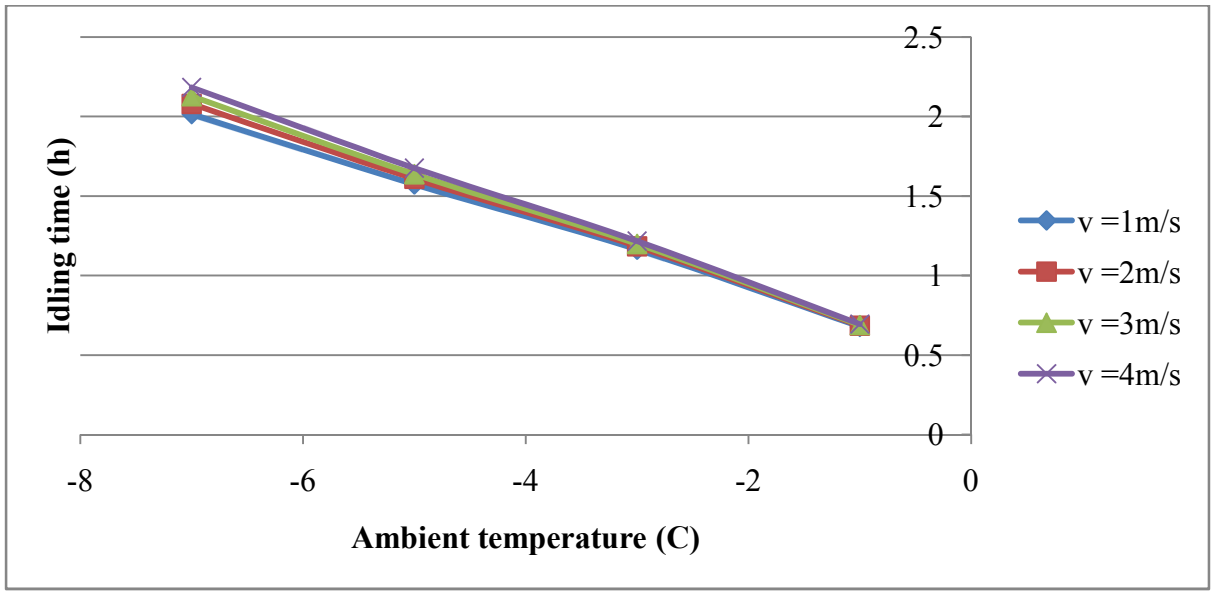

Figure 4.27 Idling time with various wind velocities

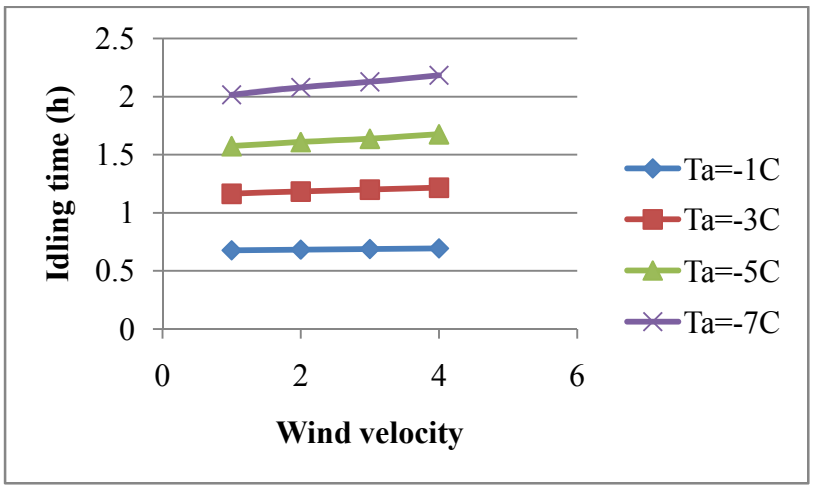

Figure 4.28 Idling time with various ambient temperatures

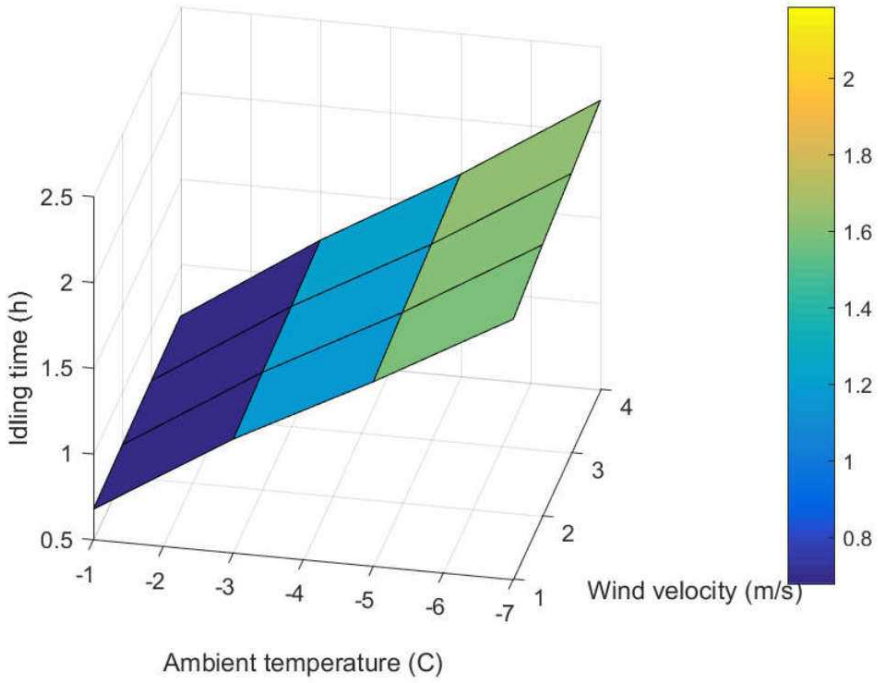

Figure 4.29 Idling time surface

The table above suggests that when environment temperature is lower and wind velocity is greater, the concrete slab takes a longer time to heat and rise to the melting point 0^0C.

The idling curves obtained at various wind velocities are close to one another as opposed to those obtained at various ambient temperatures. This suggests a slight effect of wind velocity on idling time. Therefore it can be concluded that ambient temperature is more important than wind velocity in the snow melting performance.

CHAPTER 5 - CONCLUSION

5.1 SUMMARY

In this research, a general introduction about hydronic snow melting system has been performed.

(a) Advantages and basis components of hydronic heating system were described.

(b) The applications of hydronic snow melting system can be divided into three types based on the snow-free ratio A_r: type A - level I (residential systems), type B - level II (commercial systems) and type C - level III (industrial systems).

(c) Hydronic piping system and installation techniques (insulation, tubing layout patters...) have also been covered.

Some preliminary results were obtained from steady-state and transient analysis of two-dimensional and three-dimensional finite element modeling.

(a) Surface temperature distribution is non-uniform. More specifically, the maximum surface temperature is above the hydronic pipe whereas the minimum temperature is at the midway between the every two adjacent pipes.

(b) The temperature variation of concrete surface can be categorized into four sub-stages: the starting stage, linear stage and accelerated stage and stable stage. Generally, the melting speed in the initial stages is significantly fast and then becomes slow.

(c) If three-dimensional domain is "sliced" in the z direction, the same results can be obtained for all slices. Therefore, two-dimensional simulation will be performed for all analyses.

The effects of internal working conditions represented by pipe diameter, pipe depth, pipe spacing, fluid temperature and external working conditions such as ambient temperature and wind velocity have been investigated by intensive parametric studies.

For internal working conditions, the concrete surface temperature decreases as the pipe spacing and pipe depth increase. However, concrete temperature increases as the pipe diameter and fluid temperature increase. More specifically, it can be found from this study that:

(i) Placing pipes at shallower depths decreases the surface temperature, indicating the negative role of pipe depth on the performance of snow melting process. In practice, shallow pipes cause negative effects on the structural performance of concrete slab/pavement under various loads. Also, hydronic pipes are also placed on the rebar in practice. Therefore, it is proposed that pipe should be placed about 2" above the bottom surface.

(ii) The distance between pipes plays an important role in the increase of surface temperature. Closer pipe improves surface temperature remarkably because the surface temperature absorbs more energy as the interval gets shorter. However, the maximum distance should not be over 12" due to the fact it violates the uniformity requirement for snow melting. Also, closer pipes might result in segregation of aggregate of concrete during construction. Hence, it is suggested that pipe spacing should be around 6"-12" so that the snow melting system can achieve the optimal performance.

(iii) An increase in pipe diameter results in warmer surfaces due to the absorbing energy more thermal energy. However, large pipes will cause some negative effects on the structural behaviors of concrete. The most commonly used diameter in U.S should be about 0.75".

(iv) Increasing the heating energy represented by fluid temperature, circulating through the pipes, causes to supply more thermal energy to the concrete surface. Higher value of fluid temperature also reduces the idling time during the process. This is obviously the most important parameter in the snow melting process. However, the fluid temperature should be too high

(i.e over 50^0C) as it causes bad effects on concrete. The proposed fluid temperature should be around $25^0C - 50^0C$.

These proposed values match well with the designed values in many installation guides used in the U.S. [22] [23] [24] [26]

The order of most effective options, investigated in this study associated with the increase of surface temperature and heating rate (at B): (i) fluid temperature, (ii) pipe spacing, (iii) pipe depth, (iv) pipe diameter:

(a) In terms of surface temperature at B, fluid temperature is 334% more important than pipe spacing, pipe spacing is 86% more important than pipe depth and pipe depth is 15% more important than pipe diameter. Putting these parameters on a 1-10 scale, if fluid temperature is 10 then spacing is 2.304, depth is 1.24 and diameter is 1.08.

(b) In terms of heating rate at B, fluid temperature is 152% more important than pipe spacing which is 150% more important than pipe depth and pipe depth is 5% more important than pipe diameter. Putting these parameters on a 1-10 scale, if fluid temperature is 10 then spacing is 3.97, depth is 1.59 and diameter is 1.51.

For external working conditions, ambient temperature and wind velocity have been studied. The following general conclusions can be drawn:

(i) Idling time is more sensitive to the input thermal energy (fluid temperature) as the air temperature reduces.

(ii) When environment temperature is lower and wind velocity is greater, the concrete surface takes longer time to heat and rise to the temperature above the melting point.

(iii) Ambient temperature plays a more important role in the snow melting performance in comparison to wind velocity.

5.2 FUTURE RESEARCH

The following recommendations for future research may be made:

(a) Field experiments should be performed to further verify the accuracy of this predictive computational model.

(b) The heat transfer from water to pipe as well as from pipe to concrete should be taken into consideration. Therefore, the modification of model to take the thickness of the pipe into consideration (thermal conductivity of hydronic pipe) and actual convection between fluid and pipe (coefficient of cooling water convection) should be taken into consideration.

(c) Linear and nonlinear regression can be performed to establish the formula of predictive surface temperature and idling time as a function of input parameters.

(d) Structural behaviors of concrete under mechanical loads combined with thermal loads can be made.

REFERENCES

[1] National Research Council. Where the weather meets the road. Washington, DC: National Academies Press; 2004.

[2] Lombardo L. Overview of US crashes and environment. Second Weather Information for Surface Transportation (WIST) Forum, December 4–6, 2000, Rockville, Md.

[3] Federal Highway Administration, How Do Weather Events Impact Roads? [Online]

[4] Salt Institute, Highway Deicing and Anti-icing for Safety and Mobility. [Online]

[5] Daniel L. Kelting and Corey L. Laxson. Review of effects and costs of road deicing with recommendations for winter road management in the Adirondack Park.

[6] Hou, Z.F., Li, Z.Q., Tang, Z.Q., 2002. Research on making and application of carbon fiber electrically concrete for deicing and snow-melting. Journal of Wuhan Institute of Technology (Natural Journal Edition) 24, 32–34.

[7.1] Liu, X.B., Spitler, J.D**.**A Simulation Tool for the Hydronic Bridge Snow Melting System. Submitted to the 12th International Road Weather Conference- 2015.

[7.2] Liu X, Ree SJ, Spitler JD. Modeling snow melting on heated pavement surfaces. PartⅠ:Model development. Applied Thermal Engineering - Volume 27, Issues 5–6, April 2007, Pages 1115–1124.

[7.3] Liu X, Ree SJ, Spitler JD. Modeling snow melting on heated pavement surfaces. Part II: Experimental validation. Applied Thermal Engineering - Volume 27, Issues 5–6, April 2007, Pages 1125–1131.

[8] Chapman WP. Design of snow melting systems. Heat Vent 1952;49:88-95

[9] ACI Committee 207, Mass Concrete. ACI Manual of Concrete Practice, Part I, 207.1, 1994 p.21-3.

[10] JCI Committee on the thermal stress. The state of the art report of thermal stress evaluation in massive concrete, 1985 p. 5-9.

[11] Sikoku Electric Power Corp., A study on the preventive measure of early age cracking in a mass concrete. Technical report, 1964.

[12] https://www.braensupply.com/rock-salt-lowes-home-depot/

[13] https://www.telegraph.co.uk/motoring/news/8249314/Snow-hit-council-imports-grit-from-Peru.html

[14] https://www.usatoday.com/story/weather/2017/11/01/warnings-deadly-weather-hazard-snow-squalls-coming-winter/818248001/

[15] http://www.westlafayette.in.gov/department/division.php?structureid=178

[16] http://www.pexheat.com/Catalog/ProMelt

[17] http://www.snowmeltingcable.com/site/page/installation

[18] Snow and Ice Melting Systems. The power to melt snow and ice for safety and efficiency.

[19] Daryl L. Logan - A first course in the Finite Element Method

[20] G. R. Liu and S. S. Quek - The Finite Element Method: A practical course

[21] J. N. Reddy - Introduction to the Finite Element Method.

[22] Snow & Ice Melting Design Manual- Uponor Wirsbo

[23] Manual for ClimateMaster Training Course: Essential of Hydronics for GSHP Professionals

[24] Snowmelt Installation Guide - Infloor Heating Systems

[25] https://www.colourbox.com/vector/structural-chemical-formula-and-model-of-ethylene-glycol-molecule-vector-13701713

[26] Snow Melting System Installation Manual - S-no-Ice Viega.